INFORMATION TO USERS

This material was produced from a microfilm copy of the original document. While the most advanced technological means to photograph and reproduce this document have been used, the quality is heavily dependent upon the quality of the original submitted.

The following explanation of techniques is provided to help you understand markings or patterns which may appear on this reproduction.

1. The sign or "target" for pages apparently lacking from the document photographed is "Missing Page(s)". If it was possible to obtain the missing page(s) or section, they are spliced into the film along with adjacent pages. This may have necessitated cutting thru an image and duplicating adjacent pages to insure you complete continuity.

2. When an image on the film is obliterated with a large round black mark, it is an indication that the photographer suspected that the copy may have moved during exposure and thus cause a blurred image. You will find a good image of the page in the adjacent frame.

3. When a map, drawing or chart, etc., was part of the material being photographed the photographer followed a definite method in "sectioning" the material. It is customary to begin photoing at the upper left hand corner of a large sheet and to continue photoing from left to right in equal sections with a small overlap. If necessary, sectioning is continued again – beginning below the first row and continuing on until complete.

4. The majority of users indicate that the textual content is of greatest value, however, a somewhat higher quality reproduction could be made from "photographs" if essential to the understanding of the dissertation. Silver prints of "photographs" may be ordered at additional charge by writing the Order Department, giving the catalog number, title, author and specific pages you wish reproduced.

5. PLEASE NOTE: Some pages may have indistinct print. Filmed as received.

Xerox University Microfilms
300 North Zeeb Road
Ann Arbor, Michigan 48106

SUPPRESSION OF ICE FOG
FROM POWER PLANT COOLING PONDS

A

DISSERTATION

Presented to the Faculty of the

University of Alaska in partial fulfillment

of the Requirements

for the Degree of

DOCTOR OF PHILOSOPHY

By

Terry T. McFadden, B.E.S.M.E., M.S.M.E.

Fairbanks, Alaska

December 1974

SUPPRESSION OF ICE FOG

FROM POWER PLANT COOLING PONDS

RECOMMENDED:

T. E. Stelson

Carl S. Benson

John L. Burdick

J. B. Friedemann

E. F. Rice

Chairman, Advisory Committee

John L. Burdick

Department Head

APPROVED:

C. Bullock

Dean of the College of Mathematics, Physical Sciences and Engineering

12/9/74

Date

Earl H. Beistline

Provost

12/20/74

Date

ABSTRACT

Ice fog generated at the Eielson AFB power plant cooling pond contributes heavily to the total ice fog problem on the base. Several methods for suppression were studied and two techniques were tested experimentally. Experiments were also conducted to determine the magnitude of the various modes of heat transfer within the pond's microclimate. Values of evaporative and radiative heat loss during ice fog are presented.

Ice cover is shown to be an effective ice fog suppression technique. Monomolecular films are also shown to be effective and offer some unique advantages, such as ease of application and low overall cost.

The heat normally lost to evaporation must be dissipated by other means during suppression. With the ice cover technique this is accomplished by melting the ice cover. During suppression with monomolecular films, the heat must be dissipated by increasing radiative and convective losses.

The simplicity of application of monomolecular films, along with their lower cost, combine to make this technique attractive; however, the lower pond temperatures and increased suppression effectiveness weigh heavily in favor of the ice-cover technique. In addition, more exhaustive testing provides a better understanding of the problems involved in using the ice cover method of suppression.

ACKNOWLEDGEMENTS

In the completion and presentation of this work I am indebted to many individuals. I would like to sincerely express my gratitude for their kind help and assistance. To the members of my doctoral committee (Dr. E. F. Rice, Professor John Burdick, Dr. Carl Benson, Dr. James Tiedemann, and Dr. Tom Osterkamp) for their many hours of patient help and encouragement, both during preparation of the manuscript as well as help and suggestions at the research site during the experimentation.

Dr. Bjorn Holmgren and Dr. Glenn Shaw were a great help in securing instrumentation and reviewing the manuscript.

Mrs. Virginia Daugherty needs special thanks for her enormous effort in typing and correcting the manuscript.

I would also like to express my appreciation to the US Air Force for their cooperation and logistics support during the studies.

Last, but not least, I would like to express my sincerest gratitude to my wife Ruth, whose patience and encouragement never faltered throughout the project.

TABLE OF CONTENTS

Table of Contents (continued) Page

LIST OF FIGURES

List of Figures (continued)

List of Figures (continued)

LIST OF TABLES

LIST OF SYMBOLS

A = surface area

α = absorptivity

β = coefficient of thermal expansion

c_p = specific heat

C_B = Bowen's Constant

°C = celsius degrees

Δ = boundary layer thickness

E = evaporation per unit time

e_a = saturation water vapor pressure at air temperature

e_w = water vapor pressure at water temperature

e_{ai} = water vapor pressure at air temperature

ε = emissivity of surface

F_c = convective heat transfer during evaporation

g = acceleration of gravity

Gr = Grashoff number

h = convective heat transfer coefficient

h_o = overall heat transfer coefficient

h = height of cloud base

K = thermal conductivity

K_h = eddy diffusivity of heat

K_w = eddy diffusivity of water vapor

K_r = coefficient of reflection

K_t = coefficient of transmissivity

λ = wave length of radiant energy

L = latent heat of evaporation

m = meters

m = minutes

μ = absolute viscosity

N = cloud cover in tenths

Nu = Nusselt number

Pr = Prandtl number

P = atmospheric pressure

Q_a = atmospheric radiation

Q_{ac} = atmospheric radiation under cloudy skies

Q_E = evaporation heat loss

Q_H = convective heat loss

Q_{in} = rate of heat added

Q_{iw} = net long wave heat added

Q_n = net radiation under clear skies

Q_r = net radiation under cloudy skies

Q_o = outgoing radiation

Q_R = radiative heat loss

Q_s = rate of increase of heat storage

Q_{sw} = net shortwave radiation

ρ = density

R_B = Bowen's ratio

Re = Reynolds number

s = seconds

S = shape factor

St = Stanton number

σ = Stephan Boltzman constant

T_a = air temperature

T_f = fog temperature

T_m = mean temperature

T_o = absolute temperature

T_w = water surface temperature

τ = transmissivity

u = wind speed

x = horizontal distance

y = vertical distance

ν = kinematic viscosity

w = watts

INTRODUCTION

Ice fog is caused by extremely small ice crystals (8μ to 35μ diameter) dispersed in the air. It forms whenever temperatures fall below approximately -30° C and water vapor is introduced into the air in excessive quantities.

Several studies have delved into the nature and causes of ice fog. Benson (1965) made the first comprehensive study into the makeup of the phenomenon and estimated that power plant cooling water produces over 60 percent of the total ice fog in the Fairbanks urban area. Ohtake (1970) studied the nature of the fog crystals and the mechanisms of fog formation. Suppression of ice fog was largely ignored until McFadden (unpublished work) designed and tested a small exhaust-gas dehydration unit in 1968. In 1969 Tedrow (unpublished, personal communication) designed and tested a successful exhaust dehydrator on an Army 2-1/2 ton truck. Furnace stack dehydrators have been used sporadically with mixed results, until finally McKay (personal communication) designed and tested a stack dryer for a boiler in 1971. Suppression of emissions from power plant cooling water had not been approached prior to this study.

In 1969 the Alaskan Air Command, recognizing the problems associated with ice fog at Eielson Air Force Base, asked the Arctic Health Research Center to investigate ice fog suppression on the base. It was proposed that the major contributor be considered first, and knowledge gained in this effort could then be used to formulate attacks on the remaining

sources. The purpose of this study was to test ideas for ice fog suppression on the power plant cooling pond and to report on the results.

The Eielson AFB power plant cooling pond is located on the east side of the base. Terrain to the east of the pond rises to an altitude of 500 m MSL. The pond is 168 m wide and 305 m long, and is divided into two units, 76 m wide and 305 m long, by a 15 m wide dike. Surface area is 46,360 square meters. Depth is 3 meters and very uniform.

Power plant cooling water at approximately 25° C is injected into the north pond (which has been designated the receiving pond) and drawn out of the south (intake) pond at 15° C. Flow through the pond is uniform at 0.38 m^3-sec^{-1}. Heat input to the pond averages 1.8 x 10^7 watts.

During the winter of 1969 a preliminary study was conducted to gain background information on the pond and its operation. A dewatering pump was used to divert the water from the receiving valve house to the intake side of the pond. This was found to be a feasible means of isolating the receiving side of the pond so that it could cool and form an ice cover. Short-circuiting the pond in this manner did not appear to pose any significant overheating problem, and plans were made to conduct a full scale experiment during the following winter season.

The winter of 1970-71 was one of the mildest on record. Temperatures did not drop sufficiently to permit any worthwhile experimentation, and work on the project was postponed until the winter of 1971-72. Plans were made to install a flood control pump to divert the water from point #1 (see Figure 1-1) to point #2, thus short-circuiting the normal flow pattern and isolating the receiving side of the pond completely.

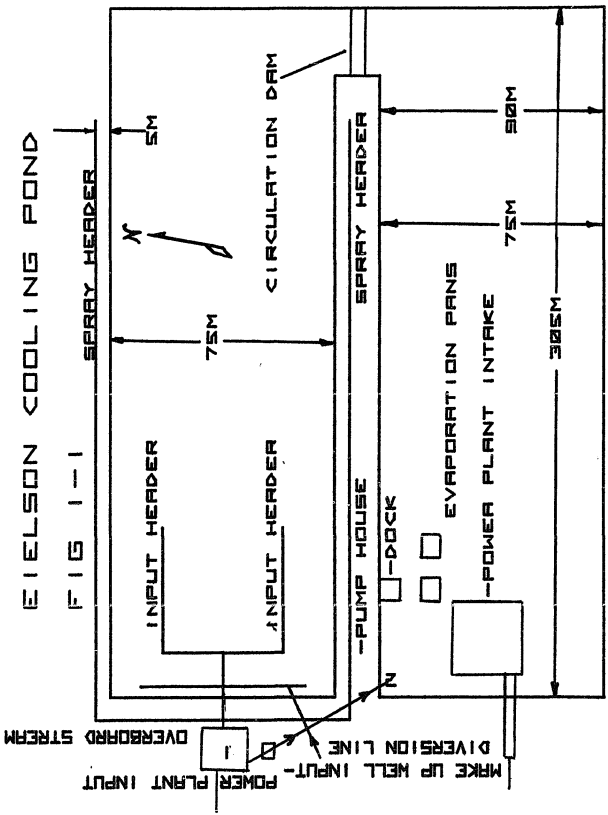

In the summer of 1972 the required installations were completed and the experiment was readied for the coming winter season. During the winter of 1972-73, the project was operated on a 24-hour a day, seven days a week basis, from early December to mid March. The entire pond was frozen over and ice fog suppression was achieved, while melting ice consumed the excess heat load of the power plant. A heat balance was determined for the pond, and radiative and evaporative heat losses were measured. Various spray and flooding techniques were investigated for their efficiency in ice building, and freezing rates were measured. Evaporation suppression was measured while using monomolecular films of hexadecanol, and also while using ice cover. Approximately 3.6×10^6 kg of ice were formed on the pond and subsequently melted by the cooling water from the power plant. Heat transfer from pond water to the ice sheet was monitored, and heat transfer coefficients were determined for comparison with calculated values. Temperature and wind velocity profiles above both open water and ice were measured to establish the film coefficients of heat transfer in these cases.

Chapter One is a short review of ice fog, its causes and effects. In Chapters Two, Three, and Four, the various components of the heat budget equation are discussed. Chapter Five reviews suppression techniques and experiments in suppression using monomolecular films. Chapter Six presents the experiments in ice fog suppression using ice cover. Chapter Seven presents recommendations and conclusions.

CHAPTER ONE - ICE FOG

Ice fog is a phenomenon peculiar to locations where temperatures drop below -30° C and water sources are available. (Water sources such as hot springs, open water on rivers or lakes, products of combustion, and even breathing, all may contribute to ice fog.) Ice fog differs from water fog in that it is composed of very small ice crystals (8μ to 35μ diameter) rather than water droplets. Ice crystals of this size are very slow to precipitate (precipitation rates of 5×10^{-4} to 5×10^{-6} gms H_2O m^{-2}-sec^{-1} are reported by Benson [1965]), and thus they remain in the air for long periods of time. The size of the particles is a function of the cooling rate of the water droplets from which they are formed.

The major contributors to ice fog in the Fairbanks area have been identified by Benson (1965) as: open water from power plant cooling requirements, combustion by-products from power plants and homes, and exhaust emissions from automobiles. Of these, he estimates that open water from the power plant cooling ponds of Fort Wainwright, and open water on the Chena River created by the Municipal Utilities System cooling water discharge are responsible for over half of the ice fog in the Fairbanks area. Eielson Air Force Base, located 22 road-miles southeast of Fairbanks, is analogous to the Fairbanks/Ft. Wainwright area, but of somewhat smaller scale. It differs in a few major respects, however, and these should be discussed.

The power plant stacks at Eielson Air Force Base are 37 m high and they discharge their gases at a relatively high velocity. This generally has the effect of putting these gases above the critical level so they do not merge with the ice fog blanket on the ground within the confines of the Air Force Base. They are not normally a major contributor to ice fog on the base (Robinson, 1963). Only under certain conditions of prolonged ice fog, when the temperature inversion layer has thickened, will gases from the power plant stacks be forced back into the ice fog blanket. This situation rarely occurs within the base boundary. However, conditions can cause the stack gases to be a major contributor to ice fog in the surrounding residential areas.

A large percentage of the heating at Eielson is done with steam from the power plant (in contrast with Fairbanks where condenser heat is largely discharged into the Chena River). This has the effect of decreasing the ice fog in the housing areas since buildings heated by power plant steam are not emitting products of combustion from individual furnaces. The cooling pond adjacent to the power plant, therefore, becomes an even larger relative contributor than in Fairbanks. It must be emphasized that producing heating steam does not load the power plant; instead, it makes practical use of energy that cannot be used for electrical generation, and which would otherwise be wasted in the cooling pond, while forming more ice fog. (If enough "waste" energy could be used for producing heating steam, the cooling pond would be unnecessary.) Under these considerations, it is apparent that the major contributor to ice fog at Eielson must be the cooling pond. (The cooling pond is probably

the least offensive of ice fog sources since it contributes only ice crystals; products of combustion, which constitute a portion of most other sources of ice fog, are not a part of the fog rising from the pond.)

On a cold morning (-30° C or colder) a cloud of ice fog rising from the pond can be seen. It tends to rise vertically since during very cold weather there is rarely a discernible wind. The only air movement is "air drainage" flow (Ohtake, 1970) which generally moves from the hills in the east, across the base toward the west. Since the cooling pond is located on the east edge of the base, it is in position to contribute to the general ice fog condition, and further, it is located so that its fog moves into the runway area.

The mechanism of formation of ice fog has been studied at length and is well documented. Ohtake gives the following description of the formation of ice fog:

> Aerial photographs showed steam or water clouds, which are important sources of ice-fog moisture, coming from the open water of the river, slough, and cooling ponds, power plants and private heating systems. Such water droplets will freeze in several seconds within a distance of 3 to 5 m from open water under low temperature conditions. ...The humidity in ice fog lies between water- and ice-saturation, allowing the ice-fog crystals to grow, but very slowly because of the small differences of saturation vapor pressure between them. This results in ice-fog crystals having the smallest size of ice crystals and being suspended in the air for a long time. The modal size of the ice crystals changes with the changes in the moisture content of the environmental air. In an area which has less moisture than ice saturation, the crystal sizes will be smaller and smaller until the crystals disappear. ... The most important factor in the formation of steam or water droplets is not the concentration of condensation nuclei in the case of formation of steam from open water, heating plants and car exhausts under ice-fog conditions but rather the temperature differences between water (not ice) and ambient air temperature. (Ohtake, 1970, p 132-133)

As an example, on January 12, 1973, air temperature was -34° C. Light ice fog was evident along the streets of the base, but visibility was generally several miles. The air was drifting from the north-northeast. The fog cloud around the pond was visible for several miles as it rose from the pond and drifted in an ever-widening band across the southern portions of the base. The band was estimated to average 800 meters in width and was approximately 20 meters deep, as observed from outside the cloud. Upon entering the cloud of fog, visibility dropped to less than 50 meters, the sky was obscured, and the sun was not visible. These limitations in visibility cause severe restrictions in aircraft operations and make automobile driving hazardous. During this period, the plume from the power plant stacks was observed to rise, then bend over, as is typical during strong temperature inversions in the air layers near the surface. The plume eventually rejoined the cloud of fog on the ground. This junction, however, was well beyond the limits of the base and did not add to fog on base.

An efficient approach to the problem of ice fog suppression lies in suppressing ice fog at the source. Several possible ways have been proposed. They include closed circuit cooling of the condenser water and covering the cooling pond with different covers, including polyethylene, styrofoam balls, floating metal plates, and inflatable buildings. Injection wells have also been recommended as a means of disposing of the cooling water, with the new cooling water being drawn from the water table. Several of these ideas have merit and should be explored in depth. This paper, however, is limited to an exploration of some techniques of suppressing ice fog from cooling ponds.

CHAPTER TWO - EVAPORATION

Evaporation accounts for a major portion (on the order of 25%) of the heat dissipated from an open water surface during winter months. It is also recognized as a large contributor to the ice fog in the Fairbanks area. Elimination of this source of ice fog by evaporation suppression deprives the pond of one of the means of dissipating waste heat; so that for the pond to remain effective, alternate means of transferring this heat to the atmosphere or to outer space must be provided. Therefore, a knowledge of the "order of magnitude" of this heat loss is essential to ice fog suppression, so that adequate alternate heat transfer modes may be incorporated in the system.

Evaporation is a function of many interacting variables. Water temperature and surface conditions influence the vapor flux leaving the surface; while wind, air temperature, and relative humidity influence the flux of vapor returning to the water. The interaction of these variables has made mathematical predictions of evaporation difficult.

Most observers have noted that wind is an important parameter. In fact, some equations have been proposed whose form is such that if wind goes to zero, evaporation ceases. This, of course, is impossible since even in stagnant air, diffusion accounts for a net flux of vapor away from the surface.

A still greater effect is induced air movement. During ice fog conditions a unique situation develops. The air near the ground

(below 50 meters) is nearly quiescent, so that conventional wind measurements show zero velocity (that is, air movements are below the measurement threshold of conventional instruments). The air over the warm open water surface of a cooling pond is far from still, however. The temperature differences between air and water can be greater than 50° C. It is visually evident that the air near the water surface is warmed and rises convectively, since vertical air currents can be observed over the pond.[1] Therefore, although meteorological measurements in the vicinity of a cooling pond may show zero wind, convective currents are usually present and they greatly influence evaporation.

Although the extremely cold air can hold very little moisture, the continued flow of new air into the pond area to replace the air that rises vertically in the convection plume provides a mass transfer mechanism that can carry off large amounts of vapor. In addition to this, as Yen and Landvatter (1970) have found, considerable supersaturation of vapor in cold air can exist above a warm water source. It is not surprising, therefore, to find high winter evaporation rates.

It might also be expected that equations developed for warmer, windier climates may underpredict the evaporation during times when meteorological measurements indicate wind to be absent.

---

[1] The situation may be analogous to the generation of thunderstorms in the summer, where moisture-laden air, heated by a warm surface, rises to elevations of 40,000 feet and higher. Currents and turbulence within these columns of rising air have been known to destroy aircraft caught in their interior.

Bowen's Equation

To begin a discussion of the various attempts to describe evaporation in mathematical terms, it is necessary to become acquainted with Bowen's ratio, which is used in the derivation of virtually all modern evaporation equations.

Bowen (1926) concluded that "the process of evaporation and diffusion of water vapor from any water surface into the body of air above it is exactly similar to that of the conduction or 'diffusion' of specific heat energy from the water surface into the same body of air." He proposed a ratio, R_B, which has become known as Bowen's ratio.

R_B is defined as the ratio of convective Q_H to evaporative Q_E heat loss. It is assumed in Bowen's derivation that the eddy diffusivities of water vapor (K_w) and heat (K_h) are equal in air (a result derivable from kinetic theory). Several investigators have reported satisfactory results using Bowen's ratio under stable and neutral conditions (Pasquill, 1949; Dingman, Weeks, and Yen, 1967; Anderson, 1964; Veimeyer, 1964). Pasquill (1949), on the other hand, has reported that under unstable conditions, i.e. when the water temperature is greater than the overlying air temperature ($T_w > T_a$), K_h can be as much as three times as large as K_w. However, Brutsaert (1965) cites two reports that concern themselves with the subject; one found $K_h = K_w$ regardless of stability conditions, and the other confirmed that they were equal to each other except under highly stable conditions.

Working under winter conditions, Rimsha and Donchenko (1957) have successfully used Bowen's equation (with $K_h = K_w$) to calculate heat losses from open stretches of rivers. In view of these studies it seems

reasonable to assume (as did Rimsha and Donchenko) that Bowen's ratio can be used with $K_h = K_w$ for the conditions of this study. Bowen's ratio (R_B) is:

$$R_B = \frac{Q_H}{Q_E} = C_B \frac{P}{1x10^5} \frac{(T_w - T_a)}{(e_w - e_a)} \qquad 2\text{-}1$$

where:

P = atmospheric pressure $(N)(m^{-2})$

T_w = temperature of the water (°C)

T_a = temperature of the air (°C)

e_w = saturated vapor pressure at the temperature of the water $(N)(m^{-2})$ (Fig. 2-1)

e_a = vapor pressure at the temperature of the air $(N)(m^{-2})$ (Fig. 2-1)

Q_H = convective heat loss $(W)(m^{-2})$

Q_E = evaporative heat loss $(W)(m^{-2})$

C_B = Bowen's Constant $(°C^{-1})$

Bowen evaluated C_B for three wind conditions. Case I represents a condition where, in Bowen's words, "the whole quantity of air under consideration is completely changed in temperature and moisture content to that of the layer of air in contact with the water." In this case, diffusion is not the limiting factor and, therefore, K_h and K_w do not enter into the equation. For Case I, C_B is found empirically to be:

$$C_B = 0.501\ °C^{-1}$$

Case II represents the situation where diffusion dominates completely. Heat and water vapor are immediately carried away after diffusing through a stationary layer in contact with the water. For this case $C_B = f\left(\frac{K_h}{K_w}\right)$, and was empirically determined to be:

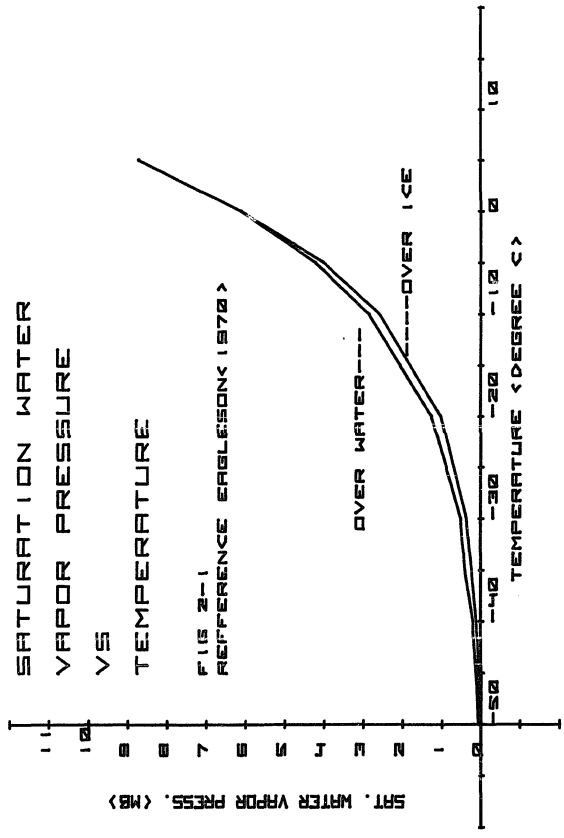

$$C_B = 0.442\ ^\circ C^{-1}$$

The final case is for the conditions where wind (u) is a function of the height above the water ($u = f(y) \simeq Ky^n$). This is the condition Bowen considers the "average wind condition"; and for this case, his analysis shows that

$$C_B = 0.46\ ^\circ C^{-1}$$

He concluded that the best value for Bowen's ratio utilized $C_B = 0.46$. Using this value, Bowen's ratio (R_B) becomes:

$$R_B = (6.1 \times 10^{-4})(P)\frac{(T_w - T_a)}{(e_w - e_a)} \qquad 2\text{-}2$$

Bowen states that this equation is valid for the situation where T_w is low enough that the volume of air is not changed significantly by the water vapor evaporated into it, and where condensed evaporated water does not precipitate back into the pond. These two restrictions are both violated to some degree at a cooling pond during ice fog conditions. This may reflect on the accuracy with which equations based on Bowen's ratio can describe the actual evaporation at these times.

Evaporation Equation

Traditionally, there have been two basic approaches to develop the theory for predicting evaporation: the "aerodynamic" method and the energy-budget method.

The "Aerodynamic" Method Approach: Most empirically derived equations of the aerodynamic method have the same basic form as Dalton's Law (Dalton, 1802):

$$E = (f(u))(e_w - e_{ai}) \qquad 2\text{-}3$$

where:

E = the evaporation in a unit of time and area

e_{ai} = the water vapor pressure in the air at the 2-meter level

e_w = the saturation vapor pressure at the temperature of water surface

$f(u)$ = a function of the wind speed

The form of the wind function is usually taken such that:

$$f(u) = (a + bu)$$

where "a" and "b" are empirically derived constants and u = average wind speed 2 meters above the surface.

At ice fog temperatures e_{ai} can be replaced by the saturated vapor pressure (e_a) without significant error,[1] and therefore, equation 2-3 can be rewritten:

$$E = (a + bu)(e_w - e_a) \qquad 2\text{-}4$$

where e_a = saturated vapor pressure at the temperature of the air. The constants "a" and "b" must be evaluated experimentally.

---

[1] It must be remembered that this approximation will only be usable at temperatures well below 0° C. For water temperatures of +10° C, the maximum error introduced by this approximation is:

T_a	e_w	e_a	$e_w - e_a$	$e_w - e_{ai}$	% Error
-20	12.3	1.25	11.05	12.3	10
-30	12.3	0.51	11.79	12.3	4
-40	12.3	0.19	12.11	12.3	1.5

Error this large will be produced if the air entering the pond area is completely dry ($e_{ai} = 0$), and air leaving the pond is saturated (R.H. = 100%). If the air entering is close to saturation, the error approaches zero.

Dingman, Weeks, and Yen (1967) propose a form of Dalton's equation which they attribute to Kohler's work that is "a simple, well-accepted formula for calculating daily evaporation rates":

$$E = (0.525 \times 10^{-2} + 1.0007 \times 10^{-2}\ u)(e_w - e_a) \qquad 2\text{-}5$$

where u = windspeed in m/sec and e_w and e_a are in mb.

Multiplying by the latent heat of vaporization, Equation 2-5 becomes an expression of evaporation heat loss, Q_E:

$$Q_E = (1.518 + 2.911\ u)(e_w - e_a) \qquad 2\text{-}6$$

where:

Q_E = evaporation heat loss (watts)(m^{-2})

u = wind velocity (m)(sec^{-1})

e_w = saturation vapor pressure at water temperature (mb)

e_a = saturation vapor pressure at air temperature (mb)

Using Dalton's equation and evaluating the constants "a" and "b", Behlke and McDougall (1973) found that values of a = 13.82 and b = 0 gave the optimum correlation to their measured data. Their results in the form of evaporation heat loss rate were:

$$Q_E = 13.82\ (e_w - e_a) \qquad 2\text{-}7$$

where:

Q_E is in (watts)(m^{-2})

e_w is in mb

e_a is in mb

Their study is of particular interest since it was conducted in interior Alaska during one of the same winters that the cooling pond studies (of this paper) at Eielson AFB were in progress. The two

investigations, however, differed markedly. The Behlke-McDougall experiments were conducted on the roof of a four-story building located on a hill above the valley floor, and were influenced by the surrounding buildings and the local "heat island" of the university complex. The evaporation studies at Eielson were, in contrast, isolated from all other structures by at least 1000 feet. The site is on the valley floor and, additionally, the evaporation pans were subject to the microclimate of the open water of the pond. Nevertheless, it is interesting to note that in spite of these differences, neither study showed appreciable wind effect (see page 36). The conclusion follows that during ice fog conditions in interior Alaska the wind is not a significant factor in evaporation. This is because wind is absent during these times. If wind were present, it would not only cause even greater evaporation but would also disperse the ice fog, alleviating this problem.

Another study using the "Dalton equation" approach was reported by two Russian scientists investigating ice formation. Rimsha and Donchenko (1957) concluded (after comparisons of actual heat loss) that for winter conditions on rivers and reservoirs throughout Russia, the convective heat loss rate (Q_H) could be expressed by:

$$Q_H = (F_c + 1.89\ u)(T_w - T_a) \qquad \text{(watts)}(m^{-2}) \qquad 2\text{-}8$$

where:

u = the windspeed in (m)(sec^{-1}) at 2 m above the surface

F_c = the portion of heat transferred by free convection

F_c was determined empirically by them to be:

$$F_c = 3.87 + 0.17\ (T_w - T_a) \qquad 2\text{-}9$$

Applying the Bowen ratio (assuming pressure = 1000 mb), the rate of evaporative heat loss, Q_E, is determined to be:

$$Q_E = (0.755\ F_c + 2.94\ u)(e_w - e_a) \qquad 2\text{-}10$$

Combining Equations 2-9 and 2-10 gives:

$$Q_E = (6.04 + 0.264\ (T_w - T_a) + 2.94\ u)(e_w - e_a) \qquad 2\text{-}11$$

This is Rimsha and Donchenko's "Russian Winter Equation". The advantage of this equation to the needs of this investigation lies in the term F_c. During ice fog conditions when wind is absent, Equation 2-10 reduces to:

$$Q_E = (0.755\ F_c)(e_w - e_a) \qquad 2\text{-}12$$

Evaporation is thus expressed as a function of convective conditions represented by F_c. Since F_c was determined for winter conditions in Russia, the applicability of F_c in the revised Rimsha and Donchenko equation (2-12) may represent conditions at the Eielson Pond more closely (in concept at least) than any of the other equations discussed. Their studies were addressed to open water on rivers and reservoirs; however (and this may be a significant difference), ice-free areas on rivers and reservoirs expose water that may be warmer than the surrounding air, but many degrees colder than the water surface of a cooling pond (T_{avg} = 12.6° C for the Eielson pond). In addition, the Russian studies were conducted at sites throughout Russia, many of which (e.g., Chu River, Angara River) are too far south to be considered arctic conditions. Thus the equation might be expected to yield somewhat different values than the Eielson studies.

The Energy Budget Approach: The energy budget approach to evaporation measurements is merely an application of the concept of conservation of energy. Williams (1963) states, "The fundamental basis of the energy

budget approach is unchallenged; the challenge is to our ability to measure or estimate all the quantities needed to exploit the principles of the conservation of energy."

In mathematical terms the method, when applied to a cooling pond, can be stated:

Rate of heat added - rate of heat lost = rate of change of heat stored

$$Q_{in} + Q_{sw} + Q_{other} - Q_{lw} - Q_E - Q_c = Q_s \qquad 2\text{-}13$$

where:

Q_{in} = rate of cooling water heat energy input to the pond

Q_{sw} = net shortwave radiation rate incoming from the sun (direct and diffuse)

Q_{other} = all other energy input rates not considered in the first two terms (i.e., seepage, ground water make up, precipitation, outflows, etc.)

Q_{lw} = net long wave radiant heat loss rate

Q_E = evaporation heat loss rate (convected and conducted from the systems)

Q_H = convective heat loss rate

Q_s = rate of increase of heat energy stored in the body

It is immediately obvious that this method is dependent on the accuracy of a number of components, some of which are difficult if not impossible to evaluate (e.g., seepage of warm springs into the bottom of the pond). In addition, because of the problems in accurately assessing the change in the heat storage term Q_s, this method is difficult to apply accurately (especially for short periods of time). This is particularly true for small bodies of water such as cooling ponds, since the heat storage can and does change rapidly, due to fluctuations of both pond level and heat input from the incoming cooling water.

However, this method has been used with apparent success in studies at Lake Hefner for time periods of seven days or greater (Kohler, Nordenson, and Fox, 1955). The method would probably also be adequate when applied to cooling ponds if time periods were long enough to average out short term storage changes.

In an effort to derive a relationship that is based upon a limited number of reasonably easy to obtain meteorological values, Penman (1947) combined the energy balance approach with the "aerodynamic" approach of Dalton. The derivation is lengthy and the reader is referred to Penman's paper listed in the bibliography. The Penman equation is usually written:

$$Q_E = \frac{0.48}{\Delta+\gamma} (Q_r \Delta + \gamma E_a L) \qquad 2\text{-}14$$

where:

Q_E = evaporative heat loss rate (watts)(m^{-2})

Δ = slope of the curve of saturation vapor pressure (mb) vs temperature (°C); $(\frac{d(e)}{dT})$ at air temperature T_a

E_a = the evaporation given by an equation of the form of Equation 2-4 (watts)(m^{-2})

Q_r = net radiant energy, expressed in the units of $E_a L$

$$\gamma = R_B \frac{(e_w - e_a)}{(T_w - T_a)} = C_B P \text{ (mb)}(°C^{-1}) \qquad 2\text{-}15$$

$$L = R_B \frac{(e_w - e_a)}{(T_w - T_a)} = C_B P \text{ (mb)}(°C^{-1})(\text{cal})(\text{gm}^{-1})$$

An advantage Penman claims for this approach is that "it eliminates the need for water surface temperature, the parameter most difficult to measure." However, the method is based on the assumption that heat storage of the system does not change. Therefore, it must be applied over longer periods of time in order to "average out" the effects of storage fluctuations.

The term γ is a function of the eddy diffusivity ratio K_h/K_w discussed earlier; and if this ratio departs from the assumed value of 1, adjustments of γ must be made to compensate. Another disadvantage to the method is that it relies on the standard Dalton relationship for the wind function, and values for "a" and "b" in Equation 2-4 must be evaluated. It does not consider, in its present state, the special case of convective instability.

Evaporation Measurements During Ice Fog Conditions

Very few actual experiments have been conducted which measured evaporation under actual ice fog conditions. Ohtake (1970) measured the evaporation of water from two shallow pans (13.4 and 30.5 cm in diameter and approximately 1 cm deep). The pans were exposed to the atmosphere and kept from freezing with an infrared lamp. Water temperature in the pans was measured with thermometers, and was maintained above freezing by adjusting the distance from the lamp to the pan. Measurements were made at air temperatures ranging from -18° to -40° C. Water temperature was "...kept around 4° to 10° C with an occasional maximum of 15° C..." (Ohtake, 1970). A total of ten measurements yielded an average evaporation of 5000 $(g)(m^{-2})(day^{-1})$. The rather large variations of water temperatures, coupled with the short time increments, gave rather wide scatter in evaporation measurements, which ranged from 2380 to 8530 $(g)(m^{-2})(day^{-1})$. In contrast to the small scale of Ohtake's experiment, a cooling pond is large enough to create its own microclimate, and enough heat may be dissipated from the large open water surface of the pond to create substantial convective currents. This is not nearly as well

developed in the case of small pans on land, and the difference suggests that the values may not be completely representative of conditions in the larger system. Anderson (1952) and Kohler (1955) discuss this point at length.

Yen and Landvatter (1970) measured the evaporation from stretched blotter paper with below-freezing air flowing over it. Their measurements covered a water temperature range from 0.8° C to 30.4° C, and air velocities from 0.10 to 1.60 (m)(sec^{-1}). Their apparatus allowed the variables involved in evaporation to be controlled in much better fashion than is available in field experiments. A total of 64 runs was reported. Evaporation ranged from 1296 to 7058 (g)(m^{-2})(day^{-1}) for water temperatures of 1.7° C to 6.7° C and below freezing air, and 5642 to 24,019 (g)(m^{-2})(day^{-1}) for water temperatures between 24.9° and 30.3° C and above freezing air temperatures. Unfortunately, no measurements were made for water temperatures between 8.3° and 24.9° C, the range in which the Eielson cooling pond water surface temperatures fell most of the time. The emphasis in these experiments on forced convection suggests that they may not be closely representative of the conditions on the cooling pond where air movement is predominately free convection. The scale in this case, also, is different. Nevertheless, these measurements represent evaporation under conditions which are more nearly similar to those predominating at the cooling pond than for most of the evaporation measurements reported in the literature, and agree, in order of magnitude at least, to those which were taken at the Eielson cooling pond. Table 2-2, page 30, points this out. If only those runs with below freezing air are considered, the average values of Ohtake, and Yen and Landvatter are

within 28% of each other, with Yen and Landvatter showing the lower average. On the other hand, if the higher water temperature and above freezing air values of Yen and Landvatter's study are included, then their average value is greater than Ohtake's by 27%. This suggests that good agreement of the values of evaporation might have been obtained if both studies had covered the same temperature range.

Evaporation Measurements at Eielson Power Plant Cooling Pond

Two standard Colorado floating pans were placed in the pond (Figure 2-2). The pans were read concurrently in the same location and the values were compared (Table 2-1). The average difference between all values for the two pans increased as spring approached. In January an average difference of 2.1 percent was recorded for measurements covering a period of 118 hours, but in March the difference between the pans had increased to 17.6 percent over a period of 166 hours. This is probably a function of a number of variables. Air movement across the pond, increased solar radiation as spring approached, and warm currents in the pond could all have contributed to the difference. As solar radiation increased, the degree to which the pans were in the sun would influence their evaporation. If the shadow from the pump house on the pond (Figure 1-1) selectively shaded one pan and not the other, a differential evaporation would result. Another possibility is that of warm currents in that area of the pond (from the nearby warm water diversion inlet); should one pan be selectively warmed by such a current, it would experience higher evaporation. Finally, when the pans were in close proximity to each other, air movement from either east or west could affect the

Figure 2-2. Colorado Evaporation Pans.

Table 2-1

Evaporation Data
Standard Colorado Floating Pans

Date	Pan No.	Duration (hrs)	Air temp. °C	Water temp. °C	Avg wind velocity m/s	Evaporation $\frac{gms}{m^2\ day}$
1/2/73	2	95.0	-16.0	8.4	0	3720
1/5/73	2	72.5	-16.0	11.1	0	3812
1/11/73	1	23.5	-11.0[1]	10.8	0	3633
	2	25.0	-11.0[1]	10.9	0	4079
1/12/73	1	25.1	-31.0	9.5	0	3996
	2	24.8	-31.0	9.0	0	3972
1/13/73	2	24.2	-38.5	10.2	0	6853
1/14/73	1	25.2	-38.0	9.0	0	5485
	2	24.2	-38.0	9.3	0	5622
1/15/73	1	23.5	-40.0	8.4	0	5728
	2	23.8	-40.0	8.6	0	5476
1/18/73	1	69.8	-33.0	9.5	0	5247
	2	70.0	-33.0	9.3	0	5013
1/20/73	1	46.8	-36.0	7.5	0	6738
	2	48.2	-36.0	8.8	0	6603
1/21/73	1	28.5	-39.0	8.2	0	4854
1/23/73	1	46.8	-38.0	8.2	0-0.50	7656
	2	49.5	-38.0	8.5	0-0.50	3980
2/6/73	1	25.0	-18.0	10.0	0.20	3364
	2	24.5	-18.0	10.0	0.20	3731
2/7/73	1	24.0	-18.0	12.2	0.05	4676
	2	24.5	-18.0	12.0	0.05	5617
2/8/73	1	23.8	-17.0	13.4	0.15	7700
	2	24.0	-17.0	13.4	0.15	4676

[1] These temperatures are from Air Force measurements at Eielson, approximately 2 miles from the site.

Table 2-1 (continued)

Date	Pan No.	Duration (hrs)	Air temp. °C	Water temp. °C	Avg wind velocity m/s	Evaporation $\frac{gms}{m^2\ day}$
2/9/73	1	23.6	-20.0	13.5	0	2821
	2	23.5	-20.0	13.5	0	7488
2/10/73	1	26.9	-15.0	12.5	0	8301
	2	26.2	-15.0	12.5	0	5894
2/11/73	1	25.2	-19.0	11.0	0.90	4440
	2	25.2	-19.0	11.0	0.90	7508
2/12/73	1	24.0	-21.0	10.5	3.00	5495
2/13/73	2	22.8	-26.0	11.5	1.50	5823
2/15/73	1	49.5	-22.0	13.5	0.12	6253
	2	49.5	-22.0	14.0	0.12	6184
2/21/73	1	24.0	-5.0	15.6	1.40	6105
	2	23.8	-5.0	15.7	1.40	4834
2/22/73	1	24.8	-4.0	14.9	0.10	5393
	2	24.8	-4.0	15.0	0.10	5996
2/23/73	1	23.5	-4.5	13.8	0	4183
	2	23.8	-4.5	14.0	0	4990
2/24/73	1	23.0	-12.0	13.6	0.62	5141
	2	22.8	-12.0	13.6	0.62	3835
2/26/73	1	48.7	-24.0	11.0	0.50	4669
	2	49.0	-24.0	11.1	0.70	4604
2/27/73	1	22.8	-16.0	5.4	0.70	5835
	2	22.4	-16.0	5.3	0.70	5971
3/7/73	2	23.2	-11.0	7.0	0.35	1931
3/8/73	1	24.0	-10.0	9.7	0.20	3839
	2	24.5	-10.0	10.0	0.20	3732
3/9/73	1	26.0	-9.5	12.4	0.30	1965
	2	25.6	-9.5	12.6	0.30	2603
3/10/73	1	22.3	-13.0	12.6	1.60	4270
	2	22.8	-13.0	12.9	1.00	4725

Table 2-1 (continued)

Date	Pan No.	Duration (hrs)	Air temp. °C	Water temp. °C	Avg wind velocity m/s	Evaporation $\frac{gms}{m^2\ day}$
3/11/73	1	24.20	-9.5	13.3	0.15	5420
	2	23.75	-9.5	13.4	0.15	4363
3/12/73	1	22.20	-15.0	13.6	1.15	5740
	2	22.60	-15.0	13.9	1.15	6672
3/14/73	1	50.00	-12.0	14.3	0.70	6045
	2	49.50	-12.0	14.4	0.70	5856
Small Pan Data:						
1/27/72	S-1	6	+18	10.2	1.50	2850
	S-2	6	+18	10.2	1.50	3270
1/28/72	S-1	4	+16	10.2	0	2440
	S-2	4	+16	10.2	0	2820
2/1/72	S-1	5	+14	0.5	1.50	1122
	S-2	5	+14	0.5	1.50	1230
3/1/72	S-1	4	-23	3.0	0	2119
	S-2	4	-23	3.0	0	2650
	S-3	4	-23	3.0	0	2119
3/2/72	S-1	6	-26	2.0	0	3470
	S-2	6	-26	2.0	0	3060
3/3/72	S-1	3	-24	2.0	0	1410
	S-2	3	-24	2.0	0	3760
	S-3	3	-24	2.0	0	3290
	S-4	3	-24	2.0	0	3530
3/7/72	S-1	4	-20	5.0	0.75	7900
	S-2	4	-20	4.0	0.75	4690
	S-3	4	-20	4.0	0.75	3670
	S-4	4	-20	2.0	0.75	5770
3/8/72	S-1	4	-14	4.5	3.00	3840
	S-2	4	-14	3.0	3.00	3770

Table 2-1 (continued)

Date	Pan No.	Duration (hrs)	Air temp. °C	Water temp. °C	Avg wind velocity m/s	Evaporation $\frac{gms}{m^2\ day}$
3/10/72	S-1	5	-20	5.5	0	4000
	S-2	5	-20	5.0	0	3300
	S-3	5	-20	4.5	0	1890
3/14/72	S-1	5	-18	6.5	0	4070
	S-2	5	-18	6.0	0	4240
	S-3	5	-18	5.5	0	3110
	S-4	5	-18	5.5	0	4240

first pan it encountered; at the same time, this pan would provide a shelter for the second pan. As weather warmed from January to March, both the magnitude and frequency of wind increased over the pond (Table 2-1), which may help explain the increase in the difference between the pans as spring approached. The overall difference between the pans of less than 9 percent, however, is within reasonable expectations for evaporation field measurements even under temperate conditions (see data spread for laboratory measurements of Yen and Landvatter, Table 2-2). The total spread in evaporation measurements at Eielson was less than reported by either Yen and Landvatter, or Ohtake, in their measurements (see Table 2-2).

The rate of evaporation from the pans was determined by measuring the volume of water evaporated each day. This was done by raising the pan partially out of the water with a lift, and leveling it. Water was then added to the level of a point gage installed in the pan. The added volume of water was measured with a graduated cylinder to the nearest 10 milliliters. Precision of the point gage in the pans was determined experimentally in the laboratory and found to have a standard deviation of 38 milliliters over 40 measurements. Evaporation volumes for each day were in the order of several thousand milliliters in each pan, so that measurement errors were less than one percent.

To obtain data on evaporation from cooler surface areas of the pond, three 33-cm diameter pans were used to measure evaporation at different locations on the pond (Figure 2-3). These smaller, more mobile pans were compared with each other and with the larger Colorado pans. Measurements were taken in the same manner as the Colorado pans, except that the

Table 2-2

Evaporation Rates During Ice Fog Temperatures

	Average Evaporation $gm(m^{-2})(day^{-1})$	mm/day	Water temperature range	Number of measurements	Data spread
Ohtake (1970)	5040	5.0	4°-15°	10	0.9-5.9
Behlke and McDougall (1973)	4464	4.5	2.7°-11.9°	10	2.6-4.3
Yen and Landvatter (1970)[1]	6912	6.9	0.8°-30.3°	64	0.9-16.7
Yen and Landvatter (1970)[2]	3600	3.6	0.8°-7.9°	37	0.9-4.9
Eielson Cooling Pond Studies[3]	5040	5.0	0.0°-16.0°	79	1.3-5.8
Russian Winter Equation[4]	5393	5.4	+10°	--	---
Revised Russian Equation[4]	4314	4.3	+10°	--	---
Eielson Form, Dalton Equation[4]	5045	5.0	+10°	--	---
Kohler Equation[4]	585	0.5	+10°	--	---
Modified Penman Equation[4]	3456	3.4	calculated for 12°	--	---
Thompson (1970)[5]	2736	2.7	calculated	--	---

[1] Laboratory measurements, all values included.
[2] Only values for air temperatures below freezing included.
[3] Values for the Eielson cooling pond were the average values for all conditions during the testing throughout the winter.
[4] Values were calculated for -20° C air temperature and +10° C water temperature.
[5] Using Thornwaite and Holzman's equation (reported by Ohtake, 1970).

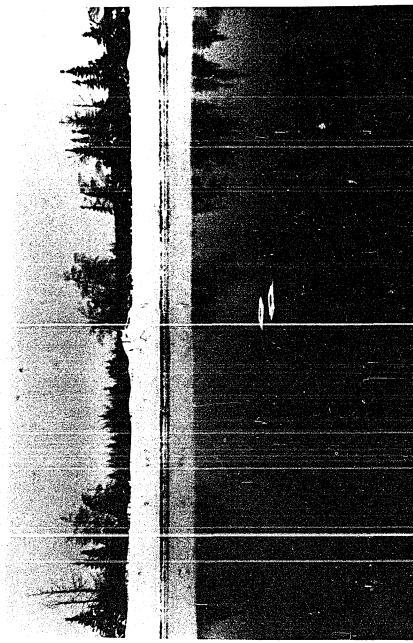

Figure 2-3. Small Evaporation Pans.

period of measurement was much shorter since the pans were in colder water and would freeze when left out overnight. It was not convenient to stabilize the smaller pans before measurement; therefore, the accuracy of these data points is subject to more influence from outside factors (such as waves which rocked the pan slightly, causing reflections that made measurement difficult).

A total of 57 measurements was made with the Colorado pans, covering a time span of 495 hours of evaporation. The smaller pans were used over short time spans, usually not exceeding 6 hours. Since the temperature of the water in the small pans often approached 0° C, ice sometimes formed over a portion of the surface. This was stirred away at the hourly checks. Average temperature in these pans was 3.8° C, while the large Colorado pans averaged 11° C.

Traditionally, a "pan constant" for the evaporation pans has been used to account for the difference in temperature between the water in a lake or river and that in the pan. Kohler (1954) states, "The practice of applying a coefficient to pan evaporation to estimate that occurring from an adjacent lake is of long standing, even though the reliability of this approach has always been subject to question." Since the water temperature in the pans under measurement conditions encountered during most studies was warmer than that of the adjoining lake, a pan coefficient of less than 1 is applied (values of 0.86 to 0.95 are usually used for floating Colorado pans) (Kohler, 1954; Anderson, 1952). In the measurements made at Eielson, however, the pan water temperature was colder than that of the surrounding pond in all cases (averaging 2.47° C lower).

This would indicate the use of a pan constant greater than 1. However, since the temperature over the surface of the pond graded from 0° at the edge of the ice cover, to as high as 16° C near the inlet, the pans can be assumed to indicate evaporation from those areas of the pond where the surface temperature is the same as that of the pans. Since the average pan temperature is slightly higher than the average temperature of the open water surface of the pond, a pan constant of less than 1 might be indicated.

Another factor should be considered. The surface of the water in the pond lies approximately 2 meters below the dikes that make up the sides. As air moves across the pond, the dikes produce a sheltered area on the lee side (a distance of approximately 10 meters). This area is affected very little by the wind, and is visible as still water next to rough water, even during light breezes. Although there weren't even light breezes during ice fog events, a sizable portion of the evaporation data was taken during warmer weather. The remaining part of the pond (70 meters) received the effect of the wind. The evaporation pans have a similar configuration with respect to the wind in that their sides, which float approximately 10 centimeters above the pond surface, shelter the surface of the water within, in much the same manner as the dikes shelter the pond. The pans, however, have a somewhat different geometrical aspect when compared with the pond and, therefore, the effect of the wind on evaporation from the pans is different and most likely a bit less than that on the pond itself. This would indicate the use of a pan constant slightly greater than 1, at least for windy periods.

Since horizontal air movement during ice fog events is so slight, the "shadow effect" of the dike was probably minimal during these times. It seems reasonable to select a pan constant of 1.0, for the evaporation from the pans must have fairly well matched that from the pond. The effects of the "wind shadow" and slightly elevated pan temperatures tend to compensate for each other.

Data Analysis

Because of the many diverse factors affecting evaporation it is difficult to obtain a precise mathematical description of the process in terms that will allow the prediction of evaporation under specific conditions. (For that matter, it is quite impossible to predict with any great confidence what environmental conditions will occur at any time in the future.) We must be content with approximations which give a range of values for evaporation heat loss which will include the actual value. The data spread shown in the evaporation values in Table 2-2 for the various investigators in this field bears this out. Even the well controlled laboratory studies of Yen and Landvatter (1970) show as much spread for a water temperature range of 0° to 8° C as the field studies at Eielson did for a water temperature range of 0° to 16° C. The average values of Ohtake show a still larger spread for a temperature range of 4° to 15° C.

Behlke and McDougall's values of average evaporation compare very closely to those of the Eielson experiments. The water temperature range covered by their experiments was 2.7° to 11.9° C and their average value of evaporation was within 12% of both Ohtake and the Eielson studies, and

was within 22% of Yen and Landvatter's. In spite of the spread of data, it is interesting to note that the average values from all investigations fell between 3600 and 5040 $(g)(m^{-2})(day^{-1})$. This is a maximum difference of only 33%. Considering the differences in measurement technique, environmental setting, and water temperature range, the average values given in Table 2-2 are considered to be in rather good agreement, and probably represent the actual magnitude of evaporation under unstable conditions ($T_w > T_a$) rather well.

Comparison of the measured values of evaporative heat loss to the various formulas proposed, yields some interesting results. The constants "a" and "b" in Dalton's fundamental evaporation formula have been evaluated for the Eielson data. To do this, a computer program was developed to substitute different values of "a" and "b" into Dalton's equation and, using the wind and vapor pressure data for each measurement at Eielson, to calculate the theoretical value of evaporation. This value was then compared to the actual measured evaporation. New values of "a" and "b" were then tried until the difference between the calculated and the measured evaporation was a minimum. This was done for each of the 78 data points. The result was an optimum "a" and "b" for each data point. These values were averaged to yield an equation of the Dalton form which gave optimum correlation with the Eielson data. The value for "a" was found to be 13.1. The optimum value for "b" was found to be 0.132. Referring to Table 2-1 and the discussion of wind during ice fog conditions, it would be instructive to ignore wind (which was absent during ice fog) and calculate the value of "a" under this restriction. This resulted in a value of "a" equal to 13.4. The standard errors of these

two equations are within 1% of each other, confirming that the effect of wind during ice fog is minimal. The two resulting equations are:

$$Q_E = (13.1 + 0.132\ u)(e_w - e_a) \qquad \text{(watts)}(m^{-2}) \qquad 2\text{-}16$$

and

$$Q_E = (13.4)(e_w - e_a) \qquad \text{(watts)}(m^{-2}) \qquad 2\text{-}17$$

Behlke and McDougall, who made a similar correlation for their data, arrived at optimum values of 13.82 for "a" and zero for "b". It is interesting to note how closely these two experiments agree. Figures 2-4 and 2-5 show the evaporation data plotted against the Eielson forms of Dalton's equation (Equation 2-16 and Equation 2-17).

Figures 2-6 and 2-7 show the evaporation data plotted against the Kohler equation and the Russian Winter equation. The Kohler equation underpredicts the measured evaporation, while the Russian Winter equation slightly overpredicts it. In light of the agreement between the various investigators on the measured values, the conclusion is that currently suggested formulas are not adequate for describing the evaporation under the highly unstable conditions prevailing during ice fog. This is probably due to the fact that most equations fail to address the convective activity during these conditions, and those few that do (primarily the Russian Winter equation) use empirical values obtained from the open water of rivers and lakes, which is different from the convective activity that is present over the warmer water of a cooling pond.

The Kohler and Penman equations contain a wind term to describe increased evaporation during air movement but they fail to account for the fact that, although meteorological wind measurements show zero wind during periods of ice fog, there is considerable air movement due to the

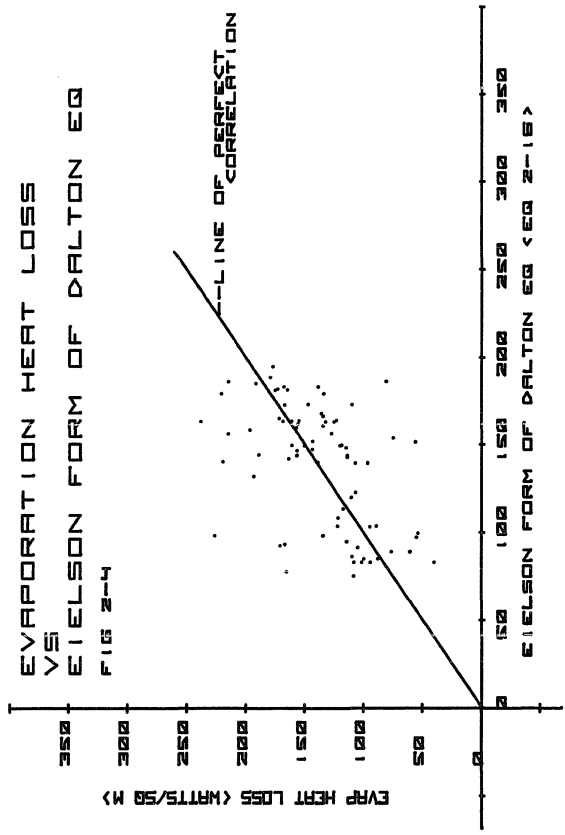

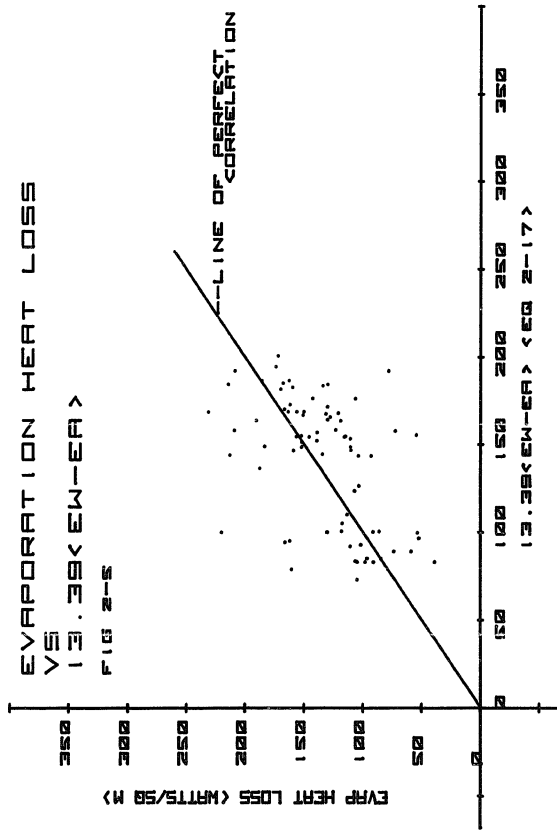

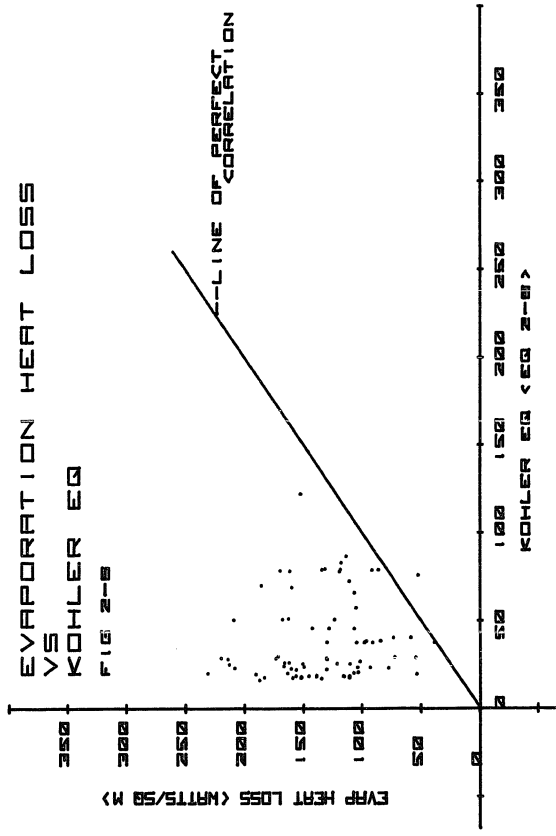

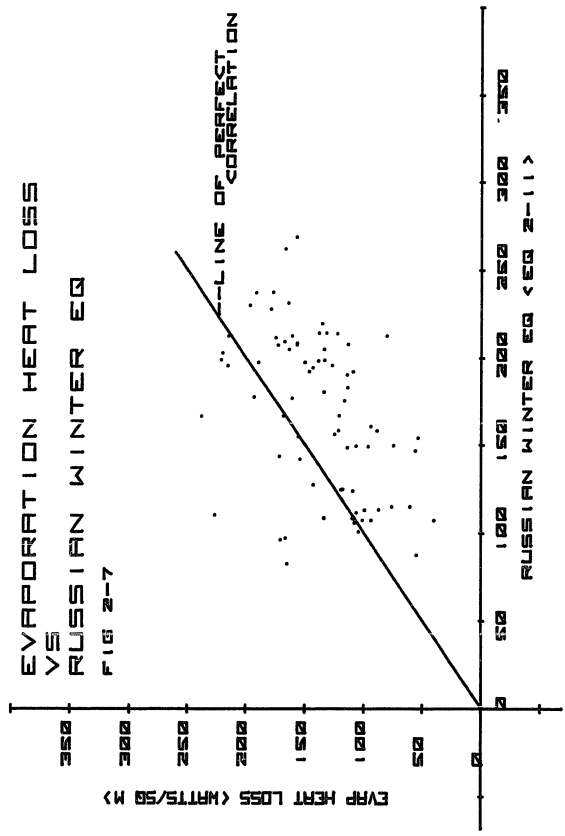

unstable convective conditions. This causes evaporation fluxes that are higher than the equation predicts. The Russian Winter equation, on the other hand, is much closer to the actual measured conditions and even overpredicts the measured values. This suggests that a revised form of the Russian Winter equation type might be formulated that will give a better correlation than either the Eielson form of Dalton's equation (equation 2-16) or the existing Russian Winter equation (2-11). Figure 2-8 shows the data plotted against an equation of the form:

$$Q_E = (4.84 + 0.21\ (T_w - T_a))\ (e_w - e_a) \qquad \text{(watts)}(m^{-2}) \qquad 2\text{-}18$$

This equation was obtained using the fitting technique discussed above, and gives the optimum fit to the data from the Eielson cooling pond. This fit considers data over the entire temperature range encountered during the studies. The temperature difference $(T_w - T_a)$ that is of interest during ice fog temperatures, however, is that of $\Delta T > 40°$ C, since the pond water temperature is relatively stable at +10° to +12° C, and air temperatures of at least -30° C are required for ice fog. This is also the area of greatest divergence between the fitted equations and the Russian Winter equation (Figure 2-9). Restricting attention to this area only and fitting an optimum curve (of the Dalton form) to the data, the following equation is obtained:

$$Q_E = 14.21\ (e_w - e_a) \qquad \text{(watts)}(m^{-2}) \qquad 2\text{-}19$$

This should represent the evaporation from a cooling pond during ice fog conditions rather well, while Equation 2-18 would give a better estimate of average evaporation for general conditions during winter months in interior Alaska.

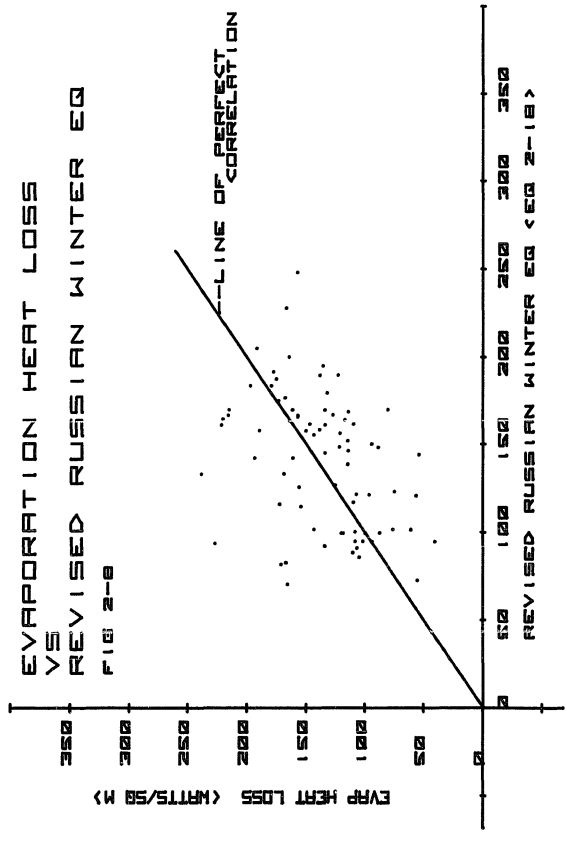

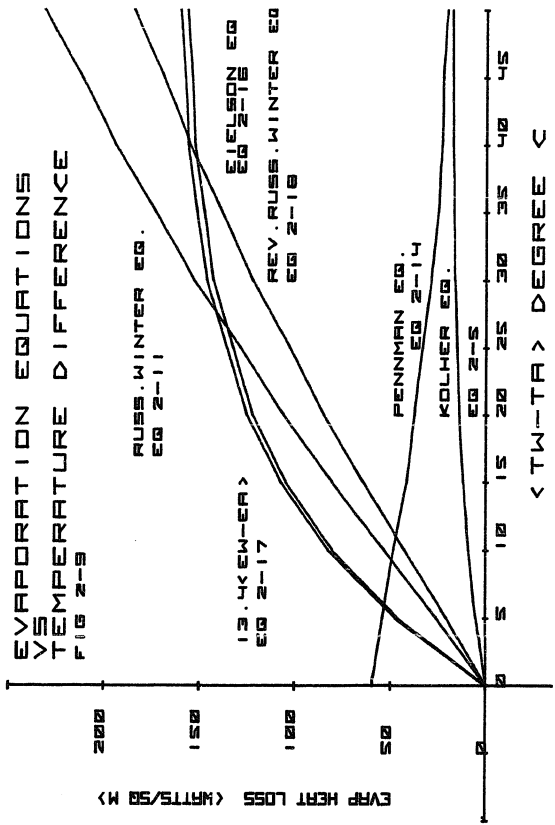

Figure 2-9 compares all of the equations discussed above with each other. It could be argued that the equation which yields the maximum values should be used for calculations of evaporative heat loss (i.e., the Russian Winter equation). This can be supported by the argument that the extreme instability supports the higher evaporative flux. However, the greatest instability occurs because the overlying air is at its coldest. Under these conditions, a greater condensation fall-back might reduce the magnitude of the net flux. This would partially explain the difference in the constants obtained for ice fog conditions (equation 2-18) as opposed to winter conditions in general (equation 2-11). Many of the measured values for evaporative flux at Eielson were above the asymptotic maximum of the Dalton form equations (equations 2-16 and 2-17); therefore, equation 2-18 is considered to be the best equation of those discussed for calculations during ice fog conditions.

CHAPTER THREE - RADIATION DURING ICE FOG

The net radiation loss during ice fog from an open water area such as a power plant cooling pond is dependent on several variables. The emission from the water surface is dependent on the temperature and emissivity of the surface. Although surface temperature is a difficult parameter to measure with high accuracy (Penman, 1948), it can be measured to within one celsius degree with reasonable care. The emissivity of a water surface has been established by several investigators, and the value of 0.97 is well agreed upon (Raphael, 1962, p 97). Calculation of the radiation leaving the surface, therefore, is a relatively easy task.

The radiation incoming to the pond can be divided into two distinct categories: short wave radiation from the sun; and long wave radiation from the atmosphere, surrounding geographic features, or man-made structures.

Short wave radiation received from the sun is a function of the zenith angle of the sun, the turbidity of the atmosphere, cloud cover, atmospheric composition, and reflectivity of the surface. Scott (1964) gives the maximum daily solar radiation arriving at the earth's surface under clear sky conditions for various latitudes in the northern hemisphere. On a clear December 22 at the latitude of Fairbanks, Alaska, a daily total of less than eight langleys[1] of short wave radiation is received at the surface. Koberg (1964) estimates the clear sky radiation

---

[1] The unit of solar radiation is the langley. It is equal to one g cal per square centimeter.

for latitudes up to 50° N. Extrapolating his computed curves yields a value of less than 10 langleys of radiation reaching the surface on December 21. Behlke and McDougall (1973) calculate a minimum clear sky solar radiation reaching the ground at the latitude of Fairbanks of 7 langleys per day. Therefore, the magnitude of short wave radiation reaching the surface during December should lie between 7 and 10 langleys.

Clouds and ice fog will reduce this value even further. Eagleson (1970) gives an extinction factor for the effect of clouds on the incoming solar radiation. Table 3-1 lists the values of this factor for various cloud covers and cloud heights. During ice fog the cloud height is zero, and cloud cover is 10/10. This yields an extinction factor of 0.18. Multiplying this factor by the clear sky radiation received at the surface gives a value of less than three langleys of solar radiation received per day by a horizontal surface during ice fog at this time of the year. On February 4 the solar radiation arriving at the surface under ice fog conditions had risen to slightly less than 10 langleys per day. Comparing this to the average measured value of long-wave radiation from the atmosphere (430 langleys per day, Table 3-2), it is clear that the incoming solar radiation during this time of the year is a negligible portion (≈2%) of the radiation heat balance of an open water surface during ice fog.

The outgoing long-wave radiation emitted by any body can be calculated from:

$$Q_o = \varepsilon \sigma T_o^4 \qquad 3\text{-}0$$

where:

Q_o = outgoing long-wave radiation (watts)(m^{-2})

Table 3-1

Cloud Attenuation Factors (1 - (1 - .18 - .024z) N)
for short-wave radiation.

N = cloud cover in tenths

	Height of cloud base (feet) (z)					
N	0	100	1000	4000	8000	16000
.1	.918	.918	.920	.928	.937	.956
.2	.836	.836	.841	.855	.874	.913
.3	.754	.755	.761	.783	.812	.869
.4	.672	.673	.682	.710	.749	.826
.5	.590	.591	.602	.638	.686	.782
.6	.508	.509	.522	.566	.623	.738
.7	.426	.428	.443	.493	.560	.695
.8	.344	.346	.363	.421	.498	.651
.9	.262	.264	.284	.348	.435	.608
1.0	.180	.182	.204	.276	.372	.564

Table 3-2

Long Wave Radiation Data

Date	T_w	T_{air}	Day or Night	Fog Cover**	Net LW rad outgoing	Avg wind
	(°C)	(°C)		(tenths)	(w)(m^{-2})	m/s
Over Water:						
1/9/73	12.9	-18.0	D	-	89	0
	12.9	-18.0	D	-	102	0
1/18/73	15.0	-28.0	N	-	159	0
1/20/73	12.0	-33.0	D	-	106	0
1/21/73	14.5	-38.0	N	-	102	0
1/22/73	13.0	-40.0	D	-	82	0
1/23/73	12.0	-40.0	N	-	122	0
1/27/73	3.5	-20.0	N	-	63	0
2/5/73	8.8	-22.0	D	0.0	112	0
	7.5	-14.0	D	0.0	128	0
	8.5	-22.0	N	0.8	114	0
2/6/73	12.0	-22.0	D	0.9	106	0.20
	12.0	-18.0	D	0.0	126	0.20
	12.5	-16.0	N	0.0	128	0.20
2/7/73	13.5	-20.0	D	1.0	108	0.05
	15.0	-13.0	D	0.0	142	0.05
2/8/73	15.8	-19.5	D	0.2	152	0.15
	16.6	-16.0	D	0.2	128	0.15
2/9/73	16.7	-23.0	D	0.5	114	0
	16.8	-18.0	N	0.0	162	0
2/10/73	14.0	-15.5	D	0.2	158	0
2/11/73	12.0	-19.0	D	0.5	159	0.90
	13.8	-16.5	N	0.0	182	0.90
2/12/73	12.3	-18.5	D	0.0	186	3.0
	12.5	-23.5	N	0.0	187	3.0

Table 3-2 (continued)

Date	T_w	T_{air}	Day or Night	Fog cover**	Net LW rad outgoing	Avg wind
	(°C)	(°C)		(tenths)	(w)(m^{-2})	m/s
2/13/73	13.0	-26.5	D	0.2	165	1.50
	13.2	-19.5	D	0.2	184	1.50
	14.0	-17.5	D	0.5	164	1.50
2/14/73	12.7	-32.0	D	0.9	130	0.25
3/7/73	7.5	-7.5	D	0.1	65	0.05
3/8/73	11.1	-10.0	D	0.9	77	0.20
	11.1	-10.5	D	0.9	67	0.20
	11.1	-9.5	D	0.9	50	0.20
	11.1	-10.0	D	0.8	76	0.20
3/9/73	13.8	-9.5	D	0.5	113	0.30
3/10/73	14.4	-13.0	D	0.1	122	1.60
	14.4	-13.5	D	0.9*	79	1.60
3/11/73	14.5	-7.5	D	0.9*	96	0.15
	14.8	-7.0	D	0.0	121	0.15
3/12/73	14.5	-15.0	D	0.4*	137	1.15
	14.5	-15.0	D	0.3*	109	1.15
3/14/73	15.8	-12.0	D	0.9	90	0.85
3/16/73	14.0	-15.0	D	0.9*	83	1.30
3/19/73	15.0	-5.6	D	-	144	3.45
3/21/73	9.1	-9.0	D	0.0	98	0.10
3/22/73	6.5	-9.0	D	0.6	103	0.90
Avg	12.7	-17.9			119	0.60

* Indicates high altitude overcast.
** Fog cover was estimated visually by the observer.

Table 3-2 (continued)

Date	T_{ice}	T_{air}	Day or Night	Fog cover**	Net LW rad outgoing	Avg wind
	(°C)	(°C)		(tenths)	(w)(m^{-2})	m/s
Over Ice:						
1/27/73	0.0	-15.0	N	-	66	0.25
1/28/73	0.0	-15.0	N	-	66	2.0
	-4.5	-20.5	D	0.8	60	2.0
	-1.5	-1.0	N	0.9	27	2.0
1/29/73	-0.5	-1.0	D	0.9	8	3.0
	-1.0	-10.5	N	0.9	34	3.0
1/30/73	-1.0	-23.5	D	0.9	49	0.75
	-1.0	-24.5	N	0.6	42	0.75
1/31/73	-1.5	-25.0	D	0.9	35	0.15
	-1.5	-25.5	D	0.0	77	0.15
2/1/73	-2.0	-30.0	D	0.9	52	0
	-2.0	-30.0	N	-	34	0
2/2/73	-2.5	-4.5	D	-	73	3.50
	-2.5	-9.0	N	-	6	3.50
	-2.5	-4.5	D	0.5*	50	3.50
2/14/73	-	-20.0	D	0.0	75	0.25
	-	-20.0	D	0.0	79	0.25
	-	-19.0	D	0.0	70	0.25
	-	-19.0	D	0.0	68	0.25
	-	-17.0	D	0.0	70	0.25
	-	-20.0	D	0.0	70	0.25
	-	-20.0	D	0.0	73	0.25
Avg	-1.6	-17.0			54	1.20

* Indicates high altitude overcast.
** Fog cover was estimated visually by the observer.

ε = emissivity of the radiating body

σ = Stefan-Boltzman's constant (watts)$(m^{-2})(°K^{-4})$

T_o = the absolute temperature (°K)

The problem of estimating the net radiation loss during ice fog conditions is therefore reduced to that of estimating the effective back radiation from the atmosphere and subtracting it from the outgoing radiation (equation 3-0). Outgoing radiation is fairly straightforward; however, back radiation is not so simple, and several investigators have proposed empirical equations to estimate its value.

Brunt's Equation

One equation, widely used for atmospheric radiation, was proposed by Brunt (1944). This equation uses the vapor pressure at the surface to estimate atmospheric radiation. Approximating conditions of the layers of air at various heights in terms of the conditions at the surface obviously leaves much to be desired, but can be justified because data on the various strata of air above the ground are seldom available. Anderson (1952), for example, found that twice daily radiosonde balloon flights were not adequate to accurately measure the temperature and humidity conditions of the various strata of the atmosphere. This equation could be very useful if it can be shown to have sufficient accuracy. Brunt's equation is:

$$Q_a = (a + b\sqrt{e_a})(\sigma T_a^4) \qquad 3\text{-}1$$

where:

Q_a = atmospheric radiation (watts)(m^{-2})

e_a = vapor pressure of the air at 2 m height in (mb)

σ = Stefan-Boltzman constant

T_a = air temperature at 2 meters (°K)

a & b = empirically derived constants

Ångstrom Equation

Ångstrom (1920) proposed an equation similar to Brunt's, but with slightly different form. It is, however, somewhat more awkward to use. Ångstrom's equation also bases the prediction of incoming atmospheric radiation on the vapor pressure of the air near the surface - in this case, at 4 meters.

Ångstrom's equation is:

$$Q_a = (a-b \exp [-\gamma e_a])(\sigma T_a^4) \qquad 3\text{-}2$$

where:

exp = the Napierian base, e = 2.72

a, b & γ = empirically derived constants

Elsasser's Equation

Elsasser (1942) proposed still another form for atmospheric radiation using vapor pressure at 4 m:

$$Q_a = (a+b \log e_a)(\sigma T_a^4) \qquad 3\text{-}3$$

The above equations attempt to relate the atmospheric radiation to local vapor pressure only. While these make convenient equations, they are obvious oversimplifications of the complex meteorological systems governing atmospheric radiation. A "true" equation should be related to the total vapor content of the atmosphere, the carbon dioxide content, the ozone content, and perhaps the aerosol content; the relationship is

clearly not simple. These equations can only be looked upon as estimates of the average atmospheric radiation, and evaluations for the constants involved in each equation will pertain only to the conditions prevailing for that set of data. As an example, Anderson (1952) gives values for the various constants in Brunt's and Ångstrom's equations for various localities. Differences as great as 135% exist in some of the constants between different studies.

Cloud Cover

None of the above equations considers the effect of cloud cover. To compensate for this effect, most investigators have relied upon an empirical polynomial equation to allow back radiation to increase as cloud cover increases. One such method is the Karadag-Chumikova factor (Kondratyev, 1965). This technique applies a reduction factor to the net loss of long-wave radiation from the surface. From observations at Karadag-Chumikova in southern Russia, it was found that a non-linear polynomial could be used to express net radiation during times when the skies are cloudy. Net radiation was then expressed as:

$$Q_r = Q_n (1 - 0.02N - 0.004N^2) \qquad 3\text{-}4$$

where:

Q_r = net radiation under cloudy skies

Q_n = net radiation under clear skies

N = cloud cover in tenths

A more direct approach is reported by Anderson (1952). He found in studies at Lake Hefner that a linear equation could be used to express atmospheric radiation from cloudy skies. He recognized that cloud height

(in addition to amount of cloud cover) must be taken into account. Anderson's cloudy sky equation is:

$$Q_{ac} = ([a+b\ N \exp(-0.058h)] + [c-D\ N \exp(-0.06h)][e_a]) \sigma T_a^4 \qquad 3\text{-}5$$

where:

Q_{ac} = atmospheric radiation from cloudy skies

h = cloud height in thousands of feet

a, b, c, D are empirically derived constants

This equation was tested for cloud heights of 1600 feet and greater. Anderson states that the radiation increases as cloud height decreases and probably continues to increase for cloud heights below 1600 feet. He contends that accuracies of 5 to 10% are possible using this equation.

Reflection

The amount of the atmospheric radiation that is absorbed by the surface is a function of the reflectivity of the surface. For water surfaces, Raphael (1962) gives a graph of reflection as a function of cloud percent and incident angle. For angles above 50 degrees, the reflection asymptotically approaches 0.05 for overcast skies. Anderson (1952) reports that studies at the Physical Standards Laboratory of the US Geological Survey set the reflectivity of water for long-wave radiation at 0.03. An absorptivity (α) of 0.97, therefore, seems to be reasonable.

The net radiation heat loss under clear skies during ice fog temperatures can be expressed as:

$$Q_n = Q_{out} - \alpha Q_{atmos} \qquad 3\text{-}6$$

$$Q_n = \sigma \varepsilon_w T_w^4 - (\sigma \alpha T_a^4)(a + b \sqrt{e_a}) \quad \text{Brunt} \quad 3\text{-}7$$

$$= \sigma \varepsilon_w T_w^4 - (\sigma \alpha T_a^4)(a - b \exp(-\gamma e_a)) \quad \text{Ångstrom} \quad 3\text{-}8$$

$$= \sigma \varepsilon_w T_w^4 - (\sigma \alpha T_a^4)(a + b \log e_a) \quad \text{Elsasser} \quad 3\text{-}9$$

The choice of which equation to use for atmospheric back radiation is not critical, since as Anderson (1952) points out: "The difference between Brunt's and Ångstrom's equation and between Brunt's and Elsasser's equation is only 10%. This is not a significant difference since the scatter of the observations is considerably greater."

Using Brunt's equation and Kondratyev's Karadag-Chumikova factor for cloudy skies, the net radiation (Q_r) can be expressed as:

$$Q_r = \sigma(\varepsilon_w T_w^4 - T_a^4 (a+b \sqrt{e_a}))(1 - 0.02N - 0.004N^2) \quad 3\text{-}10$$

or expressing atmospheric back radiation with the cloud equation proposed by Anderson yields:

$$Q_r = \sigma \varepsilon_w T_w^4 - [(a + b N \exp(-0.058h)) + (c - D N \exp(-0.06h))(e_a)] \alpha \sigma T_a^4 \quad 3\text{-}11$$

Comparison of the above equations will be presented later in this chapter.

Field Experimental Results

At the Eielson field station radiation measurements were taken several times daily for a period of two and one-half months, from January to the middle of March. Three different instruments were used: a pyrgeometer, a net radiometer, and a precision radiation thermometer. The pyrgeometer and the net radiometer were mounted on a cantilevered beam projecting out over the pond surface at a height of 0.5 m (Figures 3-1 and 3-2).

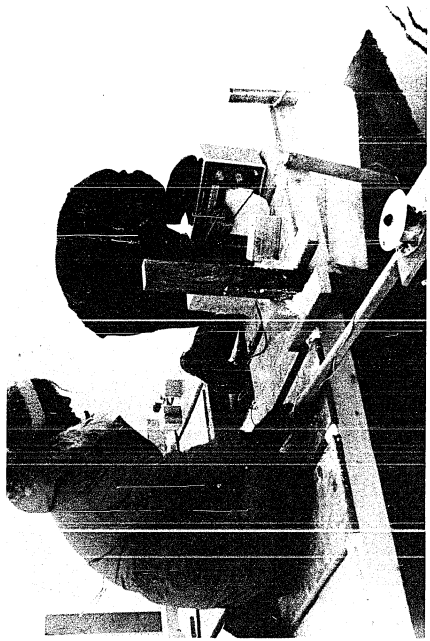

Figure 3-1. Net Radiation Measurements with the Radiation Pyrgeometer.

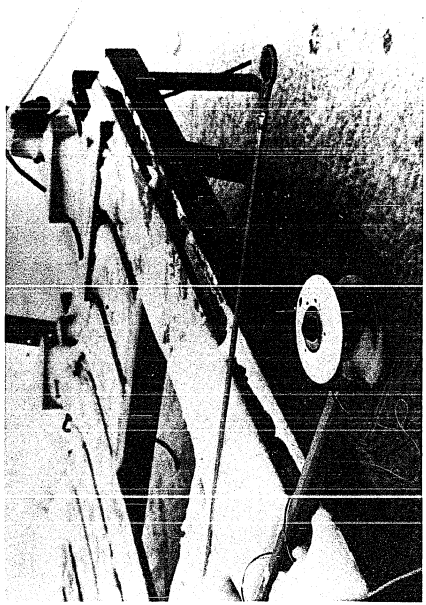

Figure 3-2. Radiation Instrumentation.

Radiation values were measured using a Leeds & Northrup millivoltmeter bridge housed in a trailer laboratory at the site. Calibration of the instruments was performed at the laboratory of the University of Alaska Geophysical Institute. Measurements were made at frequent intervals throughout the day during two months of the investigation period. The long-wave pyrgeometer was turned toward the surface and then toward the sky, and the difference between the two values yielded a "net radiation" which was compared to the net radiometer readings. Comparing values from the two instruments showed a correlation coefficient at night (when all incoming solar effects were absent) of 0.984. As spring approached, the effect of incoming solar insolation rapidly increased each day.[1] A radiation thermometer was used to measure water and ice surface temperatures, and to calibrate thermocouples at strategic locations.

The average value for outgoing long-wave radiation at a water temperature of 10° C averaged 10% below the theoretical maximum (Figure 3-3). This is probably caused by the attenuating effect of fog between the instrument and the water surface, and the field of view ("shape factor") of the instrument. Since the instrument was mounted approximately 0.5 meters above the water surface, the water vapor and ice fog in this layer attenuated the measured outgoing radiation value.

---

[1] The radiation pyrgeometer used at Eielson was temperature compensated down to -25° C. Values below this temperature are therefore open to suspicion.

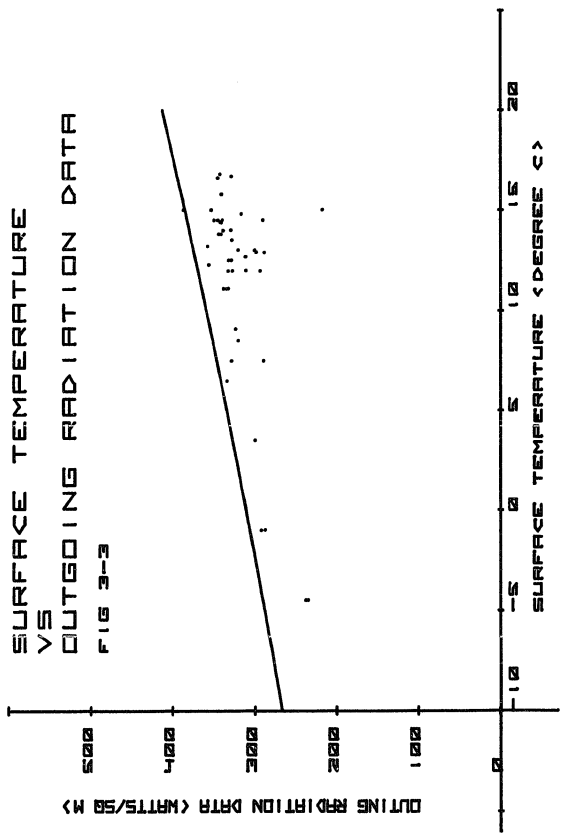

Wexler (1940) measured the radiation incoming from the atmosphere at Fairbanks, Alaska, during the winter months. Considering only values below 0° C, the average air temperature at the time measurements were made by Wexler was -15° C, while at Eielson the average was -17° C. The corresponding average atmospheric radiation values are:

Wexler	188 (watts)(m^{-2})
Eielson	214 (watts)(m^{-2})
% Difference	10.8%

It is interesting to note that the time lapse between these two studies was 34 years. The difference between the average values is not significant since the spread in both Wexler's data and the Eielson data is greater than 10.8%. Wexler reports values from 132 to 279 (watts)(m^{-2}), while the Eielson data contained values from 144 to 304 (watts)(m^{-2}). For both studies this represents a spread of ±36% about the average. Variations of as much as 69.7 (watts)(m^{-2}) were reported by Wexler at a specific temperature. Although data are not sufficient to be conclusive, the overall average of atmospheric radiation appears to be in this range.

Analysis of Experimental Results

The net long-wave radiation heat loss is a function of the atmospheric conditions prevailing over the pond. The equations above have addressed the atmosphere at altitude; however, the ice fog plume rising from the pond has not been considered by these equations. The back radiation from this cloud has a direct effect on the net radiation heat loss. Figure 3-4 shows the net radiation from Table 3-2 averaged and plotted against fog cover. This illustrates the effect of fog cover on the net

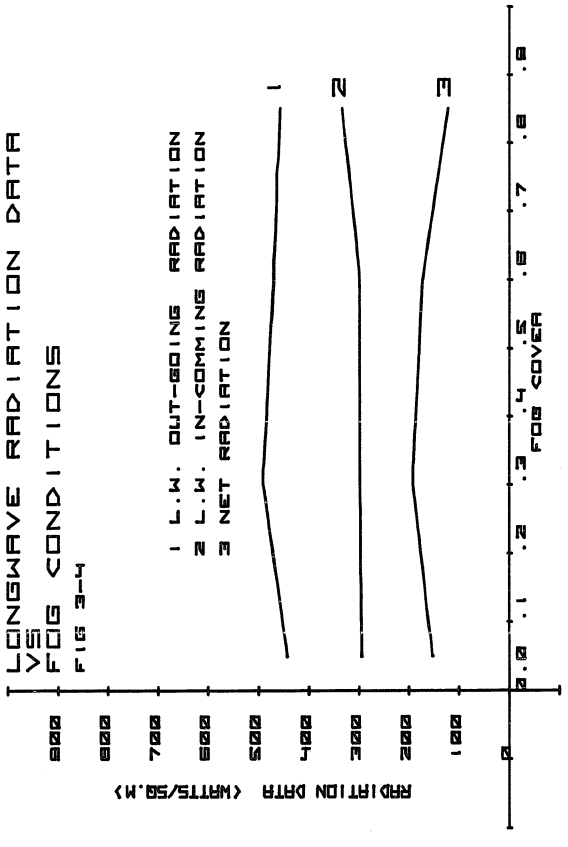

radiative loss of heat from the water surface. The average measured radiation loss during -30° C air temperatures (Table 3-2) is 37 percent less than the calculated value for clear skies, using the corrected equation discussed below. A corresponding decrease of 40 percent is found when net measured radiation is compared with cloud cover (Figure 3-4).

Wien's Law states that the wave length of maximum intensity of radiation emitted by a surface times its absolute temperature is a constant according to the relation:

$$T\lambda_{max} = 0.2897 \text{ cm } °K \qquad 3\text{-}12$$

The average temperature of the water surface during the winter months was 12.6° C. At this temperature, the maximum intensity of radiation from the surface occurs at a wavelength of 10 microns. The absorption spectrum of water vapor has a window from 9 to 12 microns. The spectrum of the radiation is wider than the window, so that a significant portion of the total emission is absorbed by water vapor. However, approximately 30 percent of the total is in the wavelength range of the window and is lost into space. Geiger (1965) states: "In these ranges, streams of radiation can escape into space. ...No matter how heavily the atmosphere is laden with water vapor, it can afford no protection." Although much smaller in magnitude, somewhat similar absorption features exist in both ice and liquid water absorption spectrums (Shaw, personal communication; Kondratyev, 1954). (Water has much more intensive absorption bands in the infrared.) In addition, the shape factor from pond to fog approaches unity, while the factor from ice fog to pond is closer to zero. Therefore, of the radiation emitted by the ice fog, only a small fraction goes back to the pond.

Radiation Equations for Ice Fog

The development of a precise equation for the net radiative heat loss from an open water surface is extremely difficult due to the many diverse factors affecting the various components of the radiation heat balance of the system. Many of these factors cannot be measured continuously; others are difficult to measure accurately. We must be content with approximations which use readily available parameters as models of the overall system. This, of course, lacks the desirable precision, but in this manner usable average values and their bounds can be calculated for use as design parameters.

Each of the above equations for atmospheric radiation contains constants which must be determined empirically. Each of the authors has determined average values for these constants, as have other users as well. None of the equations addresses the situation of fog immediately over the water surface, and none mention ice fog. To account for these effects, each of the constants was evaluated using data from the Eielson cooling pond.

To evaluate the constants, a computer program was developed which substituted various values into the equations and compared the results with values of atmospheric radiation measured at Eielson. The difference between the calculated and measured values was computed and a search was made for constants that would reduce the difference to a minimum. The average value of the constants thus derived was found and is displayed in Table 3-3. The resulting equation was again compared to the measured data, and a standard error calculated.[1]

[1] Standard error is defined by the equation: $S.E. = \left[\frac{(X_{calc} - X_{meas})^2}{n-1}\right]^{1/2}$

Table 3-3

Atmospheric Radiation Equations $(w)(m^{-2})$

Equation Constants as Presented by Original Author

	a	b	c	d	γ	Eq. No.	Percent std error
Brunt's Eq.	.60	.042	---	---	---	3-1	27.0
Ångstrom's Eq.	.806	.236	---	---	.115	3-2	24.3
Elsasser's Eq.	.21	.22	---	---	---	3-3	73.8
Anderson's Eq.	.74	.025	.0049	.00054	---	3-5	18.5
Constants Resulting from Eielson Data							
Brunt's Eq.	.807	.029	---	---	---	3-13	13.7
Ångstrom's Eq.	.658	.201	---	---	.375	3-14	14.6
Elsasser's Eq.	.848	.039	---	---	---	3-15	14.1
Anderson's Eq.	.814	.110	.0054	.00059	---	3-16	10.7

Although the differences in standard error are not great, it is interesting to note that the equations originally proposed by the various authors generally exhibited considerably greater standard error than did the equations resulting from the Eielson studies (Table 3-3). This suggests that an increase in accuracy of 8% to 60% can be obtained when calculating atmospheric radiation during ice fog conditions by the use of the equations correlated to the Eielson data.

The final form of each equation is:

Revised Brunt's Eq. $Q_a = (.807 + .029 \sqrt{e_a})\ \sigma T^4$ 3-13

Revised Ångstrom's Eq. $Q_a = (.658 - .201 \exp(-.375\ e_a))\ \sigma T^4$ 3-14

Revised Elsasser's Eq. $Q_a = (.848 + .039 \log e_a)\ \sigma T^4$ 3-15

Revised Anderson's Eq. $Q_a = ((.814 + .11N \exp(-.0584h)) + (e_a)$
$(.0054 - .000594N \exp(-.06h))) \sigma T^4$ 3-16

These are not necessarily the best or most representative equations that could be found to represent ice fog conditions. However, the use of these "familiar and well used" forms allows the resulting calculations to be compared with other data taken in different localities by other investigators. The standard error of 10.7% found for the revised form of the Anderson equation (Table 3-3) indicates that the results of calculations using this equation will be well within the limits of the measured data of both this and other studies. Figures 3-5 through 3-8 compare the above equations with the data gathered at Eielson.

Transmissivity of Ice Fog

It was noted above that the measured outgoing radiation fell 10% below the theoretical value for the various pond temperatures at which it was measured (Figure 3-3). This is caused by two factors; first, the measuring probe was positioned 0.5 meters above the water surface. In this position it received radiation not only from the surface of the pond, but also from the much colder banks of the pond. Therefore, a radiation "shape factor" should be applied to compensate for this error. In addition, the 0.5 meters of air between the water surface and the probe contained water vapor and ice fog particles which absorbed some of the emitted radiation from the water and re-emitted at the temperature of the vapor and ice fog crystals. This suggests that an approximation of the transmissivity of ice fog could be obtained by calculating the radiation shape factor and applying it to the data; the difference between

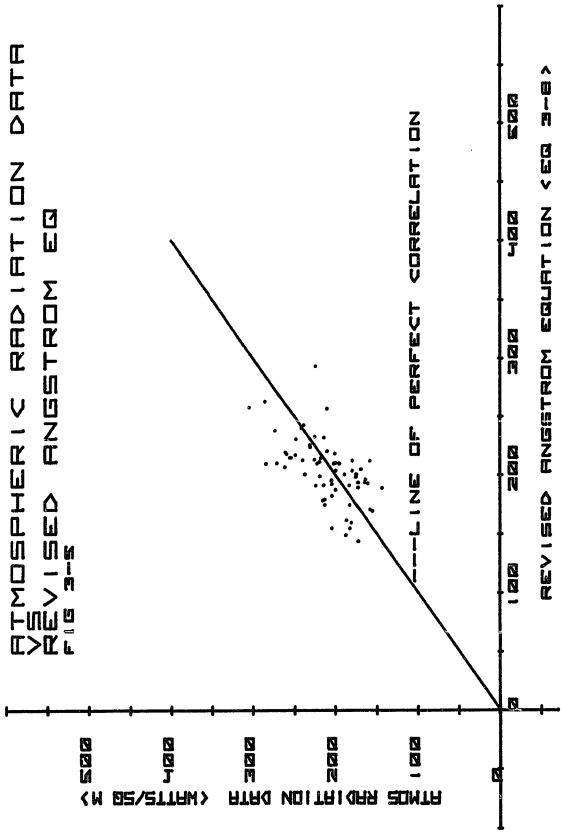

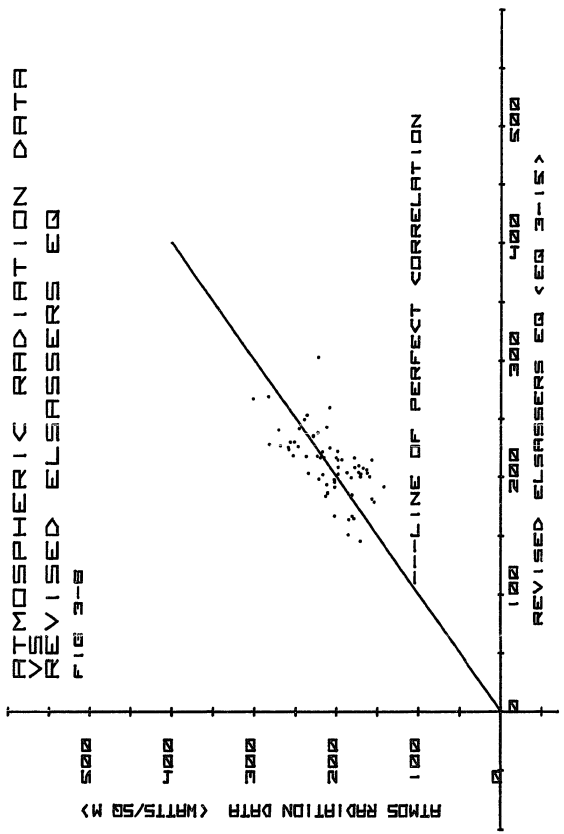

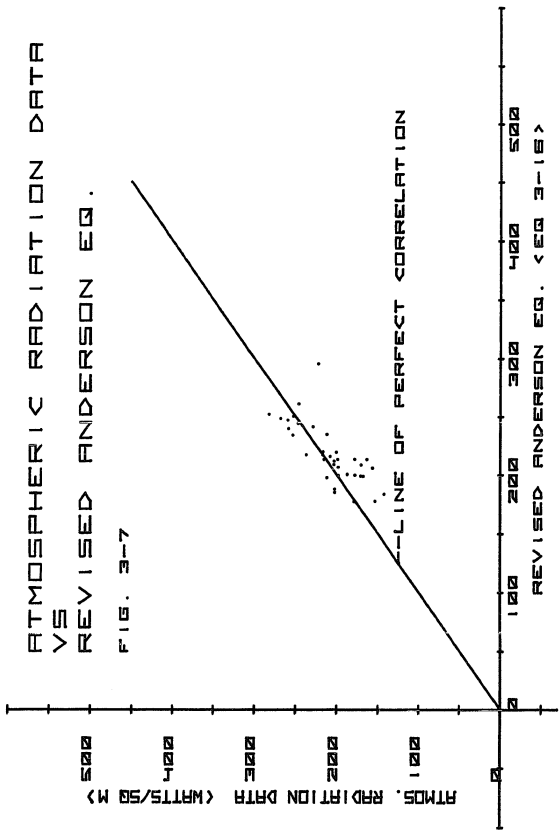

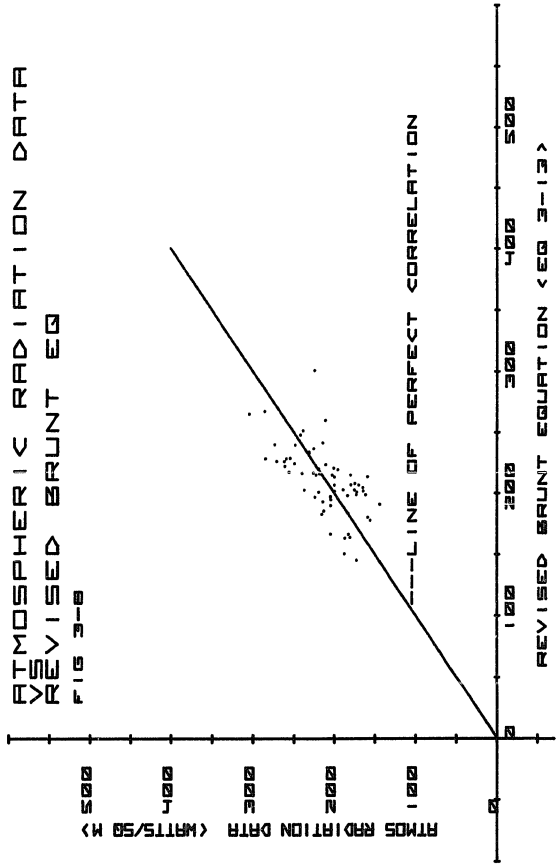

the data and theoretical value would then represent the transmissivity of the ice fog.

The radiation probe is a hemispherical dome that admits radiation from all angles below the flat plate upon which it is mounted. The solid angle thus represented is 2π steradians. The area of the pond which falls into the "field of view" of the probe represents the base of a cone whose vertex lies at the center of the probe. The solid vertex angle of this quasi conical surface represents a good approximation of the view factor of the radiometer. This can be calculated by integrating the plane vertex angle through the 360-degree field of view of the probe. Since the base of the conical surface is difficult to express as a continuous function, the technique of numerical integration can be used to arrive at the value of the solid angle. A computer program was set up to evaluate this angle, and is presented in Appendix B. The resulting value of the shape factor is 0.956.

A computer program was developed to determine the difference between the measured values and the theoretical value. A correction factor for the theoretical equation was found which gave a minimum standard error between the measured data and the formula. This value was found to be 0.895, and is a function of the emissivity (ε), the shape factor (S), and the transmissivity (τ) of the ice fog.

$$S_B \varepsilon_B \sigma T_B^4 \tau + \varepsilon_f \sigma T_f^4 + S_w \varepsilon_w \sigma T_w^4 \tau = 0.895 \sigma T_w^4 \qquad 3\text{-}17$$

where subscript B refers to the bank, subscript w refers to the water surface, and subscript f refers to the ice fog. Rearranging and cancelling terms, the value of the transmissivity is found to be:

$$\tau = \frac{0.895\ T_w^4 - \varepsilon_f\ T_f^4}{S_B\ \varepsilon_B\ T_B^4 + S_w\ \varepsilon_w\ T_w^4} \qquad 3\text{-}18$$

All of these terms have been discussed above except the emissivity of the banks (ε_B) and the emissivity of the ice fog (ε_f). The emissivity of the banks can be assumed to be that of snow, $\varepsilon = 1$ (Eagleson, 1970). If the emissivity of the fog is assumed to be represented by any one of the revised atmospheric radiation equations above (equation 3-13, 3-14, 3-15, or 3-16) an order of magnitude value of 0.8 is representative. These equations are designed to measure the radiation from the entire atmosphere. Since the thickness of fog viewed by the pyrgeometer (300 meters maximum) is a small fraction of the thickness of the atmosphere (0.1 at best), an emissivity of 0.08 should give a reasonable approximation of this value. An approximate value of the transmissivity is then:

$$\tau = \frac{(0.895)(283)^4 - (0.08)(243)^4}{(.044)(243)^4 + (.97)(.956)(283)^4} \qquad 3\text{-}19$$

$$\tau = 0.9 \qquad 3\text{-}20$$

constituting an absorption of 10% by the ice fog in the wavelength range of emitted radiation.[1]

Figure 3-9 shows the data, corrected for transmissivity and shape factor, plotted against formula 3-0.

Figure 3-10 compares the four equations for atmospheric radiation which can be used for calculating net long wave radiation lost from the water surface.

---

[1] This assumes that the density of the ice fog is constant, and can be represented by the lowest half meter.

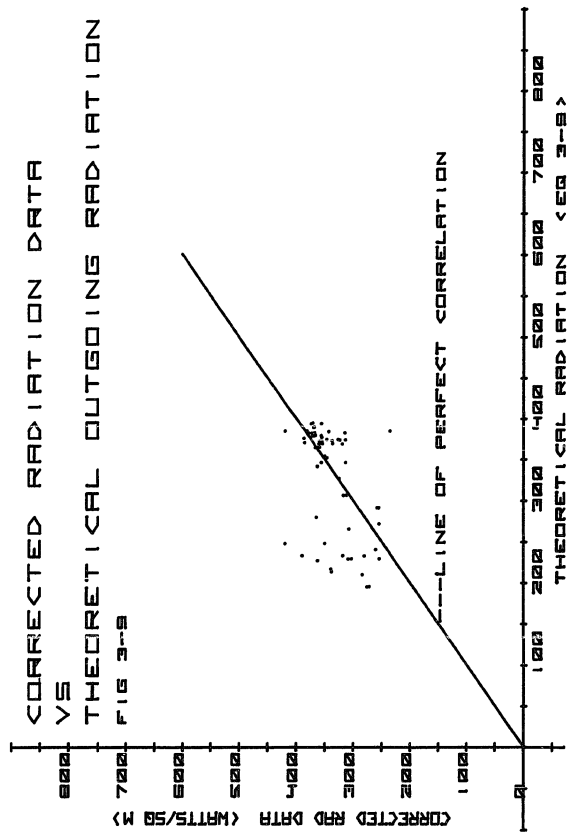

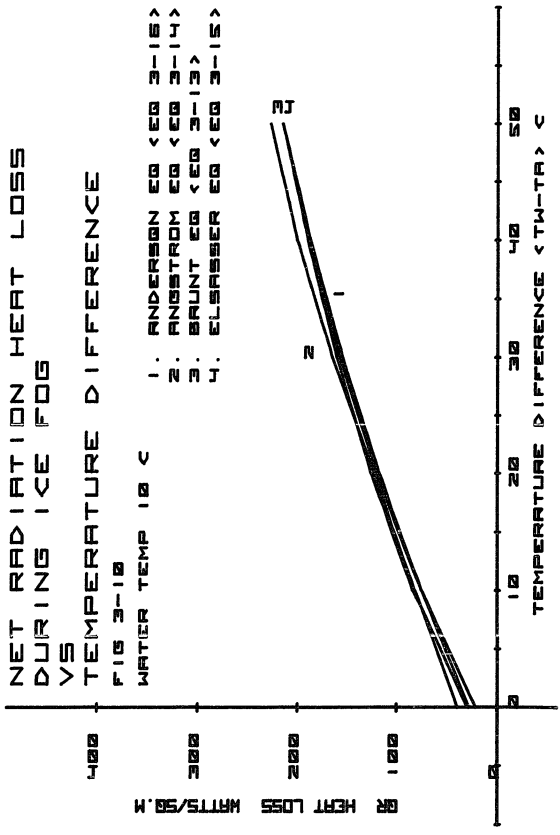

Radiation Model

A model of the radiation balance of the pond during ice fog conditions may be constructed in the following manner. The water surface will be considered to radiate with an emissivity of 0.97 ($R_{out} = .97\ \sigma T_{wo}^4$).[1] Some of this outgoing radiation is reflected by the cloud over the pond. The ice fog cloud radiates at the rate of $\varepsilon\sigma T_{ao}^4$. This is a function of the thickness and density of the fog layer. A portion of this will be directed back to the pond. Finally, the sky above the pond is radiating long-wave energy, some of which is directed at the pond. The amount reaching the surface is a function of wavelength, air temperature, transmissivity of the ice fog cover, and shape factor between the two bodies. If an approximate effective sky temperature (T_{so}) is assumed, then the net radiation lost (R_{net}) is:

$$R_{net} = R_{outgoing} - R_{reflected} - R_{ice\ fog} - R_{sky}$$

and the first approximation is:

$$R_{net} = \varepsilon_w \sigma T_{wo}^4 - K_r S_{fP} \alpha_w \sigma T_{wo}^4 - \varepsilon_f S_{fP} \alpha_w \sigma T_{ao}^4 - \varepsilon_s \alpha_w K_t \sigma T_{so}^4 \qquad 3\text{-}21$$

where:

ε_f = emissivity of fog

ε_w = emissivity of water

K_r = coefficient of reflection of ice fog cloud

K_t = transmissivity of fog layer

S_{fP} = shape factor between the fog and the pond

ε_s = emissivity of atmosphere

---

[1] The subscript (o) will be used to indicate absolute temperatures.

α_w = absorptivity of water

T_{wo} = water surface temperature

T_{ao} = air temperature

If an effective sky temperature (T_{so}) is assumed to be a function of the air temperature (T_{ao}), it can be seen that as the air temperature declines, the last two terms of the equation diminish, thus causing R_{net} to increase. As fog forms over the pond, however, the magnitude of the radiation from this term begins to increase due to increasing ε_f; this will have the effect of attenuating the magnitude of net radiation lost and an inflection point in the curve of radiation loss vs air temperature will result. As the air temperature continues to decrease, however, the decreasing value of T_{ao}^4 will overshadow the increase in ε_f (which will be approaching the maximum value) and a second inflection point will occur after which the net radiation lost will again increase with decreasing temperature. The effective sky temperature is influenced by the amount of water vapor in the upper layers of air above the pond. Pond surface temperature also varies. The degree to which T_s is a function of T_a is still another variable. The interaction of these variables causes considerable scatter (e.g., see Wexler, 1940).

Wind Effect

The effect of wind on radiation losses is significant since the ice fog cloud and its back radiation can be greatly reduced or eliminated completely by it. When the wind velocity is high, the vapor-laden air above the pond is swept away before it forms the traditional cloud or plume over the pond. Under these conditions the area above the pond is

predominately air from the surrounding environment, and does not reflect the normal vapor-laden conditions present when wind is absent. The back radiation from the atmosphere under these conditions will be considerably lower than when the ice fog plume rises over the pond undisturbed. It was evident in the measurements that air movement played a significant effect on the net radiative loss. Comparing average radiative losses on windy days to average losses on days in the same temperature range without wind, shows a 26 percent higher loss on windy days (Table 3-2). Data are not extensive, but it does appear that wind plays an important role in radiative as well as other heat losses.

Summary

Ice fog plays a significant role in attenuating the radiative heat losses from an open water surface. This effect is more pronounced as the temperature falls, due to increased back radiation from the fog layer. Back radiation reaches a maximum and then declines as the temperature drops further. Approximately one-third of the emission from a body radiating at the temperature of the cooling pond is in the 9 to 12 μ wavelength range of the absorption window for water vapor. Absorption features for liquid water fogs and ice particle fogs are altered, but still exist in somewhat diminished form.

Solar radiation can be ignored for December and January, but should be considered during daylight hours of other winter months.

The outgoing radiation from the water surface at +11° C is 350 $(w)(m^{-2})$. Outgoing radiation from the ice surface at an average -2° C

is 286 $(w)(m^{-2})$. Using Anderson's equation for the back radiation from the ice fog, a value of 162 $(w)(m^{-2})$ is obtained.

The average net radiation heat loss if the entire pond is open therefore can be 8.7×10^6 watts at -30° C. This is 48% of the average net heat input to the pond (see Chapter Six). If half of the pond is ice covered, then 24% of the total heat is dissipated by radiation from the water surface and 15% from the ice surface. This represents a significant portion of the heat budget of the pond.

CHAPTER FOUR - CONVECTION

Heat losses by convection are usually the largest single component of the heat budget of a body of water (Dingman, Weeks, and Yen, 1967; and Rimsha and Donchenko, 1958). Convection may be divided into two classifications: laminar and turbulent. However, Gebhart (1969) points out, "Many of the natural convection processes found in nature are of such a large size scale and of such long duration that the detailed transport mechanism is largely turbulent." Visual observations of open water during ice fog tend to support this point of view. The vapor rising and condensing over the water provides an excellent visual reference of the local eddies and overall transport of the vapor-laden air near the surface, which is seen to be turbulent with laminar flow predominating only in the first few centimeters above the water. Theoretical studies of turbulent heat transfer have been made by many researchers (Kays, 1966; Gebhart, 1969; Rotem and Claassen, 1967; and others). However, only Rotem and Claassen have addressed the subject in a manner that is applicable directly to free convection heat transfer in the environment. Their approach, although rigorous in theory, "found only moderate agreement with experimental data." Kays, on the other hand, using an equally rigorous theoretical approach, demonstrated good agreement between theoretical equations and laboratory experiments. A question arises as to which approach to use - the free convection approach of Rotem and Claassen (which leaves something to be desired in verification), or the

forced convection approach of Kays (which correlates well with conditions that may be far removed from those encountered in the environment).

A third alternative is available, however, and that is to rely on a purely experimental approach, as did Rimsha and Donchenko in deriving an empirical formula for convective heat loss from data collected throughout the Soviet Union in the winter months.

Other empirical approaches have attempted to determine the convective heat loss by direct measurement of the volume of air and its temperature rise while passing over a pond (Pruden, et al, 1954). This approach has the advantage of yielding values that are not dependent on other variables; however, it is a difficult and time-consuming process to use and does not lend itself to accurate heat loss predictions.

This chapter will compare the various approaches and discuss their correlation.

Convective Heat Transfer Theory

Consider a plane facing upward (e.g., a water surface with air above). The minimum convective heat loss (zero) will come during periods of zero temperature difference (ΔT) between the water and the air. As ΔT increases, the convective heat transfer (Q_H) increases; and for every temperature difference, there is a maximum and minimum Q_H depending on air movement, which is described by the convective heat transfer coefficient (h) of the air-water boundary layer.

The Prandtl number is the ratio of thermal boundary layer[1] thickness

[1] The thermal boundary layer is defined as the thin layer next to the wall, whose thickness extends to the interface where conductive heat transfer is equal to convective heat transfer.

to velocity boundary layer thickness. When these two are of nearly equal thickness ($Pr \simeq 1$), then the two boundary layers may be considered equal. Fluids and gases with Prandtl numbers approaching 1 can be treated as though their boundary layers were the same. For these cases, the momentum and energy equations of flow can be assumed identical; this greatly simplifies the derivation of heat transfer coefficients and equations.

The Prandtl number (Pr) may also be defined as:

$$Pr = \frac{c_p \mu}{k} \qquad 4\text{-}1$$

where:

c_p = specific heat

μ = absolute viscosity

k = thermal conductivity

For air at temperatures between -35° to 0° C, this turns out to be 0.72.

The Grashoff number (Gr) is a dimensionless number that has been found to characterize free convective flow, much the same as Reynold's number characterizes forced flow. The Grashoff number is the ratio of buoyancy forces to viscous forces in a free convection flow system.

The Grashoff number (Gr) may also be defined as:

$$Gr = \frac{g\beta x^3 (T_w - T_a)}{\nu^2} \qquad 4\text{-}2$$

where:

g = acceleration of gravity

β = coefficient of thermal expansion = $\frac{1}{T_{abs}}$

x = distance downstream from the leading edge of the plane

$T_w - T_a$ = temperature difference across the boundary layer

ν = kinematic viscosity

The Nusselt number (Nu) is the ratio of the length along the surface (x) to the boundary layer thickness (δ).

$$Nu = \frac{x}{\delta} = \frac{hx}{k} = f\ (Pr, Gr) \qquad 4\text{-}3$$

where:

h = convective heat transfer coefficient

k = thermal conductivity

It is the function of the product of Prandtl number and Grashoff number.

The convective mechanism prevailing over an open body of water during periods when much colder air covers the area is one that approximates a single large convection cell. Air near the surface of the water is heated by contact with the water and by latent heat of evaporation as vapors condense. The heated air rises due to the buoyancy forces created during the heating process. The rising warm air is replaced by cold air which enters the area around the periphery of the pond, lake, or river. This gives rise to a horizontal flow across the surface of the water (while the air is heating) that gradually changes into a vertical flow.[1] Because of this change in direction of flow it is difficult to use the conventional convection parameters which involve the distance (x) along the plate. It is customary in such cases to define a "characteristic dimension (x)" to be used for computing the Grashoff and Nusselt numbers.

Values of the Grashoff number above 10^9 are usually considered to be turbulent (in environmental heat transfer, values of 10^8 are sometimes

---

[1] If any wind is present, it is superimposed upon the convective flow, and changes the shape of the plume accordingly.

found to be turbulent) (Holman, 1972). A characteristic length for turbulent conditions can then be calculated from Equation 4-2:

$$x = \sqrt[3]{\frac{(Gr)(\nu)^2}{(g)(\beta)(T_w - T_a)}} \qquad 4\text{-}4$$

For air at -20° C, over water at +10° C:

$$x = \sqrt[3]{\frac{(10^9)(9.3 \times 10^{-6})^2}{(9.8)(1/253)(30)}} \qquad 4\text{-}5$$

$$= 0.42 \text{ m}$$

This is confirmed by visual observations. It is apparent that virtually all flow under ice fog conditions can be considered turbulent.

Rotem and Claassen Equation

A theoretical approach to free convective heat transfer above a horizontal surface was presented by Rotem and Claassen (1968). They were able to obtain a similarity solution for the partial differential equations of momentum, continuity, and energy by considering a semi-infinite heated plate facing upward, and assuming that density effects were negligible except for the buoyancy terms, for a Prandtl number of 0.7. Numerical integration was used to solve the boundary value equations, and the results were compared to experimental results using a "semi-focusing color-schlieren apparatus." Their experiments indicated that a critical Grashoff number for turbulent transition was as low as 10^6. They concluded that the horizontal plate is much less stable than the more widely studied vertical and inclined plates.

The Rotem and Claassen equation is:

$$Nu = \frac{-0.598\ Gr^{1/5}}{(1+2n)} \qquad 4\text{-}6$$

where:

n is the power of the temperature difference function (θ) (i.e., $\theta = T_{x^1} - T_{x^2} = c\, x^n$)

where:

c is a constant

x is the distance from the leading edge of the plate

T_x is the surface temperature at position x

Figure 4-1 shows a plot of Nusselt numbers vs the distance (x) along the plate.

Kays' Approach

The classical approach to convective heat transfer problems is presented by Kays (1966). Starting with the differential equations for momentum, energy, and continuity, and applying them to the boundary layer, he develops generalized equations for heat transfer by convection. For the external boundary layer, assuming that Reynolds' analogy is valid, Kays develops the following equation for convective heat transfer:

$$St = \frac{0.0295\ Re^{-0.2}}{(1 + 0.172\ Re^{-0.1}\ (5\ Pr + 51\ n\ (5\ Pr + 1) - 14))} \qquad 4\text{-}7$$

where:

St = Stanton number[1]

Re = Reynolds' number[2]

Kays states that this equation is a "little awkward to use; ...in the Prandtl number range of gases it is quite well approximated by the

---

[1] The Stanton number is defined as $\frac{Nu}{Re\ Pr}$.

[2] $Re = \frac{u_\infty x}{\nu}$

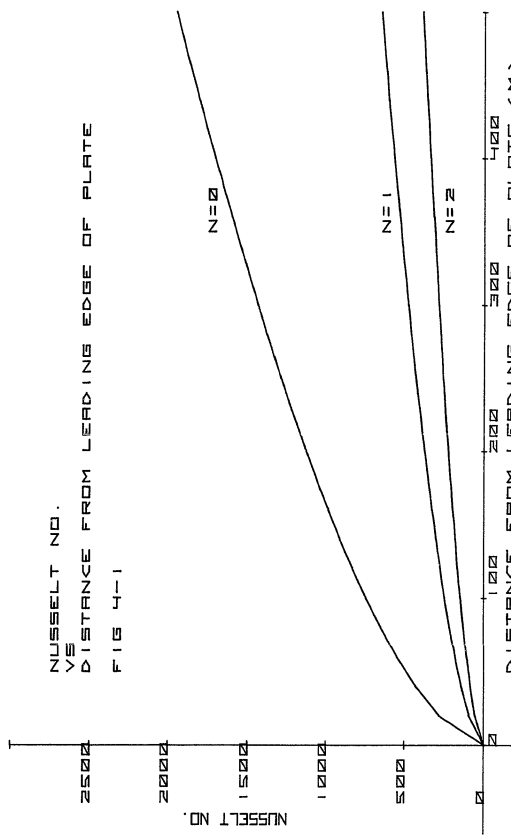

following more simple expression:"

$$St = \frac{0.0295\ Re^{-0.2}}{Pr^{0.4}} \qquad 4\text{-}8$$

For the Prandtl number range of 0.5 to 10, the various assumptions involved in deriving these equations have been shown to be reasonable by experimentation. Good experimental data are available, and both Eq. 4-7 and 4-8 are shown to be in excellent agreement with the data (Kays, 1966).

The Stanton number can be written:

$$St = \frac{h}{\rho\ c_p\ u_\infty} = \frac{hx}{k\ Re\ Pr} \qquad 4\text{-}9$$

where:

k is the thermal conductivity

u_∞ is the wind velocity of the unaffected stream

ρ is the density

h is the convective heat transfer coefficient

c_p is the specific heat

Combining Equations 4-9 and 4-8, the convective heat transfer coefficient can be written:

$$h = St\ (\frac{k}{x})\ Re\ Pr = 0.0295\ (Re)^{0.8}\ (Pr)^{0.6}\ (\frac{k}{x}) \qquad 4\text{-}10$$

The convective heat loss is then calculated from:

$$Q_H = h\ (T_w - T_a) \qquad 4\text{-}11$$

or

$$Q_H = 0.0295\ (Re)^{0.8}\ (Pr)^{0.6}\ (\frac{k}{x})\ (T_w - T_a) \qquad 4\text{-}12$$

where:

T_a is the temperature of the air above the water

T_w is the water temperature at the surface

Russian Approach

Rimsha and Donchenko of the Soviet Union have reported success in predicting convective heat losses from open water during winter months in the Soviet Union, using an empirically derived equation (Rimsha and Donchenko, 1958). They found that they could express the convective heat loss by the following equation:

$$Q_H = [3.9 + 0.17\ (T_w - T_a) + 1.9\ u]\ (T_w - T_a) \qquad (w)(m^{-2}) \qquad 4\text{-}13$$

This equation has two advantages; first, it is supported by data taken under winter conditions, so it has the best correlation with measurements of any of the above equations. Secondly, like Kays' equation, it considers the effect of the wind and is therefore more general than the free convection equation of Rotem and Claassen. Although wind conditions are probably not a significant factor during ice fog, for other winter conditions the effect of the wind must be considered.

Figures 4-2, 4-3, and 4-4 show the three equations plotted as a function of the temperature difference $(T_w - T_a)$ for wind speeds of 0, 1, and 2 m/s.

Analysis

The three equations considered differ markedly both in derivation and form, yet agreement between them for the lower temperature differences is good. At temperature differences of as much as 20 celsius degrees, there is only 10% difference between the Rimsha and Donchenko

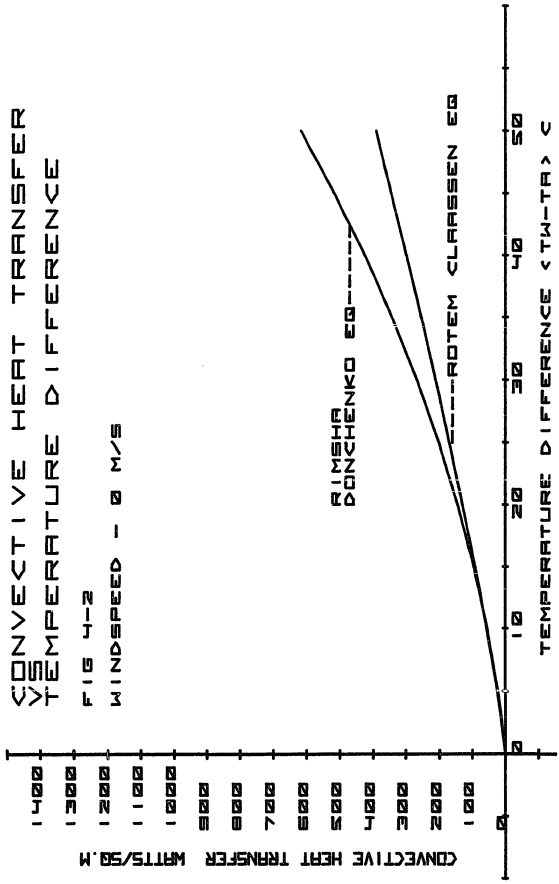

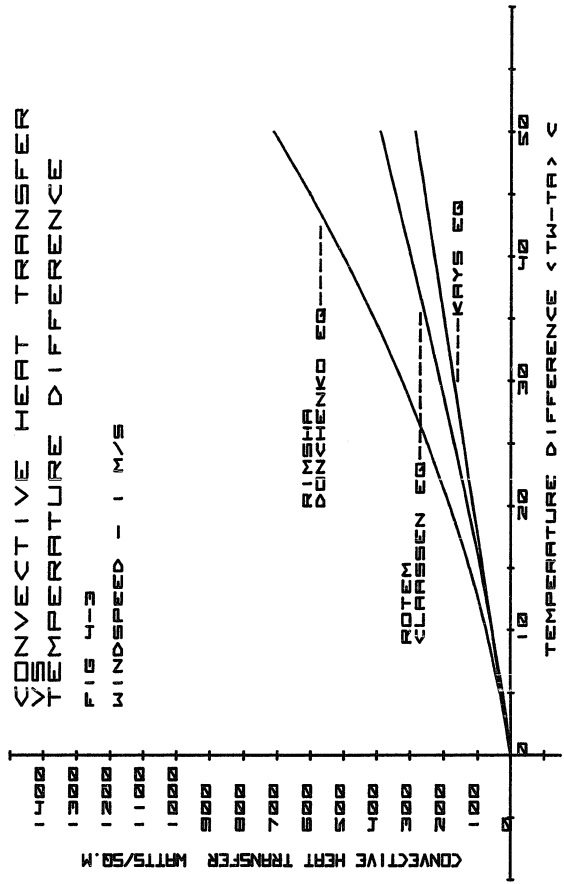

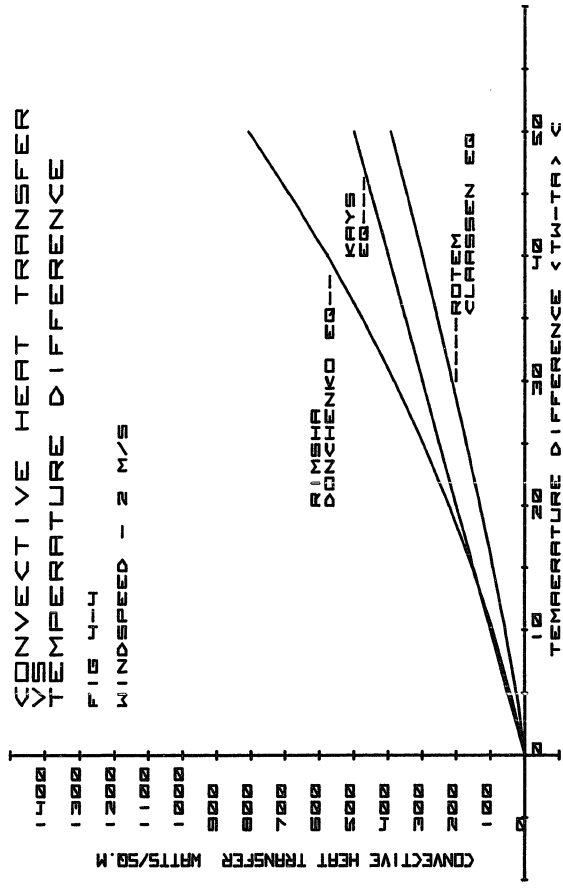

and the Rotem and Claassen equations for free convection. At 3 m/s wind, the Rimsha and Donchenko equation and the Kays equation are essentially equal for temperature differences less than 30 celsius degrees. Since the Rotem and Claassen equation is derived for free convection and contains no wind term, it does not apply to the cases of wind greater than zero; however, it is included in Figures 4-2, 4-3, and 4-4 for reference.

The empirical approach of Rimsha and Donchenko applies throughout the entire wind speed range. Kays' equation, however, does not begin to compare favorably with the others except for winds over 2 m/s. This is to be expected, since Kays' equation was derived for an external boundary layer and should not be valid for conditions of free convection where the traditional boundary layer does not exist. This is the realm that Rotem and Claassen addressed; and their equation exhibits fair agreement with the experimental approach of Rimsha and Donchenko when a value of $n = -0.4$ is used. (The isothermal plate situation (i.e., $n = 0$) yields values of Q_H that grossly underpredict Rimsha and Donchenko's equation.) Above 2 m/s, however, Kays' equation agrees closely with the Russian empirical formula (Figures 4-5 and 4-6).

During ice fog conditions, the wind is essentially absent, suggesting the use of the Rotem and Claassen or the Rimsha and Donchenko equations. However, since considerable difference exists between these two equations for the higher temperature differences present during ice fog, another comparison would be desirable to verify one equation or the other. The Bowen ratio provides such an opportunity for comparison. Bowen's ratio can be written (Bowen, 1926):

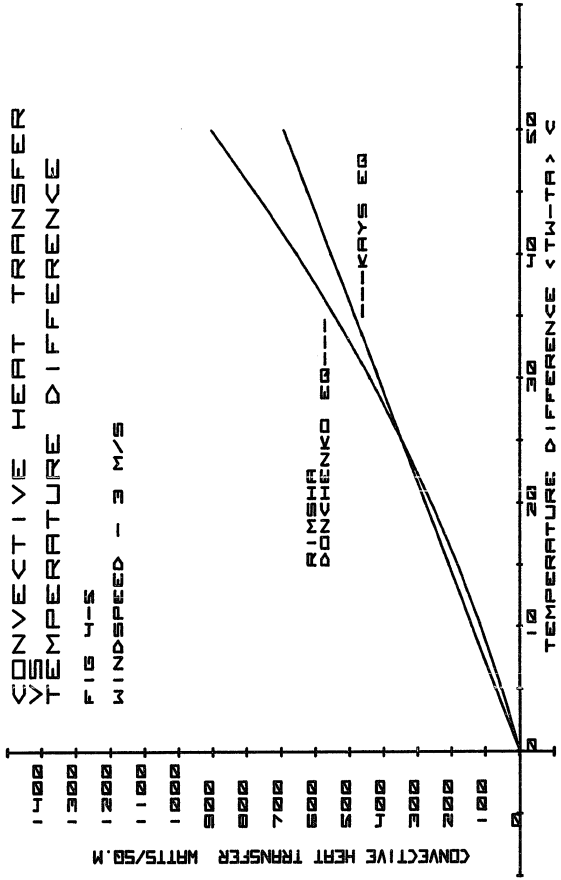

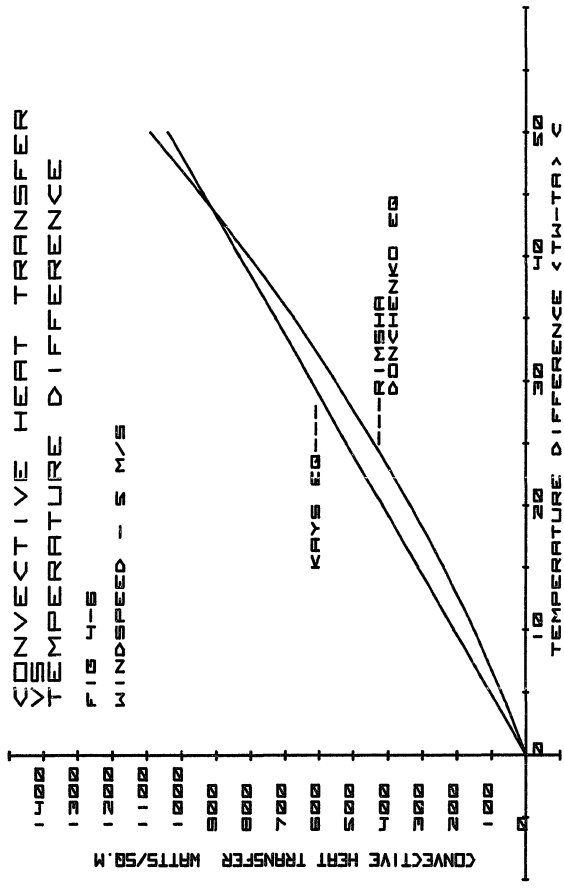

$$R_B = \frac{Q_H}{Q_E} = (6.1)(10^{-4})\ P\ \frac{T_w - T_a}{e_w - e_a} \qquad 4\text{-}14$$

where:

Q_H is the convective heat loss

Q_E is the evaporative heat loss

P is the pressure in the same units as "e"

T_w is the water surface temperature

T_a is the air temperature

e_w is the saturation water vapor pressure at the water surface temperature in the same units as "P"

e_a is the water vapor pressure at the air temperature[1]

A comparison of Bowen's ratio, using Equation 4-14 for conditions over open water at 10° C, evaporation data from Chapter Two, and the convective heat loss predictions of Equations 4-6 and 4-3, is shown in Table 4-1.

It is interesting to note that for higher values of temperature difference, Rotem and Claassen underpredict the Bowen ratio, while Rimsha and Donchenko overpredict. This would suggest that still another equation might be found that would compare more favorably with the Bowen ratio shown in Table 4-1. Figures 4-7 and 4-8 show plots of two other equations proposed for convective heat transfer in the environment. Fishenden and Saunders' equation (Sutton, 1953) applies only to free convection, while Devik's equation (Devik, 1932) is an empirical relation that was derived from measurements in Norway.

---

[1] Saturation vapor pressure can be used with very little error at ice fog temperatures.

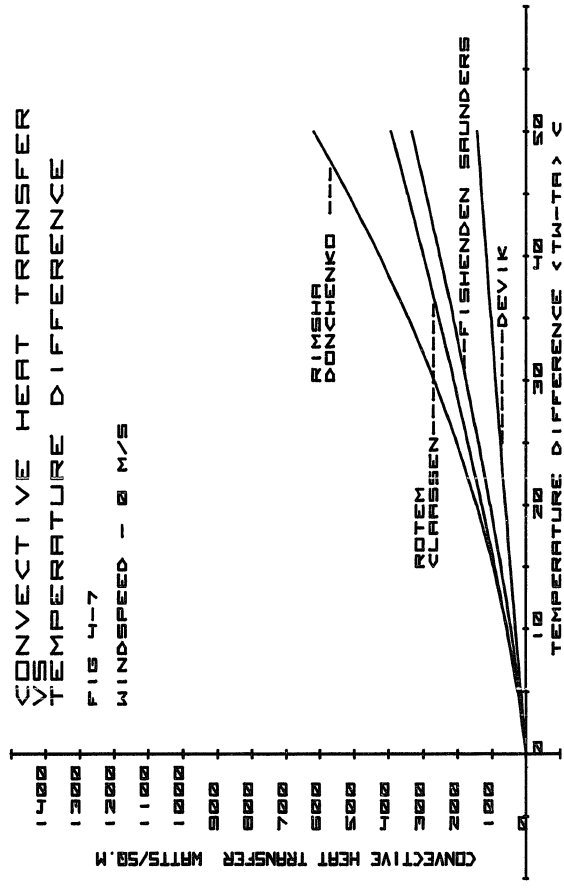

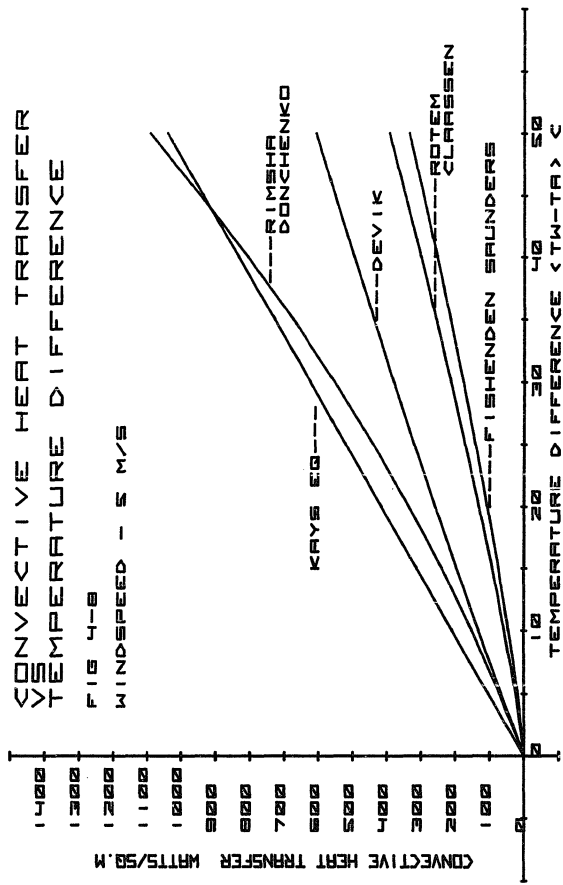

Table 4-1

Bowen's Ratio

T_w = 10° C; P = 1030 mb

T_a	$T_w - T_a$	$e_w - e_a$	R_B	Q_E[1] Avg	Bowen's Ratio Rimsha et al[2]	Bowen's Ratio Rotem et al[2]
0°	10	6.168	1.020	140	.45	.45
-10°	20	9.412	1.375	148	1.04	.94
-20°	30	11.021	1.710	155	1.70	1.40
-30°	40	11.766	2.140	163	2.60	1.80
-40°	50	12.086	2.600	171	2.80	2.30

[1] Q_E are from Table 2-1, curve averaged for Q_E vs ΔT (w)(m^{-2}).

[2] From Figure 4-2.

Fishenden and Saunders' equation is:

$$Q_H = 2.5\ (T_w - T_a)^{5/4} \qquad \text{(watts)}(m^{-2}) \qquad 4\text{-}15$$

Devik's equation is:

$$Q_H = 0.0213\ T_m \sqrt{u + 0.3}\ (T_w - T_a) \qquad \text{(watts)}(m^{-2}) \qquad 4\text{-}16$$

where:

$$T_m = \left(\frac{T_w + T_a}{2}\right) + 273^\circ\ C \qquad 4\text{-}17$$

Obviously agreement between different theories and studies is not forthcoming, since neither of these equations shows a good correlation to either each other or to the others previously discussed.

Heat Budget at the Surface

A heat balance at the water surface may now be written:

$$Q_{in} = Q_E + Q_H + Q_{R_{net}} \qquad 4\text{-}18$$

Air temperatures (T_a) of -30° C are characteristic of average ice fog temperatures. The surface temperature of the cooling pond will be assumed to be +10° C. The average evaporation at these temperatures is 155 (w) (m^{-2}) (Figure 2-9). From Chapter Three the average radiation heat loss for these conditions (using the revised Anderson equation for atmospheric radiation) was found to be 188 (w)(m^{-2}) (Figure 3-10).

From Figure 4-7, Rotem and Claassen predict the convective heat loss to be 300 (w)(m^{-2}); the percentages are given in Table 4-2. Other values in Table 4-2 are computed in the same way. Figure 4-9 shows the components of the heat balance during ice fog plotted against temperature differences.

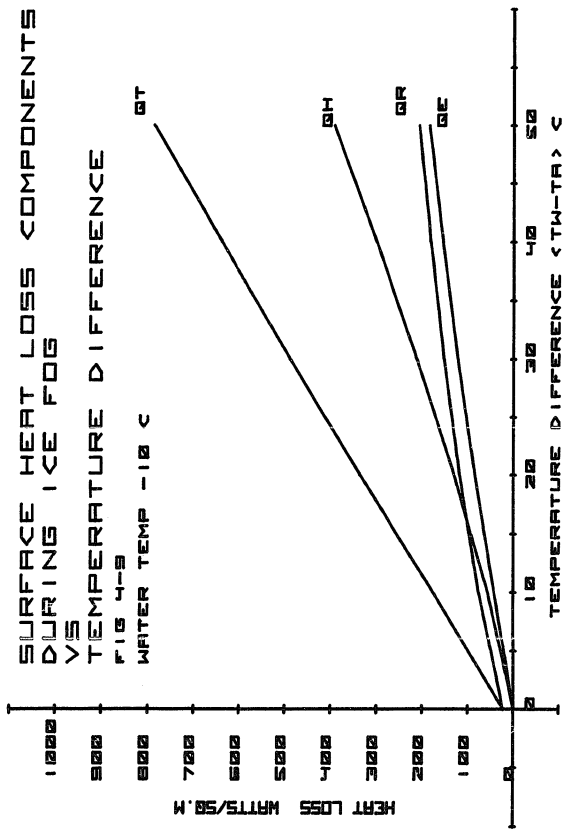

Table 4-2

Temp diff.	% Heat Budget at the Surface Q_E	Q_H	Q_R	Q_T	h_o
	%	%	%	$(w)(m^{-2})$	$(w)(m^{-2})(°C^{-1})$
10	25.5	25.5	49	157	15.7
20	25	38	37	319	15.9
30	25.5	43	32	490	16.3
40	24	47	29	643	16.1
				Avg	16.0

Since all three heat losses are a function of temperature difference, an overall heat transfer coefficient (h_o) can now be defined such that:

$$Q_T = h_o (\Delta T)$$

where:

Q_T = total heat flux $(w)(m^{-2})$

It is interesting to note that the value of h_o remains nearly constant through the range of temperature differences considered.

This overall heat transfer coefficient could be used for quick calculations of total heat transfer from an open water surface during winter conditions.

Conclusions:

The large volume of experimental data reported by Rimsha and Donchenko from many different sites in the Soviet Union, along with the relatively good agreement with the theoretical approach of Kays at 5 m/s wind speeds, lends support to the use of this equation for convective heat transfer during windy conditions. In addition to this, the good agreement

with the theoretical approach of Rotem and Claassen for free convection conditions, along with the very close agreement with the Bowen ratio, gives support to these equations for free convective heat transfer for temperature differences up to 20 celsius degrees. When ice fog exists, high temperature differences are combined with very light wind. This condition needs much study to develop conclusive relations for convective heat transfer during these times.

Convective heat loss represents a significant portion of the overall heat loss from an open water surface during ice fog conditions. For temperature differences of 30 celsius degrees and winds of 1 m/s, the convective heat loss according to the Rimsha and Donchenko equation is 340 (w)(m^{-2}) (Figure 4-2). If the entire pond were open water, this would be as large as 90% of the heat input (as shown in Chapter Six). If this condition should exist, the high rate of heat loss would cause an increase in ice cover, restoring the heat balance between convection, radiation, and evaporation.

CHAPTER FIVE - ICE FOG SUPPRESSION TECHNIQUES

Ice fog is usually confined to an area near the source, and boundaries of the cloud are usually sharply defined. A short distance outside the cloud, visibility can be unlimited; while only a few feet inside the cloud, it may be less than 15 meters. A typical experience of pilots during winter operations in Alaska is to find unlimited visibility all along their route, but at their destination a mound of ice fog covers the airport, making landing impossible. (Often visibility down through the relatively shallow layer of fog is such that the airport and surrounding buildings are visible from directly above, but as the approach for landing proceeds, the runway must be viewed through an increasingly greater thickness of ice fog; consequently, the visiblity problem becomes such that the runway disappears during the final stages of the approach.) This leads to the speculation that perhaps the problem could be eliminated by a means of controlling the location and path of the cloud so that the runway (or other critical visibility area) is outside it. At the Eielson Air Force Base runway an abundance of clear air exists outside the perimeters of the base. The only off-base concentration of population sufficient to cause ice fog in observable quantities is in the Moose Creek settlement, to the northwest. To the west and south of the runway, clear air is inexhaustible.

Fans

Moving clear air over the runway to exclude the ice fog offers an interesting possibility; a line of blowers or fans along the west edge of the runway might be used to blow the ice fog away. The fans, properly spaced and moving air at the correct velocity so that turbulence and crosswind are not a problem for landings, should eliminate the landing visibility problem. Assuming that the length of the runway (14,000 feet) must be kept clear, that a height of 30 feet would be sufficient, and that a velocity of 2 m/s (4 knots) would not cause a disruptive crosswind for aircraft operations but would be strong enough to overcome the density gradient flow of the ice fog (usually in the order of 1 meter per second), the power required to move the necessary air would be approximately 150,000 horsepower. Ignoring transmission line losses, this would require an additional power generation of over 110,000 kilowatts at the power plant, thus compounding the ice fog problem in that area. The capital equipment cost, both in air handling equipment adjacent to the runway and additional generating capacity at the power plant, is somewhat discouraging; however, the biggest problem probably would be one of stopping the creation of local eddies of ice fog from flowing around behind the fans into the negative pressure area created by their suction, thereby negating their usefulness. The ducting required to prevent this on a scale the size of the runways makes the capital investment prohibitive.

A more logical and efficient approach to ice fog suppression is to eliminate the contaminant at its source. The source is diverse;

therefore, this approach also has its limitations. However, since the cooling pond is a major producer of ice fog (Benson, 1965), elimination of its contribution would be a significant step in the overall suppression problem.

Injection Wells

In eliminating the cooling pond's use during the winter months, water could be drawn from the make-up wells to be used directly for cooling, and then be disposed of in an injection well downstream of the intake wells. In order to avoid using water that is too cold, a recirculating loop would be used to temper the incoming well water. With this installation in operation, the cooling pond could then be isolated and allowed to freeze. Since no heat would be injected into the pond, no open water would be present to produce ice fog.

Several advantages exist for this proposal, along with a few disadvantages. The system is simple and it offers a positive elimination of ice fog from the pond. It would require very little manpower to operate and the basic components are reliable. However, it would require more frequent cleaning of the condenser tubes, due to heavier mineral deposits from using raw water directly from the well. Further, should a pump fail, the plant would face a cooling crisis; therefore, backup systems would have to be provided. (An injection well would also have to be installed.) The present cooling pond could serve as emergency backup, either as a water source or as a replacement for the injection well. The well would have to comply with health and safety regulations since the potential exists for injecting contaminated water into the groundwater, which is

used by residents of the area for drinking water. Even with these considerations, however, it appears to be a more practical approach than the fans discussed earlier in this chapter.

Latent Heat Storage

Another approach to eliminating ice fog from the pond is to maintain an ice cover over the pond while the pond is still used for the primary cooling source. This requires that the heat from the power plant be dissipated by conduction through the ice and by melting of the stored ice reserves. The advantage of this plan is mainly its economy. The present installation can be used with only a minimal modification, and all equipment necessary for the modifications is available from surplus Air Force equipment. The water available for cooling is of better quality, having been treated by passage through the pond, and all the necessary backup equipment is already installed. In addition, no adverse effects to the groundwater aquifer need to be studied before the system can be installed and tested. Chapter Six discusses this technique and its testing and performance in detail.

Monomolecular Films

Another method of suppressing the ice fog from the pond is to use heavy alcohols for suppression of evaporation from the surface. This has been successfully used in a number of reservoirs in warmer climates to reduce evaporation losses (Bean and Florey, 1968; Crow, Allen and Fry, 1969). Success has been good, by all reports, with evaporation suppression ranging from 6 percent to 62 percent. The heavy alcohols form a

monomolecular film over the water surface. Although one (mono) molecular film is theoretically all that is necessary, in practice it is found that several layers exist due to difficulties in application. It is easier to apply an excess of the relatively inexpensive chemical than to risk not applying enough for complete coverage.

Several methods of application have been tried, including dissolving in appropriate solvents, spraying slurries of water and alcohol, and hand spreading from a boat.

The problem of heat transfer through the film is of concern, since the function of the cooling pond is to dissipate waste heat from the power plant. Since there is no ice to melt with this technique and little evaporation, heat must be dissipated another way. If the temperature of the pond is to remain relatively constant, conduction and storage will not change. Radiation, however, will increase significantly since the water surface, no longer covered by ice, will radiate at a much higher flux than the colder ice surface. Convection losses will also increase, for the same reason. From the heat budget measurements during the melting experiments (described in Chapter Six, Table 6-1), the average heat loss to melting is seen to be 6.4×10^6 watts. Subtracting the radiation losses measured over ice cover (Table 3-2) from the net radiation measured over open water, gives a net increase of radiation for the uncovered pond of:

$$119 - 54 = 65 \text{ (watts)}(m^{-2})$$

Estimated net convection losses (Figure 4-3) for a 1 m/s wind and -30° C, average approximately 520 (watts)(m^{-2}). Subtracting the losses

during melting, when the pond was ice covered (1 m/s and 10 celsius degrees), gives a net increase of convection losses for the uncovered pond of:

$$520 - 90 = 430 \text{ (watts)}(m^{-2})$$

These two losses add up to 496 (watts)(m^{-2}). It therefore requires 12,903 square meters of pond surface to replace the "melting heat loss" that is not available by this technique. Slightly less than 30% of the area of the pond is therefore needed to dissipate the required amount of heat for power plant operation at these air temperatures. The remaining 70% of the pond is available as reserve cooling capacity. The use of monomolecular films, therefore, appears to be technically feasible for this application.

To test the effectiveness of the evaporation retardant during below freezing conditions, two evaporation pans were used on the Eielson cooling pond. After establishing an evaporation base line, hexadecanol was added to one of the pans. Figure 5-1 shows the results. Evaporation in the treated pan dropped by over 80 percent the first period, and continued to remain significantly lower than the control pan until the test was suspended 120 hours later. The average suppression during the period was 84 percent. On March 22 hexadecanol was spread over the entire pond surface. Figure 5-2, although of poor photographic quality, shows the results. A breeze from the right side of the figure had concentrated the film on one side of the pond. The boundary of the film can be seen as a sharp line between the surface without vapor and the uncovered water surface with a normal vapor cloud visibly rising from the surface. This also points out one of the major problems to be resolved in using these

FIGURE 5-1

EVAPORATION SUPPRESSION WITH HEXADECANOL

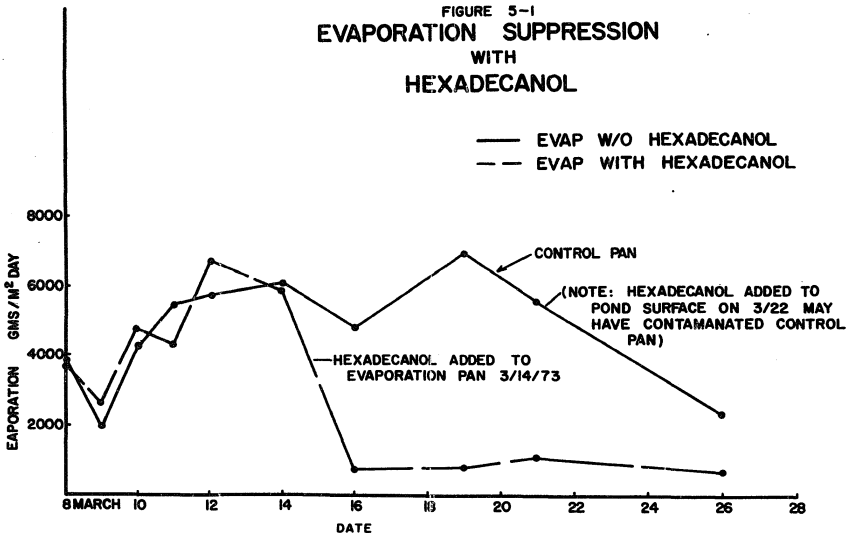

Figure 5-2. Hexadecanol Film Boundaries on the Water Surface.

films for evaporation retardation; i.e., maintaining the integrity of the film. Even the slightest breeze or water movement will move the film to one side of the pond, leaving areas of open water. This problem was not apparent in the pan, partially due to the fact that a large surplus of hexadecanol was available to maintain the film, and partially because of the size of the surface. The film has enough internal strength to keep itself intact on the smaller pan surface. This leads to the speculation that the problem could be solved with a floating grid which breaks the pond into small areas on which the film can maintain a continuous cover.

One other problem needs to be considered, that of bacterial degradation of the film. Flavobacterium and Pseudomonas, among others, are commonly found in ponds and lakes, and reportedly thrive on the film (Chang, et al, 1962). As the film is applied, the population of these bacteria increases sharply, feeding on the film and its degradation by-products. As the population of these bacteria increases, the film life decreases, until the utility of the film is destroyed. Although no observations of this problem were made at Eielson, two factors are favorable for reducing the magnitude of the problem when heavy alcohols are used for ice fog suppression. The first is the temperature of the film. During ice fog, the film temperatures are significantly below those found during the experiments reported in the literature. Lower temperature should do much to suppress the growth of the bacteria. Secondly, the pond can be disinfected by either adding a bactericide to the hexadecanol, or by adding it between applications of the alcohol during periods without ice fog.

This technique offers several advantages. It is the simplest and least expensive of any approach thus far investigated. Chemicals for an entire ice fog season would not cost more than a few hundred dollars. Applications can be done by one person in an hour and require only a small boat and a spreading device such as a hand-held lawn seeder. (Actually, the chemicals can be spread by "hand sowing" if the seeder is not available.) Application need be repeated only every few weeks during the ice fog period. No manpower is required between applications for monitoring or operation of equipment.

On the negative side, however, several items need to be resolved and a few disadvantages do exist. First, the floating grid discussed above must be designed and built, and the design problems worked out. Secondly, the bacterial degradation needs to be examined under cold weather conditions, and the disinfecting techniques need to be worked out.

Other heavy alcohols are available and indications are that some of them may be even more efficient. It appears from present investigations that the longer the alcohol chain, the more effectively it suppresses evaporation (Dressler, 1969). In this respect, hexadecanol (C_{16}) may be surpassed by heptadecanol (C_{17}), octadecanol (C_{18}), nonadecanol (C_{19}), or eicosonal (C_{20}). None of these other chemicals have been tried under ice fog conditions; however, during tests in warmer (above freezing) temperatures, they are reported to surpass hexadecanol by a considerable margin (Noe and Dressler, 1969). Evidence also exists to suggest that combinations of the different alcohols may have some advantage (Dressler, 1969). An organized testing program should be implemented to determine the optimum chemical under actual conditions.

Finally, a disadvantage to the technique is that the suppression is not complete. The 84 percent suppression obtained with hexadecanol may be optimized to an even higher value with some of the other chemicals listed above. However, some evaporation will still take place and a percentage of evaporation will still produce ice fog. This should not be of too great a concern, however, since the pond is reduced to the category of a minor ice fog producer instead of the largest source in the area.

The technical problems and unresolved questions concerning this technique seem to be much smaller in magnitude than any of the other techniques investigated thus far. It certainly warrants further investigation before any expensive capital investments are made to implement any of the other techniques considered.

Up to this point attention has been focused on dissipating heat in the pond in a manner that would not produce ice fog. It is perhaps prudent to recognize the possibility of practical use of at least a portion of this heat input. Average incoming water temperature was 25° C. This, of course, is too low for direct use in heating of residences. However, the magnitude of heat input (17.9×10^6 watts) suggests that some practical use might be found (especially in light of the current energy crisis). Such possibilities as using the water to heat hangar floors, parking lots, unheated garages, and warehouses should be analyzed for their economic implications. Heat pumps and turbines using Freon cycles should be investigated. Perhaps this waste heat might be used to warm the solid waste landfill to stimulate the biological processes

therein. This would be better than the complete waste of this resource in the cooling pond. Economics, of course, will have to prevail; however, in light of today's concern with the environment, and the awareness of dwindling energy supplies, perhaps new costs will make some of these proposals economically practical.

CHAPTER SIX - LATENT HEAT STORAGE EXPERIMENTS

Any method for ice fog suppression is subject to two overriding considerations. First, the method must be inexpensive (i.e., cost less than the cost of the ice fog). Secondly, the method must be applicable to use in the extreme cold of ice fog conditions. When applied to power plant cooling ponds these considerations quickly eliminate a number of large scale solutions (such as enclosing the entire cooling pond in an "astrodome"). One technique that appeared to warrant investigation, however, was to cover the open water surface with a thick layer of ice. This not only greatly suppresses the ice fog[1], but also furnishes a sink of latent heat that can absorb the heat output of the power plant cooling water. Thus, the power plant can continue normal operation without any negative effect from the suppression. The cost of the operation would be low since it would use normal arctic weather to provide cooling, and the only energy requirements would be the pumping required to enhance the freezing process.

Freezing Rates

As an ice sheet grows in thickness, all the heat loss necessary for freezing must be transferred through the ice sheet to the cold air above.

---

[1] The vapor pressure over ice is only slightly lower than over water, but the surface temperature of the evaporating ice surface is several tens-of-degrees colder than that of open water, reducing the evaporation to the point where it is no longer visible.

A first approximation to the rate of growth of the sheet can be made by equating the latent heat of the freezing water to the normal conductivity of the ice sheet. This yields Stephan's Law for ice growth (Pounder, 1965):

$$x = \sqrt{\frac{2k\ D}{L\rho}} = C\ \sqrt{D} \qquad 6\text{-}1$$

where:

x = the thickness of the ice sheet

k = the thermal conductivity of the ice

L = the latent heat of fusion of the water

ρ = density of water

D = the freezing exposure at the surface of the sheet in degree-time

$C = \sqrt{\frac{2k}{L\rho}}$

The ice growth rate is seen to be proportional to the square root of the freezing exposure. Thus, time required for the sheet to grow increases as the square of thickness. When building ice sheets for suppression, this situation is intolerable; an ice sheet of several feet must be formed in a matter of days and then grown again after each ice fog episode. To avoid this restriction, the sheet must be thickened by freezing on the top where each new layer of water is in direct contact with the cold air, thus eliminating the insulating effect of the ice (or at least restricting it to the skim ice on top of the layer of water). To accomplish this, water must be applied to the surface of the ice in successive layers of the proper thickness to freeze at an optimum rate.

Cooling Pond

The Eielson power plant cooling pond (Figure 6-1) is 168 meters wide and 305 meters long with a dike 15 meters wide dividing it into two ponds 76 meters wide and 305 meters long. A channel 30 meters wide connects the two sides at the east end of the pond. During normal operation, water enters the receiving pond and proceeds through this pond around the east end of the center dike to the west end of the intake pond, where it is pumped back to the power plant. In the winter, ice forms naturally over approximately the west one-half of the intake pond, leaving the remaining portion of the intake pond and all of the receiving pond unfrozen (3.48×10^4 m^2). Average pond depth is 3 meters, giving a volume of 1.04×10^5 m^3.

An 8-inch pipe runs along each side of the receiving pond with 36 spray nozzles spaced every 12 meters. This provides a means of spraying water onto the surface of the pond. The header was supplied with water from beneath the ice cover by a 6-inch centrifugal pump. Valving was arranged to permit spraying on either or both sides of the pond. The header on each side can be drained separately to avoid freeze-up. A diversion line was installed from the west end of the receiving pond to the west end of the intake pond, enabling the cooling water from the power plant to be "short-circuited" directly to the intake pond. In this manner the receiving pond side is isolated from hot water input from the power plant.

Two plastic sheet dams were installed across the connecting channel at the east end of the dike (Figure 6-2) to eliminate density gradient

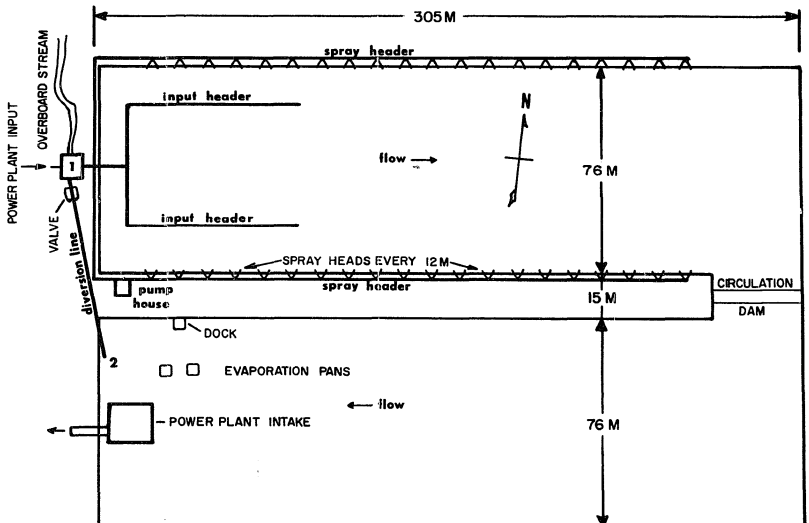

FIGURE 6-1

Figure 6-2. Polyethylene Film Circulation Dam.

circulation of warmer water from the intake pond to the receiving pond. The receiving pond was therefore free of all heat inputs, so that freezing could take place by natural means.

As soon as the natural ice sheet was 5 cm thick, spraying would commence to start thickening the ice cover. When a layer of water one centimeter deep had been applied to one side of the pond, the valves would be switched and the opposite side of the pond sprayed. At the end of spraying for the day (usually around midnight), a 3 cm layer of water would be built up on each side. It was found that 3 cm would freeze in an 8-hour period. When an ice fog event began (i.e., the temperature dropped below -25° C), all spraying would cease. The diversion of the water to the intake pond would be stopped and the water would be directed back into the receiving pond. This would then give the open water of the intake pond an opportunity to freeze. Ice cover on this pond was found to form in approximately 25 hours at air temperatures of -25° C. When the intake pond was frozen, the ice cover of the entire pond was established.

Ice fog would not be generated from this source until the warm cooling water of the power plant, injected into the receiving pond, melted enough ice to form a hole in the ice sheet and expose open water. The time required for open water to appear was a function of the air temperature and thickness of the sheet at the beginning of the episode.

Early in the freezing experiments, it became apparent that the system had some inadequacies. The pump supplying spray water was not producing sufficient pressure to spray the water far enough out onto the ice sheet. The flow and freeze characteristics of the water at the

working temperatures were such that it would not flow more than 12 m before freezing. The result was that a strip along each side was thickened, but the center was left unflooded to thicken by "natural" means.

The first spray nozzles had a 0.95 cm diameter opening. It was found immediately that the spray from these nozzles was too finely divided. At -20° C none of the water leaving the nozzle would reach the ground in the liquid state. Instead, snow was created which built up in large mounds along the bank (Figure 6-3). This added little to the thickness of the ice cover. After experimenting with different sizes of nozzles, a 1.9 cm diameter was found to be optimum[1]. Larger nozzles, of course, had lower head loss and a greater flow; however, this generated a problem of its own. The larger stream impinging on the sheet of ice had great erosive power. This was partly due to mechanical erosion and partly due to melting caused by the 4° C water. The stream would erode through a 30 cm ice sheet in 60 minutes. As soon as a hole was opened, any unfrozen water on the surface would drain back into the pond. This was corrected by installing a rotatable nozzle (Figure 6-4). The stream was then changed to a new position every 15-30 minutes.

---

[1] An additional problem with the smaller nozzles was their tendency to freeze closed, stopping the flow through that portion of the pipe. When this happened at the end of the header, the water in that portion of the header pipe would freeze and that portion would be lost. The larger nozzles showed no tendency to freeze even when used at -50° C.

Figure 6-3. Snow-Ice Buildup around Spray Nozzle.

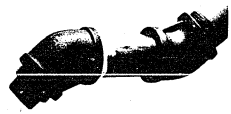

Figure 6-4. Rotatable Nozzle.

Ice Building

The rate at which an ice sheet can be thickened is a function of many variables. Outside air temperature, flood water temperature, wind conditions, cloud cover, initial ice temperature, and method of flood water application, all combine to determine the rate at which ice will form. In previous chapters most of these factors have been discussed in some detail. The only variable that has not been discussed (the only variable that is usually controllable) is the method of application.

Ideally, the water should be applied in thin layers at 0° C. As latent heat is removed, crystals of ice start to form and the layer becomes a slush that has very poor flow characteristics. If flow proceeds after this, a spongy porous ice is produced. The result is low density ice with lower latent heat capacity and relatively thin unflooded areas between flooded sections - an undesirable configuration. At the other extreme, when the water is applied well above freezing, the heat content of the water, as well as the latent heat of fusion, must be removed. A top skim of ice forms first, and thereafter the rate of freezing is subject to the limitations of Equation 6-1.

Nonuniform thickness is undesirable since it allows subsequent melting to open up areas of open water and form ice fog before the bulk of the latent heat stored in the thicker portions of the sheet is used. Therefore, a compromise must be made in the freezing technique. This compromise will vary with each change in the weather conditions, and is therefore difficult to optimize. Several methods of application were tried. Each one will be discussed separately. However, all methods are

subject to the maximum amount of heat that the system as a whole can remove.

Ice Growth Rate - Maximum System Limitation

The active air mass that covers the pond is approximately 7.5 meters deep. The intake pond area is 2.3×10^4 m^2, giving an effective air volume of 1.7×10^5 m^3.[1] An ice growth rate of 2.54 cm per hour over the entire receiving pond surface requires a pumping rate (F) of:

$$F = (2.3 \times 10^4)(2.54 \times 10^{-2}) \frac{1}{60} = 9.7 \ (m^3)(min^{-1})$$ [2]

The heat (Q) that must be removed to freeze an area of 2.3×10^4 square meters of 4° C water 2.54 cm deep is:

$$Q = (\text{mass of water})[(\text{temperature drop})(\text{specific heat}) + (\text{latent heat to be removed})]$$

$$Q = (2.3 \times 10^4 \ m^2)(2.54 \times 10^{-2} \ (m)(hr^{-1}))(1 \times 10^6 \ (g)(m^{-3}))$$
$$[(4° \ C)(1 \ (cal)(g^{-1})(°C^{-1})) + (80 \ (cal)(g^{-1}))]$$
$$= 4.9 \times 10^{10} \ (cal)(hr^{-1}) = 56.9 \times 10^6 \text{ watts}$$

If we assume that the effective air mass passing over the pond can be raised 5.5° C (the average recorded temperature rise is 4° C, upstream to downstream), then the mass of air necessary to dissipate this heat is:

$$m = \frac{Q}{c_p \Delta T} = \frac{4.9 \times 10^{10}}{(.24)(5.5)}$$
$$= 3.7 \times 10^{10} \ (g)(hr^{-1})$$
$$= 2.5 \times 10^7 \ (m^3)(hr^{-1})$$

---

[1] This is conservative on the high side since the air mass affected cannot be much greater than the highest arch of the spray. This is generally below 6 meters.

[2] The pump installed provided a maximum of 1.5 $(m^3)(min^{-1})$ with a discharge head of 5.17×10^5 $(N)(m^{-2})$. However, it could be set up to provide 3.78 $(m^3)(min^{-1})$ if only 2.76×10^5 $(N)(m^{-2})$ were required.

The effective air volume is 1.7×10^5 m^3; therefore, 182 air changes per hour are needed. If wind blows across the shortest dimension of the pond (76 meters), then a wind velocity of (182)(76) = 13,832 m/hr = 3.8 m/s would be required to form 2.54 cm of ice per hour.

Evaporation Heat Loss - Maximum

Heat loss to evaporation will be limited by the temperature and incoming humidity.

Temp	Wt. of Water in Saturated Air
-20° C	2.6×10^{-4} kg/kg of dry air
-10° C	4.6×10^{-4} kg/kg of dry air
0° C	7.9×10^{-4} kg/kg of dry air

If we assume that air enters the pond area with relative humidity equal to zero and leaves saturated, and the effective air mass flow is:

$$M_a = 4.04 \times 10^7 \text{ kg per hour}$$

then the maximum possible mass and heat lost to evaporation is:

Temp	Mass Kg per hour	Heat loss watts
-20° C	10,504	6.6×10^6
-10° C	18,584	11.6×10^6
0° C	31,916	19.7×10^6

This heat loss will freeze the following amounts of ice:

Temp	Kg per hour	Cm per hour
-20° C	71,250	.279
-10° C	125,000	.543
0° C	212,500	.924

Realistic Growth Rate

Using the average meteorological values measured at Eielson of $\Delta T = 4.0^\circ$ C, average wind = 1.7 meters per second at 6 meters above ground, and an effective air mass of 1.5×10^5 m^3; and assuming that all heat transfer is done during the flight of the droplet before impact and that the convective heat transfer efficiency (η) is $\eta = .6$, the rate of freeze for the system can be estimated. The convective heat transfer capacity is:

$$Q_H = (\eta\,[m\, c_p\, \Delta T]) = (.6)(1.5 \times 10^5)(1.7)(3600)(.24)(1400)(4)$$
$$= 11.3 \times 10^6 \text{ watts}$$

The realistic evaporative heat transfer is probably about 30 percent of the maximum values calculated above. A maximum realistic value would then be:

$$Q_E = 5.9 \times 10^6 \text{ watts}$$

Radiative heat loss from Chapter Three would be 84 (watts)(m^{-2}). Estimating the average spray stream area at 1000 times that of the emerging jet approaches realism since the streams were compact and did not break greatly over most of their flight. The area for 18 streams, 1.9 cm in diameter and 18 meters long, is:

$$A_S = (18)(1.9 \times 10^{-2})(\pi)(18)(1000) \simeq 20{,}000 \text{ m}^2$$

This gives a radiative heat loss of:

$$Q_R = (84)(20{,}000) = 1.68 \times 10^6 \text{ watts}$$

and the total heat transfer (Q_T) will be:

$$Q_T = Q_H + Q_E + Q_R = 11.3 \times 10^6 + 5.9 \times 10^6 + 1.68 \times 10^6$$
$$= 18.8 \times 10^6 \text{ watts}$$

This will freeze the following volume of 4° C water:

$$V = \frac{(18.8 \times 10^6)(860)}{83{,}700} = 1.9 \times 10^5 \text{ kg per hour} = 190 \ (m^3)(hr^{-1})$$

or for a uniform spread over the pond, this is a growth rate (G) of:

$$G = \frac{190}{2.3 \times 10^2} \times 100 = 0.83 \text{ cm per hour}$$

This, of course, ignores the considerations of convective heat transfer from the droplet to the air, as well as the heat transfer within the droplets. It is assumed that these are not the limiting factors.

It is easily seen that under the above conditions, 1 cm per hour of freezing is overly optimistic, and .75 cm per hour is closer to the upper limits of the system.

Peyton and Johnson (1967), in their Kotzebue trials, were only able to sustain a growth rate of 8 inches in 24 hours, or 0.76 cm per hour. Johnson feels that this is the upper limit of growth rate using spray techniques. (In addition, the area in which their experiments were conducted is subject to much higher winds than are normal for the Eielson area.)

Ice Building Techniques

Spraying

The use of a spray to apply water to the surface of the ice sheet has the advantage of cooling the stream of water before it strikes the ice. The amount of this convective cooling can range from complete freezing of the stream, so that snow is produced, to merely cooling the water without any latent heat extraction. The degree of cooling can be controlled by nozzle configuration. Variable orifice nozzles have long been available that adjust from a thin compact stream to a very finely

divided mist. The cost of such nozzles is prohibitively high for a multi-station header. For the cooling pond experiment, a fixed orifice nozzle was chosen. The stream could still be varied by changing nozzles to fit the atmospheric conditions. However, at ice fog temperatures the chore of changing 36 nozzles was not looked upon with enthusiasm; and after a few changes, a good compromise nozzle was installed and rarely changed. A 1.9 cm diameter fixed orifice nozzle was found to give good compromise between distance and stream break-up for the pressure produced. The nozzle configuration consisted of a pipe plug with a hole drilled in the center. The inside of the plug was naturally curved so that some streamlining of the flow occurred. These nozzles were tested against a group of commercial nozzles and found to give comparable performance at a fraction of the cost. (Fire hose nozzles were also tested and found to give approximately one and one-half the distance of any other nozzles tested, but at a cost of several times that of the inexpensive model chosen.)

The header along each side of the receiving pond was 275 m long and contained 36 nozzles (18 on each side). Two 45° elbows were installed at each nozzle port. The elbows provided a means for rotating the nozzle about its vertical axis to give wider coverage and alleviate the erosion problem at impact (Figure 6-4).

A second spray technique involved the use of an "Intelligiant" (Figure 6-5). This machine is basically a large spray nozzle whose direction is controlled by two hydraulic cylinders. One cylinder controls rotation about the vertical axis (azimuth) and the other one moves

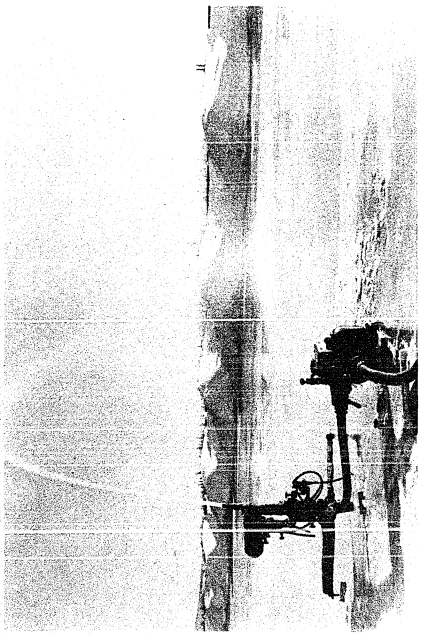

Figure 6-5. Intelligiant.

the nozzle about the horizontal axis (elevation). The rate of cylinder movement and the throw of each cylinder are adjustable, giving a very versatile spray program. The cylinders were driven by water from the pump which supplied the nozzle. A water pump is the only power source needed. The nozzle used is a fire nozzle, giving the device good range and excellent coverage. A radius of 30 meters and a sweep of 90 degrees were obtainable, providing the best coverage of any spray technique tested (730 m^2 per setting). Spray flow rate was 0.46 $(m^3)(min^{-1})$.

Flooding

Several techniques were explored for flooding the surface of the ice sheet. All suffered from the inability to spread the water evenly over large areas of the surface of the ice sheet, and the cooling realized from the spraying technique was absent. However, in some cases 0° C water could be drawn from just beneath the ice, tending to compensate for the loss of convective cooling during spraying. A short description of various flooding experiments follows:

A. A submersible pump was lowered into the water through a small hole in the ice. The discharge was directed through a "T" pipe onto the ice surface. The requirement for electrical power, and the long power lead reduced the versatility of the pump considerably. The discharge was too concentrated and, therefore, erosion was also a problem. Nor was the pressure head great enough to permit a spray discharge. Pump capacity was approximately 0.12 $(m^3)(min^{-1})$ (32 gpm) for a one-half horsepower pump.

B. A common ice auger can be used as a pump. Its pumping rate is approximately 3 $(m^3)(min^{-1})$ (800 gpm). It has the advantages of being portable so that flooding can be provided wherever more ice is needed. An additional advantage is that only one person is needed to operate it. It is fast, since it drills its own hole and then pumps out of it. On the negative side, it sprays the operator to the knees, so he must wear insulated hip boots. Another problem is that the weight of the water on top of the ice deflects the ice sheet downward so that a conical basin of water is created on the surface, with the auger hole in its center. Much of the water therefore drains back into the pond. This disadvantage can be countered by a simple drain-back shield in the form of a cylinder of sheet metal 20 to 25 cm high. This shield is frozen in place before flooding and blocks the drain-back of flood waters into the hole.

If the thickness of the ice sheet is less than the distance between convolutes of the auger (approximately 20 cm), the auger will pull into the hole by wedging the sheet between two of the convolutes and driving itself into the hole as the auger turns. In this situation a sleeve of adequate length must be inserted into the hole to eliminate the problem.

C. Outboard motors make excellent pumps, and will flood an ice surface with up to 7.56 $(m^3)(min^{-1})$ (2000 gpm). They have the same problem with drain-back as the auger, and they require a larger hole. A hole 60 cm in diameter will suffice. It can be easily cut with a chain saw (Figure 6-6). The pool of flood water from outboard flooding extends much farther than for any other type of flooding (Figure 6-7). This method was therefore better in providing uniform coverage. The operator

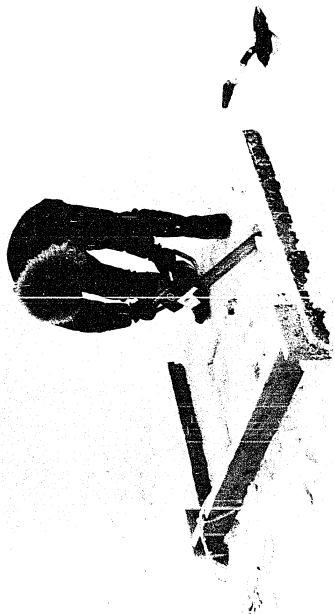

Figure 6-6. Cutting Ice for Flooding.

Figure 6-7. Flood Water on Top of the Ice Sheet.

was required to stand in ankle deep water during the flooding (Figure 6-8) and footing was treacherous unless crampons were used. Optimum angle of the outboard could be determined very quickly during operation, and the motor could be turned to direct the discharge in different directions.

The above techniques were found to be practical for localized ice building only. They were not suitable for large scale coverage on a pond of this size. An additional disadvantage was that the operator had to remain out in the cold for long periods; and, because of the time consuming nature of separately flooding each small area, the maximum depth that could be obtained in any one flood area was 7.6 cm per 8-hour day (0.95 (cm)(hr^{-1})).

D. Fire hoses were used to distribute water from the header into the center of the pond. They were extended from the header on the south side of the pond out onto the center of the ice sheet. Three 200-foot fire hoses were installed at 60-meter intervals along the header. The pressure loss in the hoses was so large that only minimal flow was achieved at the outlet. Erosion was also a big problem, and an attendant was required to change the position of the hose every half-hour. The wet 2-1/2 inch hose, partially frozen into the ice, was very difficult for one person to successfully wrestle into a new position. After 5 hours of exhausting effort, this method was abandoned. The effort yielded 10 cm of flood water in the center of the sheet; however, the area covered was only 25 percent of the pond surface, giving a net flood rate of 2.5 cm per 5 hours, or 0.5 cm per hour.

Figure 6-8. Flooding with Outboard Motor.

Ice Volume Measurements

The surface area of the ice sheet was nearly constant, varying only a few inches when the pond level changed. The volume was then easily determined by measuring the thickness. Thickness, however, varied widely due to nonuniform flooding, and therefore a large number of measurements were taken so that averages could be determined to give the total volume. A measurement net was established with lines at 60-meter intervals along the length of the pond and 15-meter intervals across the pond. This gave a total of 20 positions for monitoring thickness. Under some circumstances more holes were drilled to determine local changes that did not fit into the average pattern. During melting, the holes were redrilled every 24 hours to monitor the thickness loss. A common wood auger 1 inch in diameter, with the center screw ground away and an extension welded on for greater length, performed well. A battery-operated 3/8 inch electric drill was used to drive the auger (Figure 6-9). Thickness was measured with a hooked wire gage calibrated in inches. The wire was inserted in the hole and drawn out until the hook contacted the lower surface of the ice. The thickness was then read from the scale on the wire (Figure 6-10).

Melting Experiments

At the onset of an ice fog episode, the thickness of the existing ice sheet was monitored in the above manner. The diversion of water to the intake pond was then stopped and the entire output of cooling water from the power plant was directed under the ice. The thickness was remeasured at 24-hour intervals, and the amount of ice that had melted

Figure 6-9. Tapping the Ice Sheet for Thickness Measurements.

Figure 6-10. Ice Thickness Measurements.

in the interim was determined. Melting of the sheet was very dependent upon position. The first area to melt was directly above the input header at the west end of the receiving pond. As soon as open water was exposed above the header, the edge of the ice sheet melted from the inlet to the distal end until the entire pond was open water (Figures 6-11 and 6-12). Melting on the underside of the sheet showed a typical boundary layer pattern, with the heaviest melt occurring in the first 60 meters from the receding edge of the ice. Progressively less melting was noted as the distance from the edge increased, until at 180 meters from the edge no melting of any consequence took place (Figure 6-13). This is to be expected of flow along a quasi-infinite plate where a boundary layer between the moving fluid and the solid surface is established and continually thickens in the direction of flow. The thickening boundary layer provides progressively more and more insulation between the warm water and the ice sheet. Heat transfer to the sheet, consequently, progressively decreases.

The heat balance in the pond can be expressed by:

$$Q_{in} - Q_E - Q_c - Q_H - Q_R - Q_s - Q_m = Q_{out}$$

where:

Q_{in} = heat input to the pond

Q_E = evaporative heat transfer

Q_c = conductive heat transfer

Q_H = convective heat transfer

Q_R = radiation heat transfer

Q_s = heat storage

MELTING PROGRESS IN ICE SHEET

JANUARY/ FEBRUARY

FIGURE 6-11

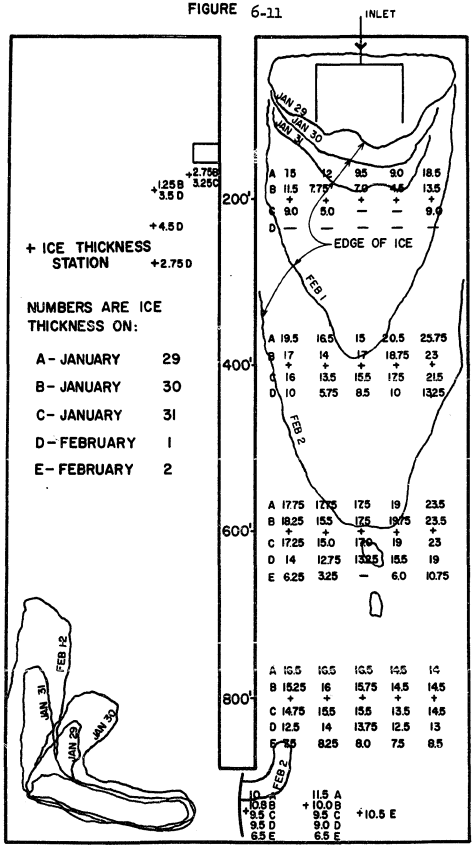

MELTING PROGRESS IN ICE SHEET

FEBRUARY

FIGURE 6-12

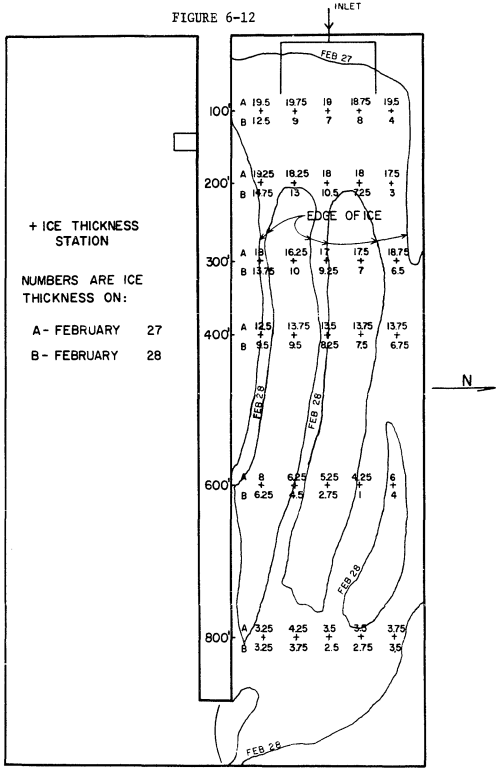

ICE THICKNESS
LONGITUDINAL CROSS SECTION
DURING MELTING 1973
FIGURE 6-13

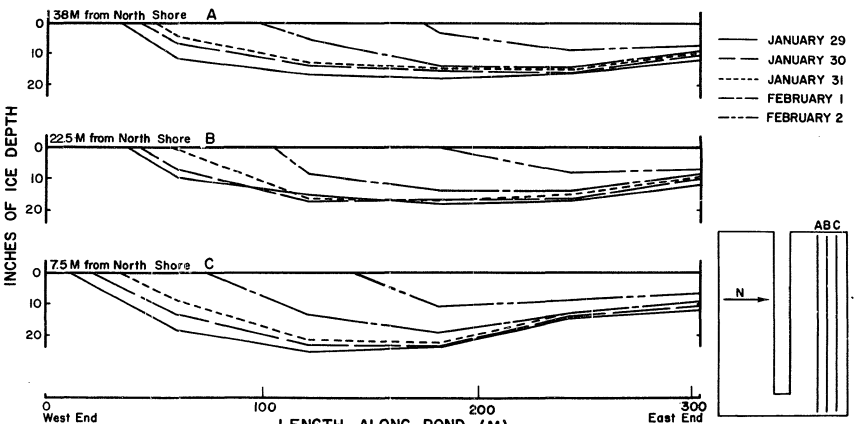

Q_m = heat of melting

Q_{out} = heat residual in water leaving the pond

Terms of the equation have varying proportions depending on the time since the beginning of the melt (Table 6-1). Heat loss through evaporation (Q_E) is initially zero, since the evaporation from the ice surface is negligible. As open water appears, Q_E starts to grow and increase in direct proportion to the open water surface area.

Total conductive heat loss (Q_c) through the ice is initially somewhat greater than that of evaporation. It decreases as the ice surface area decreases and is soon much smaller. The convective heat loss (Q_H) over the open water is a function of the air moving over the pond and the percentage of the pond that is open water. Radiative heat loss from the water (Q_{Rw}) also appears as a small portion of the total heat loss as melting begins. It is also a function of open water and surface temperature. Radiation and convective losses over the ice are accounted for in the conductive loss through the ice, and the assumption is made that they are large enough to remove all of the heat conducted through the ice sheet. Storage (Q_s) starts to increase as soon as the warm water is diverted back into the receiving pond. A component of the storage term occurs due to the influx of groundwater to make up for evaporation. This is a small portion of the storage term, however; calculations show it to be a third order term. Heat transferred to storage is small at first, but continually increases.

The heat lost to melting (Q_m) increases with time. This is a function of the temperature of the ice sheet, which initially is low and must be raised to 0° C before melting can proceed. As the temperature

Table 6-1

Heat Loss Components During Ice Sheet Melting
(watts x 10^{-5})

Period	1	2	3	4	5	Average
Date 1973	1/29-30	1/30-31	1/31-2/1	2/1-2	2/26-27	
(T_w-T_a)	20	33	38	28	23	
Open water (m^2)	3000	3600	7700	12600	3000	
Duration	27	19	24.5	24.5	24	
Q_E	2.4	4.6	11.6	15.1	2.5	7.2
Q_c	26.4	16.2	17.3	24.2	27.7	22.4
Q_s	-	2.1	40.2	5.8	66.5	28.6
Q_H	3.6	7.9	22.3	25.2	3.8	12.6
Q_{Rw}	3.6	5.8	14.5	18.9	3.7	9.3
Q_m	28.4	32.2	74.8	90.0	96.1	64.2
Q_{other}	-1.7	-9.3	-1.7	-1.2	-19.3	-6.0
Q_{in}	66.1	54.5	179.0	178.0	181.0	132.0
Q_m/Q_{in}	.42	.59	.42	.51	.53	.49

of the ice sheet rises, more of the heat transferred to the sheet will go into melting and will then show up in the measurement of ice volume lost by melting.

Instrumentation to measure the exact proportions of each of these terms was not available, nor was the required manpower. They can, however, be estimated from the measurements taken (Table 6-1). Heat lost by melting (Q_m) was determined by measuring the ice volume lost over consecutive 24-hour periods from the ice sheet thickness measurements discussed above. Evaporation heat loss (Q_E) was determined from data taken from the evaporation pans on the intake pond (see Chapter Two). Values for radiation heat loss from the water surface (Q_{Rw}) are derived using the considerations discussed in Chapter Three. The revised Anderson equation was used for atmospheric back radiation from the air above the water.

Convective heat losses (Q_H) are from values determined in Chapter Four. Storage (Q_S) was determined from measurements of the water temperature at the circulation dam in the channel between the receiving and intake ponds. Heat into the pond was calculated from measurements of the flow rate, and incoming and outgoing temperatures.

The net flow rate into the pond was measured by the following method:

Pond depth was closely monitored until a uniform depth was maintained for several days. The make-up wells were then activated until pond level had risen two inches above the base level. At this time both the wells and the hot water were stopped. The rate of fall of the surface was timed until the level had fallen to two inches below the base level.

Input water was then directed back into the pond and the level monitored to check to be sure that the level returned to the base line. Rate of flow out of the pond could then be measured with considerable accuracy.

The heat input to the pond in Table 6-1 was less during the first two days of melting, due to diversion of a portion of the input water to a small creek. Average normal heat input (reflected by the last three terms of Table 6-1) is 1.79×10^7 watts. A pan constant of 1.0 was used for evaporation (see Chapter Two).

The surface areas of the remaining ice sheet and open water could not be measured with great precision, since approaching the thin edge of the melting ice was precarious. However, a great deal of care was taken to see that the measurements were as accurate as possible.

Ice-Fog Suppression Considerations

Since nearly one-half of the heat input to the pond is used to melt ice, and most of the rest is dissipated through radiation, evaporation, and convection, and since it was possible to maintain an ice cover for several days, ice fog suppression by this technique is considered to be feasible. The limitations to the technique are primarily those of ice sheet formation. If a sustained rate of freezing of 0.75 centimeters per hour is maintained, a one-meter thick sheet of ice will be formed in 5.5 days. This volume of ice will require 12 days to melt when absorbing 50 percent of the total heat input. A 1-1/2 meter thick sheet of ice would require 8 days to form and would suppress ice fog for 18 days. (1-1/2 meters of ice on the pond is the maximum thickness without considerable modification, and one meter is probably a more practical limit.)

The longest period of continuous ice fog weather on record at Fairbanks Weather Bureau is 4 days, and 66 percent of the incidents are 8 days or less. Thus, a 1-1/2 meter thick sheet could suppress ice fog for essentially all of even the longest periods, and a one-meter thickness would suffice for the shorter ones.

Between ice fog sessions, there must be sufficient time to rebuild the ice cover. The situation of a long ice fog experience, followed by a second similar period with only 1 or 2 days between, would require the thicker 1-1/2 meter sheet. The average time interval between ice fog incidents in the last 10 years is 6.2 days. This would allow adequate time to rebuild a one-meter thick ice sheet at a rate of 0.75 centimeters per hour. On 26 occasions during the last 10 winters, a break of 2 days or less fell between ice fog incidents, but on only two of these occasions was the total sequence of ice fog events long enough to exhaust a one-meter thick ice sheet.

During the melting of the sheet, ice fog will be generated as soon as the first open water appears; however, the percentage of the normal production of fog is very small. If suppression is defined as:

$$S = \frac{\text{evaporation during suppression}}{\text{evaporation without suppression}}$$

the graph (Figure 6-14) shows the performance during the tests of this experiment in January and February 1973. Figures 6-11 and 6-12 show the limits of the ice sheet and the ice thicknesses measured during two melting experiments. Figures 6-15 and 6-16 show the pond with and without complete ice cover. Figures 6-17 through 6-20 show events and problems of interest during the experiments.

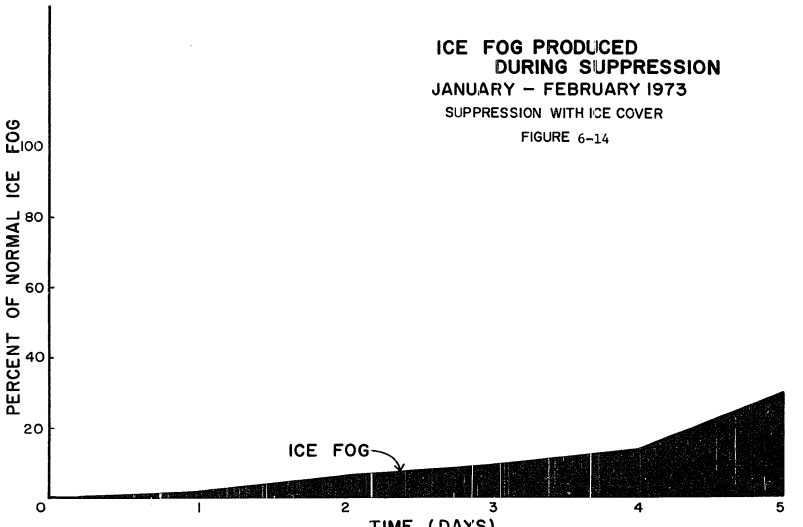

Figure 6-15. Ice Fog Suppression with Total Ice Cover (-30° C).

Figure 6-16. Ice Fog Production under Normal Conditions (-23° C).

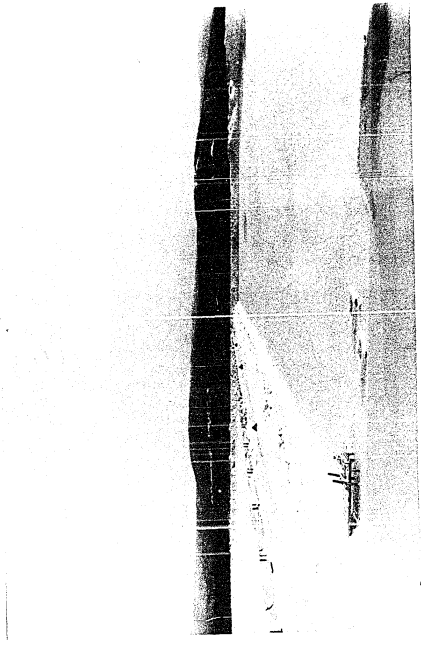

Figure 6-17. Ice Cover on the Intake Pond.

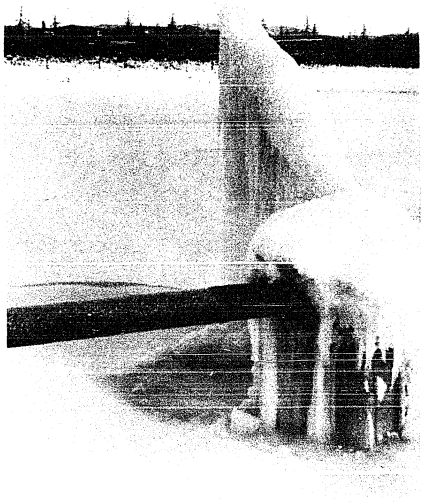

Figure 6-18. Ice Build-up Problems.

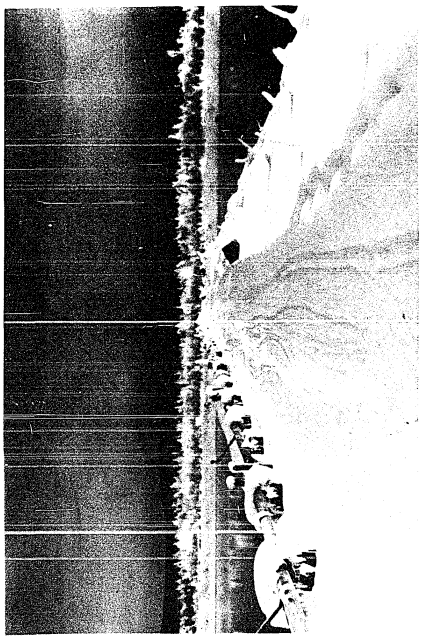

Figure 6-19. Spray Headers and Visibility Targets on the Dike.

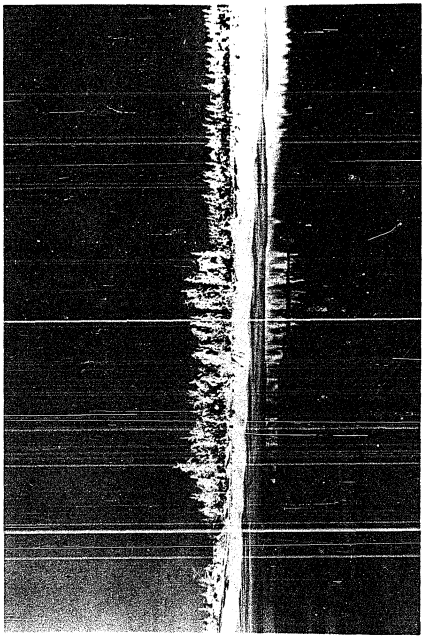

Figure 6-20. Ice Break-up during Final Stages of Melting.

Experimental Results

The unusually mild winter, coupled with the inability of the installation to form a uniformly thick ice sheet, allowed only two melting experiments. In addition, an ice sheet thickness of 53 centimeters was the maximum obtained. This is only one-half of the thickness felt to be optimum. The maximum long term freeze rate obtained during the ice building experiments was 7.5 centimeters in 24 hours (0.31 (cm)(hr^{-1})). The basic limitation was that of freezing from the top down. No way was available to prevent the water from puddling and forming a skim of ice over the top. As soon as this occurred, all further freezing was then done by transferring the heat through the ice on top of the puddles, in accordance with the limitations of Equation 6-1. This was the fundamental freeze rate limitation.

The optimum practical thickness of each applied layer of water to yield maximum growth rate is a function of the temperature and weather conditions, as well as the method of application used. An overall average of 0.46 centimeters of ice growth per hour was measured for short term experiments during the winter. Since the growth rate is proportional to the square root of time, the highest rate of freezing occurs during the first few minutes after the film of ice is formed. Thin films of water would therefore freeze much faster than the 0.46 cm film. If a very thin film could be applied at frequent intervals, the overall result might well yield an optimum growth rate of perhaps 0.75 cm per hour, approaching the theoretical maximums discussed earlier.

Although the above technique appears to offer a workable means of ice fog suppression, the limitation of ice growth rate may well be an overriding consideration that limits its practicality.

CHAPTER SEVEN - RECOMMENDATIONS AND CONCLUSIONS

The work described in this report has tested the feasibility of two techniques of ice fog suppression. Conclusive tests have not been made to determine which is the most practical or efficient. Further studies are needed, beginning with more exhaustive tests of hexadecanol. In view of the present work, it appears that hexadecanol may provide the most inexpensive and efficient solution of the problem. Should further hexadecanol experiments show this technique to be impractical, a decision would have to be made concerning the desirability of continued use of the pond during the winter months, as opposed to the injection well approach discussed in Chapter Five. If an impact study of the injection well technique shows that there will be no detrimental effects to the operation of the power plant, and the capital expenditures are within reason, then this is the next most logical approach. If the implementation of an injection well proves impractical, the installation for latent heat storage suppression appears to offer the most promise.

Hexadecanol Studies

The fundamental questions to be resolved concerning this approach are:

1. Film integrity. A floating grid or net should be fabricated and tested for effectiveness. Grid size as well as height of protrusion above water needs to be optimized. This will provide

a means for the film to maintain continuity over the entire pond, and eliminate the problem of wind concentrating the film on one side of the pond.

2. Film life. Biological degradation (see Chapter Five) is of concern in relation to film life. The extent of the problem should be determined. Methods of eliminating or reducing its magnitude by poisoning the film with a bactericide or treating the pond between applications of the alcohol need to be studied and techniques developed. Film life should be determined under ice fog conditions.
3. Alcohol blends. Several other long-chain fatty alcohols need to be tested to determine which one or which blend of two or more gives the best suppression of evaporation and longest lifetime.
4. Application technique. Many methods have been used to apply the alcohols (which come in a granular powder form) to the water surface. This can be done with a hand-held lawn spreader as was done in the studies of this report, or by spraying slurries of alcohol and water. A method compatible with the conditions of ice fog needs to be developed and implemented.

The tests thus far are not conclusive, but strongly suggest that this is an effective suppression technique. Suppression of 84% at temperatures below freezing appears to be better than the 62% reported under warmer conditions (Chapter Five). The major problem will probably be that of maintaining film integrity during wind. If practicality can be demonstrated, use of hexadecanol may be the least expensive method by a wide margin. Application should pose no technical problems.

Injection Well Suppression

Before this method can be used, several questions need to be resolved. They are:

1. Cooling water supply. Tests must be made to determine if the make-up wells can supply adequate volumes of water on a continuous basis. Tests run during the winter indicate that the wells are only producing at approximately one-half of their original capacity.
2. Raw water problems. The detrimental effects of using raw water in the condensers need to be studied and any problems resolved.
3. Injection well. Injection wells are known for gradually building up resistance to water injection due to "plugging". A well of adequate size must be developed and tested along with an emergency back-up system. (A valving arrangement to allow the cooling water to be changed back to the cooling pond would provide adequate safety.)
4. Recirculation bypass. A method of recirculating a portion of the warm cooling water needs to be designed into the system to allow the cold well water to be tempered before it is sent into the condensers.
5. Costs. The initial cost of the well drilling, injection pumps, internal piping, and valving needs to be determined to assure that this method is economically feasible.

The present well installation at Eielson is inadequate for direct use of this method. This technique provides a positive elimination of

the ice fog contribution of the ponds; however, it poses several environmental questions.

Latent Heat Storage Suppression

The critical limiting factor in this technique is the ability to form rapidly a uniform ice sheet of sufficient thickness. One means is to install spray nozzles in a 30-meter grid so that the ice sheet can be uniformly covered by spray. This could be accomplished with three headers equally spaced across the width and running the length of the pond. Nozzles capable of spraying 15 meters throughout 360 degrees would be installed every 30 meters. The headers could either be installed under the surface of the pond and be provided with an air purge so that the nozzle standpipe would not freeze in the area where it passes through the ice sheet, or alternatively, they could be set on pilings over the pond with the nozzles on the bottom of the pipe. During the experiments discussed in Chapter Six, no freezing problems developed after the larger (1.9 cm diameter) nozzles were installed.

Subject to this consideration, the technique has proven to be a practical working means of ice fog suppression. Visibility conditions in the vicinity of the pond were dramatically improved during ice fog weather when suppression was in effect. No discernible fog could be seen during this period, and bushes were visible in excellent detail across the length of the pond. Some other problems need to be considered in the application of this technique:

1. A circulation dam between the two sides of the pond must be installed to eliminate the density gradient circulation from

the warm side to the cold side of the pond. This provides the isolation needed to form an ice sheet at the maximum rate in all weather conditions.

2. To provide better control of the temperature of the intake pond, the existing make-up wells should be rerouted to empty into either side of the pond. This will enhance operating efficiency and reduce time required to switch from ice building to suppression configuration.

Of the three above recommended approaches, the hexadecanol appears to have the advantages of low initial cost and low maintenance and operating cost. The injection well, while holding a good deal of promise, needs careful study before the rather formidable initial investment is justified. The latent heat storage technique, while appearing to be the third choice, has the big advantage of having been proven in the field under ice fog conditions. We know more about this method and its requirements and performance than any of the others at this time.

Measurements of Evaporation

Evaporation into below freezing air averages 5 $(kg)(m^{-2})(day^{-1})$. Evaporation measurements are difficult under the very cold conditions of ice fog, and scatter of data points is an inevitable result. However, the data were of sufficient quantity and scatter of the same magnitude as the controlled laboratory experiments of Yen and Landvatter. This lends confidence to the average values obtained in these studies. The formulas developed from this work should be useful for ice fog evaporation

calculations, and their accuracy should be an improvement over those equations previously available.

Measurements of Radiation Loss

Long-wave radiation losses are a significant portion of the total heat losses. They are attenuated by the ice fog cover, but even with heavy ice fog, they continue to be significant. Average net long-wave radiation lost from the surface was 119 watts per square meter.

Convective Heat Losses

Convective heat losses were estimated using both Rimsha and Donchenko's equation, Kays' equation, and Rotem and Claassen's equation. Agreement between the various equations was very good at lower temperature differences; but for low winds, they diverged considerably as temperature differences increased. More work is needed to determine the convective heat loss equations at these times.

Ice Fog Suppression

The prime purpose of this paper was the investigation of techniques for the suppression of ice fog from open water of cooling ponds. Values for the various modes of heat transfer were measured during the studies. These values were used for engineering estimates of the heat budget during the melting phase of the experiments on latent heat suppression. Equations were developed to make it possible to determine the necessary heat balance components of the pond.

In the past, ice fog has been tolerated, studied, and cursed. No real attempt has been made to suppress it at its source. It is the

conclusion of this paper that suppression is feasible - and by several techniques. Suppression both by latent heat storage and by monomolecular films was proven to be effective. In an engineering assessment of the problem, both the effectiveness and the economics of each method must be considered. From a cost standpoint, the monomolecular film technique appears to be better. From the standpoint of effectiveness, the latent heat storage method was somewhat more effective, and more positive. Either way, ice fog from open water surfaces can be suppressed using the engineering techniques discussed. The reduction in the total ice fog problem should be significant, and will be visually evident to those working and living with the problem.

APPENDIX A - HEAT TRANSFER COEFFICIENT FROM WATER TO ICE

Kays (1966) develops the solution for turbulent flow of a fluid past a semi-infinite plate of constant temperature. This meets the conditions of the cooling pond at Eielson Air Force Base if we restrict the solution to low velocity flow, constant property fluids, and Prandtl numbers that range from 0.5 to 10. These restrictions are easily met for the case in question and the general formula developed should give a good comparison for measured values.

Turbulent heat transfer in the Prandtl number range of interest can be expressed by the relation:

$$St_x \, Pr^{0.4} = 0.0295 \, Re^{-0.2} \qquad \text{A-1}$$

where:

$$St_x = \frac{h_x}{\rho \, C_p \, u_\infty} \qquad \text{A-2}$$

Rearranging and substituting for St_x yields:

$$h_x = \frac{(0.0295)(\rho \, C_p \, u_\infty)}{(Pr^{0.4})(Re^{0.2})} \qquad \text{A-3}$$

Evaluating this relation for water at the following conditions:

$T_\infty = 10°$ C

$u_\infty = .152$ (m)(min^{-1})

gives:

$Pr = 7.0$

$C_p = 1.0$

$\nu = 7.8 \times 10^{-5}$(m^2)(sec^{-1})

$\rho = 999$ (kg)(m^{-3})

$$Re = \frac{u_\infty x}{\nu} = \frac{(.15)(91)}{7.8 \times 10^{-5}} = 174{,}919$$

where:

x = distance along ice sheet

then:

$$h_x = \frac{(0.0295)(\rho\, C_p\, u_\infty)(1000)}{(7)^{0.4}\ (174{,}919)^{0.2}} = 12.76\ (\text{watts})(m^{-2})(°C^{-1})$$

Evaluating the relation for air at the following conditions:

T = -20 degrees celsius

u = 1.0 (m)(sec^{-1})

x = 1 meter

gives:

Pr = 0.72

C_p = 0.24 (cal)(g^{-1})(°C^{-1})

ν = 0.93 x 10^{-5} (m^2)(sec^{-1})

Re = 107,527

then:

$$h_x = \frac{(0.0295)(1.4 \times 10^{-3})(.24)(1 \times 10^6)(1.0)(4.184)}{(0.72)^{0.4}\ (1.08 \times 10^5)^{0.2}}$$

$$h_x = 4.66\ (\text{watts})(m^{-2})(°C^{-1})$$

APPENDIX B

COMPUTER PROGRAM FOR DETERMINING RADIATION VIEW FACTOR

```
PROGRAM FOR
CALC VIEW
FACTOR
FOR
RADIATION PROBE

Ø:
SCL Ø, 3Ø5, Ø, 77 [
1:
'XE Ø, Ø; SFG 1;
SFG 5; Ø→R 18 [
2:
"AA"; Ø→A; Ø→C; Ø→R
17 [
3:
"A"; IF FLG 1=1;
((3Ø5-A-23Ø) ↑2 +
(Ø-3) ↑2) ↑.5 →R (2Ø+C)[
4:
IF FLG 1=1; ((3Ø5 -
(5+A) - 23Ø) ↑2 +
(Ø-3) ↑2) ↑.5 →R (21+C [
5:
IF FLG 1=1; 5.Ø →B;
GTO "XX" [
6:
IF FLG 2=1; ((Ø-23Ø)
↑2 + (A-3) ↑2) ↑.5 →R
(2Ø+C) [
7:
IF FLG 2=1; ((Ø-23Ø)
↑2 + (A+1-3) ↑2) ↑.5
→R (21+C) [
8:
IF FLG 2=1; 1→B;
GTO "XX" [
9:
IF FLG 3=1; ((A-23Ø)
↑2 + (77-3) ↑2) ↑.5
→R (2Ø+C) [
10:
IF FLG 3+1; ((A+5-23Ø)
↑2 + (77-3) ↑2) ↑.5
→R (21+C) [
11:
IF FLG 3=1; 5.Ø→B;
GTO "XX" [
12:
IF FLG 4=1; ((3Ø5-23Ø)
↑2 + (77-A-3) ↑2) ↑.5
→R (2Ø+C) [
13:
IF FLG 4=1; ((3Ø5-23Ø)
↑2 + (77 - (A+1)
-3) ↑2) ↑.5 →R (21+C) [
14:
IF FLG 4=1; 1.Ø→B;
GTO "XX" [
15:
"XX"; (B↑2-R (21+C)
↑2-R(2Ø+C) ↑2)/ - 2R
(2Ø+C) R (21+C) →R 1 [
16:
ACS R1→R2 [
17:
(2π/36Ø) R2→R3 [
18:
.5/R(2Ø+C) →R4 [
19:
R3* (1-R4) →R5 [
2Ø:
R5 + R17 →R17 [
21:
IF FLG 1=1; IF A≤
3ØØ; A+5→A; C+1→C;
GTO "A" [
22:
IF FLG 2=1; IF A≤
76; A+1→A; C+1→C;
GTO "A" [
23:
IF FLG 3=1; IF A≤
3ØØ; A+5→A; C+1→C;
GTO "A" [
24:
IF FLG 4=1; IF A≤
76; A+1→A; C+1→C;
GTO "A" [
25:
PRT R17 [
26:
R17+R18→R18 [
27:
IF FLG 5=1; CFG 5;
CFG 1; SFG 2;
SFG 6; GTO "AA" [
28:
IF FLG 6=1; CFG 6;
CFG 2; SFG 3;
SFG 7; GTO "AA" [
29:
IF FLG 7=1; CFG 7;
CFG 3; SFG 4;
GTO "AA" [
3Ø:
PRT "TOT SOLID A
NG", R18 [
31:
END [
R3Ø2

 2.781585381E  ØØ
 3.275551883E -Ø1
 2.Ø72488217E  ØØ
 8.269418897E -Ø1
TOT SOLID ANG
 6.ØØ857Ø676E  ØØ

VIEW FACTOR
 9.562937239E -Ø1
```

BIBLIOGRAPHY

Anderson, E. R. 1952. Energy budget studies from water loss investigations. Vol 1. Lake Hefner Studies Technical Report. US Geological Survey Circular #229, pp 91-119. Washington, DC.

Angstrom, Anders. 1920. Application of Heat Radiation Measurements to the Problems of the Evaporation from Lakes and the Heat Convection at their Surfaces. Geografiska Annaler, Vol 2, pp 237-252.

Australian Water Resources Council. 1970. Hydrological Series No. 4. Evaporation from Water Storages. Department of National Development, Canberra, Australia.

Bean, B. R., and Q. L. Florey. 1968. A field study of the effectiveness of fatty alcohol mixtures as evaporation reducing monomolecular films. Water Resources Research, Vol 4, No. 1, pp 206-208.

Brutsaert, W. 1973. Heat and Water Vapor Exchange Between Water Surface and Atmospheres. Environmental Protection Agency Office of Research and Monitoring Report #EPA R2-73 259, May 1973.

Baumeister, T., and L. Marks (Eds.). 1958. Standard handbook for mechanical engineers. 7th Ed. McGraw Hill, New York.

Behlke, C., and J. McDougall. 1973. Polyethylene Sheeting as a Water Surface Cover in Sub-zero Temperatures. Proceedings of the 24th Alaska Science Conference. University of Alaska, Fairbanks, Alaska.

Benson, C. S. 1965. Ice fog: low temperature air pollution. University of Alaska Publication, Geophysical Institute UAG 173.

Benson, C. S. 1970. Ice Fog. United States Army Cold Regions Research and Engineering Laboratory, Research Report 121. Hanover, NH.

Bilello, M. A. 1967. Water Temperatures in a Shallow Lake during Ice Formation Growth and Decay. United States Army Cold Regions Research and Engineering Laboratory Research Report 213, Hanover, NH.

Bilello, M. A., and R. E. Bates. 1972. Ice Thickness Observations, North American Arctic and Subarctic, 1967-68, 1968-69. United States Army Cold Regions Research and Engineering Laboratory Special Report 42, Part VI. Hanover, NH.

Bolsenga, S. J. 1964. Daily Sums of Global Radiation for Cloudless Skies. United States Army Cold Regions Research and Engineering Laboratory Research Report 160. Hanover, NH.

Bowen, I. S. 1926. The Ratio of Heat Losses by Conduction and by Evaporation from any Water Surface. Physical Review, Series #2, Vol 27, pp 779-787.

Brunt, D. 1944. Physical and Dynamical Meteorology. Cambridge University Press.

Chang, S., M. McClanahan, and P. Kabler. 1962. Effect of bacterial decomposition of hexadecanol and octadecanol in monolayer films on the suppression of evaporation loss of water. Retardation of Evaporation by Monolayers, pp 119-130. Academic Press, Inc. NY.

Chow, Ven Te (Editor). 1964. Handbook of Applied Hydrology. McGraw Hill, NY.

Crow, F. R., J. B. Allen, W. E. Fry, and A. L. Mitchell. 1969. Evaporation and its suppression by chemical films on Lake Hefner. Transactions of the American Society of Agricultural Engineers, Vol 12, No. 6, pp 889-895.

Devik, Olaf. 1932. Thermische und Dynamische Bedingungen der Eisbildung in Wasserlaufen. Geofysiske Publikasjones (in German).

Dingman, S. L., W. F. Weeks, and Y. C. Yen. 1967. The effects of thermal pollution on river ice conditions. United States Army Cold Regions Research and Engineering Laboratory Research Report 206. Hanover, NH.

Dingman, S. L., and A. Assur. 1969. The effects of thermal pollution on river ice conditions. Part II: A simplified method of calculation. United States Army Cold Regions Research and Engineering Laboratory Research Report 206, Part II. Hanover, NH.

Dressler, R. G. 1969. Evaporation retardants based on blends of alcohol containing odd and even numbers of carbon atoms and methods of use. US Patent Office No. 3,540,488.

Dunkle, R. V., et al. 1949. Non Selective Radiometer for Hemispherical Irradiation and Net Radiation Interchange Measurements. University of California, Department of Engineers, Thermal Radiation Project #9. Berkeley, California.

Eagleson, P. 1970. Dynamic Hydrology. McGraw Hill, NY.

Elsasser, W. M. 1942. Heat transfer by infrared radiation in the atmosphere. Harvard Meteorological Study No. 6, Harvard University Blue Hill Meteorological Observatory.

Freysteinsson, S. 1970. Calculation of Frazil Ice Production. International Association for Hydraulic Research. Proceedings of 1970 Ice Symposium. Reykjavik, Iceland.

Gebhart, B. 1969. Natural Convection Flow, Instability, and Transition. Journal of Heat Transfer - Transactions of A.S.M.E., August 1969, Paper #69 HT-29.

Geidt, W. 1958. Principles of Heat Transfer. Van Nostrand, Princeton, N.J.

Geiger, R. 1965. The Climate near the Ground. Harvard University Press, Cambridge, Massachusetts.

Goltz, S. M., C. B. Tannes, G. W. Thurtell, and F. E. Jones. 1970. Evaporation Measurements by an Eddy Correlation Method. Water Resources Research, Vol 6, No. 2, April 1970, pp 440-446.

Hatiner, G. J., and F. L. Martin. 1957. Dynamical and Physical Meteorology. McGraw Hill, New York.

Hinchen, J. D. 1969. Practical Statistics for Chemical Research. Methun and Co., Ltd. London, England.

Holman, J. P. 1972. Heat Transfer. McGraw Hill, New York.

Johnson, P. R., and C. W. Hartman. 1969. Environmental Atlas of Alaska. University of Alaska, Institute of Arctic Environmental Engineering, Institute of Water Resources, College, Alaska.

Kays, W. M. 1966. Convective Heat and Mass Transfer. McGraw Hill, New York.

Koberg, Gordon E. 1964. Methods to Compute Long Wave Radiation from the Atmosphere and Reflected Solar Radiation from a Water Surface. USGS Prof. Paper No. 272-F.

Kohler, M. A., T. J. Nordenson, and W. E. Fox. 1955. Evaporation from Pans and Lakes. US Department of Commerce, Weather Bureau, Research Paper No. 38.

Kohler, M. A., T. J. Nordenson, and D. R. Baker. 1959. Evaporation Maps for the United States. US Department of Commerce, Weather Bureau, Technical Paper No. 37.

Kohler, M. A. 1954. Lake and Pan Evaporation in Water Loss Investigations: Lake Hefner Studies Technical Report. US Geological Survey Prof. Paper 269, pp 127-149.

Kondratyev, K. 1954. Radiant Solar Energy. Gidrometeoizdat, Leningrad. (In Russian)

Kuz'min, P. P. 1951. Study of the Parameters in Formulae for Snow Melting. Trudy Gredrometeoizdat, Issue 32, 86. (In Russian)

Littleton Research and Engineering Corporation. 1970. An Engineering Economic Study of Cooling Pond Performance. EPA Project No. 16130DFX05/70.

MacRitchie, F. 1969. Evaporation Retarded by Monolayers. Science, Vol 163, No. 3870, pp 927-931.

McFadden, T. T. 1972. Ice Fog Suppression at Eielson Air Force Base. Alaska Civil Engineer, May 1972, pp 19-20.

McFadden, T. T. (Unpublished). Building Ice Sheets. University of Alaska Report.

Magin, G. B., and L. E. Randall. 1960. Review of Literature on Evaporation Suppression. Geological Survey Professional Paper 272-C. US Government Printing Office.

Michel, B. 1970. Ice Pressure on Engineering Structures. United States Army Cold Regions Research and Engineering Laboratory, Monograph III-B1b, Hanover, NH.

Michel, B. 1971. Winter Regime of Rivers and Lakes. United States Army Cold Regions Research and Engineering Laboratory, Monograph III-B1a, Hanover, NH.

Navon, U., and J. Fenn. 1971. I. Interfacial Mass and Heat Transfer During Evaporation. II. Effect of Monomolecular Films on Natural Convection in Water. Journal of Chemical Engineering Research and Development, Vol 17, No. 1.

Noe, E. R., and R. G. Dressler. 1969. Performance of Pure Odd and Even Chain Fatty Alcohols in Water Evaporation Suppression. Industrial and Engineering Chemistry Product Research and Development, Vol 6, No. 2, pp 132-137.

Ohtake, T. 1970. Studies on Ice Fog. University of Alaska Publication, Geophysical Institute, UAG R-211.

Pasquill, F. 1948. Eddy Diffusion of Water and Heat near the Ground. Proceedings of the Royal Society (London), Ser A, Vol 198, No. 1052, pp 116-140.

Penman, H. L. 1948. Natural Evaporation from Open Water, Bare Soil, and Grass. Proceedings of the Royal Society (London), Ser A, Vol 193, pp 12-145.

Peyton, H. R., and P. R. Johnson. 1967. Saline Conversion and Ice Structures from Artificially Grown Sea Ice. University of Alaska, Arctic Environmental Engineering Laboratory and the Institute of Water Resources, Research Report No. 4.

Pounder, E. R. 1965. Physics of Ice. Pergamon Press, New York.

Pruden, F. W., R. L. Wardlaw, D. C. Baxter, and I. L. Orr. 1954. A Study of Wintertime Heat Losses from a Water Surface and of Heat Conservation and Heat Addition to Combat Ice Formation in the St. Lawrence River. Report No. MD42, National Research Council of Canada, Ottawa, Canada.

Raphael, J. 1962. Prediction of Temperature in Rivers and Reservoirs. Proceedings of the American Society of Civil Engineers, Journal of the Power Division, No. P02, Paper 3200, pp 157-181.

Rimsha, V. A., and R. V. Donchenko. 1958. Winter Heat Losses from an Open Surface of Water. Trudy Gosudarstvennogo Gedrologicheskogo Institutt, Gedrometeoizdat, Leningrad. (In Russian)

Robinson, E. 1953. An Investigation of the Ice Fog Phenomena in the Alaskan Area. Stanford Research Institute Project No. 473, Menlo Park, California.

Robinson, E., W. C. Thurman, and E. J. Wiggins. 1957. Ice Fog as a Problem of Air Pollution in the Arctic. Arctic, Vol 10, pp 89-104.

Robinson, N. 1966. Solar Radiation. Elsevier Publishing Company, NY.

Rootem, Z., and L. Claassen. 1969. Natural Convection above Unconfined Horizontal Surfaces. Journal of Fluid Mechanics, Vol 38, Part 1, pp 173-192. Printed in Great Britain.

Scott, R. F. 1964. Heat Exchange at the Ground Surface. US Army Cold Regions Research and Engineering Laboratory, Monograph II-A1, Hanover, NH.

Siegel, R., and J. Howell. 1972. Thermal Radiation Heat Transfer. McGraw Hill, New York.

Starosolszky, O. 1969. Ice in Hydraulic Engineering. Division of Hydraulic Engineering, The Norwegian Institute of Technology, University of Trondheim, Report #70-1.

Stehle, N. H. 1965. Ice Engineering - Growth Rate of Sea Ice in a Closed System. US Naval Civil Engineering Laboratory, Technical Report R 396, Port Hueneme, California.

Sutton, O. 1953. Micrometeorology. McGraw Hill Book Company, NY.

Thurston, W. M. 1972. Flow into a Stratified Reservoir. Office of Research and Monitoring, USEPA, Report No. EPA R2 72 037.

US Army Corps of Engineers. 1956. Snow Hydrology. US Department of Commerce Clearing House for Federal, Scientific, and Technical Information, PB 151 660.

US Naval Engineering Laboratory. 1959. Point Barrow Trials, FY 1959 Investigations on Thickened Sea Ice. Naval Facilities Engineering Command, Technical Report R185, Port Hueneme, California.

US Naval Engineering Laboratory. 1966. Ice Construction - Survey of Equipment for Flooding. Naval Facilities Engineering Command, Technical Report R402, Port Hueneme, California.

US Naval Engineering Laboratory. 1967. Ice Construction - Methods of Surface Flooding. Naval Facilities Engineering Command, Technical Report R511, Port Hueneme, California.

Van Bover, C. H. M. 1966. Potential Evaporation: the Combination Concept and its Experimental Verification. Water Resources Research, Vol 2, No. 3, pp 453-467.

Vanderbilt University Department of Environmental Water Resources Engineering (Thackston, E. and F. Parker) 1971. Effect of Geographical Location on Cooling Pond Requirements and Performance. Water Quality Office of EPA, GPO No. EP 2.10:16130 FDQ 03/71.

Vanderbilt University Department of Environmental Water Resources Engineering. 1960. Evaporation from Lake Eucumbene. Division of Meteorological Physics. Commonwealth Scientific and Industrial Research Organization, Technical Paper No. 10, Australia.

Vanderbilt University Department of Environmental Water Resources Engineering. 1966. A Pan/Lake Evaporation Relationship. Journal of Hydrology (Amsterdam), Vol 4.

Weller, G. E. 1969. Ice Fog Studies in Alaska. University of Alaska Publication, Geophysical Institute UAG R 207.

Wexler, H. 1940. Observations of Nocturnal Radiation at Fairbanks, Alaska, and Fargo, North Dakota. Monthly Weather Review, US Department of Agriculture, Weather Bureau, Washington, DC.

Williams, G. P. 1961. Evaporation from Water, Snow, and Ice. Proceedings of the Evaporation Hydrology Symposium, No. 2, Toronto, pp 31-52.

Williams, G. P. 1972. A Case History of Forecasting Frazil Ice. Proceedings of Banff Symposia on the Role of Snow and Ice in Hydrology, Vol 2, pp 1212-1223.

Yen, Y. C., and G. Landvatter. 1970. Evaporation of Water into a Subzero Air Stream. Water Resources Research, Vol 6, No. 2, pp 430-439.